Role of Oxytocin Neurons in Obstructive Sleep Apnea Mediated Cardiovascular Disease

by Heather S. Jameson

B.S in Chemistry, May 2006, The George Washington University

A Dissertation submitted to

The Faculty of
The Columbian College of Arts and Sciences
of The George Washington University
in partial fulfillment of the requirements
for the degree of Doctor of Philosophy

August 31, 2015

Dissertation directed by

David Mendelowitz
Professor of Pharmacology and Physiology
and of Anesthesiology & Critical Care Medicine

The Columbian College of Arts and Sciences of The George Washington University certifies that Heather S Jameson has passed the Final Examination for the degree of Doctor of Philosophy as of May 28, 2015. This is the final and approved form of the dissertation.

Role of Oxytocin Neurons in Obstructive Sleep Apnea Mediated Cardiovascular Disease

Heather S. Jameson

Dissertation Research Committee:

David Mendelowitz, Professor of Pharmacology & Physiology and of Anesthesiology & Critical Care Medicine, Dissertation Director

Linda Werling, Professor of Pharmacology & Physiology, Committee Member

Katherine Kennedy, Professor of Pharmacology & Physiology, Committee Member

Dedication

For my parents. Thank your continuous encouragement over the years. Your unconditional love and support has made me the person I am and has led me through this process.

Acknowledgements

First and foremost, I would like to thank Dr. David Mendelowitz for taking a chance on me almost nine years ago and for being such a wonderful mentor. Dave, your patience, support, guidance, and friendship over the last nine years has helped shape me into the person and scientist I am today. I have had many setbacks and frustrations during my time in your lab, but you always been understanding and helped me solve the problems and overcome the obstacles in front of me. I think we both took a chance on this project, but together we managed to make it work. You're a true example of the type of scientist I hope to become in the future. It remains very bittersweet for me to leave the lab because I know I have experienced the best and anything else is going to be a letdown. Thank you for everything.

I would also like to thank the members of my committee. I appreciate all the time and energy you have all put into my dissertation defense. Dr. Werling, thank you for all your support over the years. I know that if it was not for you I would not be where I am today. I truly appreciate you always cheering me on and being there for anything I needed. I will miss your humor, laughter, and kindness. Dr. Kennedy, thank you for your enthusiasm towards my project, suggestions at my committee meetings, and for reading my dissertation. Dr. Marvar, thank you for agreeing to be a part of my committee and for all your thoughtful ideas along the way. Dr Yarbrough, thank you for agreeing to be a part of my committee.

Marc, thank you for all you do for the IBS program and for being a great friend to me over my time in Ross. I will always cherish our Friday afternoon catchup sessions and all the times we spent talking about life. You are my favorite!

Thank you to all the members of the Mendelowitz lab (past and present). You have all made it enjoyable and fun to come to work each day. Jhansi, Xin, and Olga, thanks for being great postdocs and all your contributions over the years. Ned, thanks for following up and extending some of my work, and of course for all our conversations about science and life. You're going to kill it in grad school! Pedro, I'll miss all our brigades! Thank you for doing the majority of my telemetry surgeries, making virus for me, and for always letting me keep it real! Julie, I miss your presence in the lab every day. Thank you for being such a wonderful friend, always offering me guidance, and showing me how to overcome anything. Ramon, thank you for all of your continued help over the years. My project was successful because of your previous work, ideas, and guidance.

Big cats, as someone very wise once said: you've made my bad days good and my good days better. I would not have made it through graduate school without you both making me laugh daily. The lab has never been the same for me without you two in it. Chris, if it wasn't for you I would have never worked in David's lab and made all the choice memories that I have. Thanks for mentoring me in so many ways, and always being there when I need to talk to someone about science or life. Ry, without you so much of my project would not have been possible and I'm so grateful for all your contributions. Thanks for continuing to hang with me even though you are in med school! Thanks to you both for just being an all-around awesome friends and bros.

I also want to give a very special thanks to my husband, Larry. Thank you for always being so incredibly supportive, caring, and for never putting pressure on me to graduate, even when it seemed like it might never happen. You have always believed in me when I have not believed in myself, and encouraged me to keep going. I would not have pushed through graduate school without you.

To my sistah, Sarah. You have always been there for me and it's meant even more over the past six years. Your continuous love and support have helped me through this process. I don't know what I will do without you and Gabe around the corner!

And last but certainly not least, I have to thank my parents, Bellen. Without the two of you, none of this would have been possible. Thank you for always making my education a priority, unconditionally supporting and loving me, and always reminding me of my accomplishments and strengths. I don't know where I would be without the two of you. I am so grateful for everything you have given me in life. Thank you.

Abstract of Dissertation

Role of Oxytocin Neurons in Obstructive Sleep Apnea Mediated Cardiovascular Disease

Recent work has shown oxytocin (OXT), a neuropeptide released from parvocellular neurons in the paraventricular nucleus of the hypothalamus (PVN), could be cardioprotective by exciting parasympathetic cardiac vagal neurons (CVNs) in the brainstem and reducing cardiovascular responses to stress. Obstructive sleep apnea (OSA) is a very common, yet poorly understood disease that increases the incidence of hypertension, tachycardia, stroke and other adverse cardiovascular events. For this study I test the hypotheses that the release of OXT from PVN neurons onto CVNs is diminished with exposure to chronic intermittent hypoxia-hypercapnia (CIH/H), an animal model of OSA, and furthermore, selective activation of PVN OXT neurons can reduce adverse cardiovascular consequences, particularly the elevation of blood pressure to hypertensive levels, that occur with CIH/H.

In order to elucidate the conditions required for OXT release from PVN fibers, we engineered and dispersed within the brainstem sniffer Chinese Hamster Ovarian (CHO) cells highly sensitive to oxytocin. These sniffer CHO cells were stably transfected to express the human recombinant OXT receptor, and calcium changes within these cells were visualized as these cells were also made to express the red fluorescent calcium indicator, R-GECO1. Our data show optogenetic stimulation of channelrhodopsin-2 – expressing hypothalamic PVN fibers in the brainstem evoked large, reproducible, and transient increases in calcium within sniffer CHO cells that are in close proximity to OXT

fibers. The photostimulation-elicited increase in calcium in the sniffer CHO cells upon PVN fiber activation was abolished by application of the oxytocin receptor antagonist, OTA. In animals exposed to 21 days of CIH/H the OXT dependent calcium increases in CHO cells upon photoactivation of PVN fibers were blunted. This finding indicates there is reduced oxytocin neuron activity following CIH/H, and that reduced oxytocin neuron activity and/or function could contribute to the adverse cardiovascular events associated with OSA.

We next tested if restoration of OXT neuron activity could prevent the adverse cardiovascular effects of CIH/H in vivo. To test this hypothesis we selectively expressed excitatory **d**esigner **r**eceptors **e**xclusively **a**ctivated by **d**esigner **d**rugs (DREADDs) in PVN OXT neurons, and implanted animals with telemetry devices to monitor blood pressure and EKG activity. Selective chronic activation of PVN OXT neurons decreased resting blood pressure and heart rate, blunted the responses to acute hypoxia/hypercapnia, and perhaps more importantly, chronic PVN OXT neuron activation prevented the elevations in blood pressure and heart rate that occur with CIH/H. These results indicate that excitation of parvocellular PVN fibers releases OXT at brainstem CVN targets, selective activation of OXT neurons in the PVN decreases resting blood pressure and heart rate, and chronic activation of oxytocin neurons in the PVN prevents the elevations in blood pressure and heart rate that occur after 21 days of CIH/H.

Table of Contents

Acknowledgements iv

Abstract of Dissertation vii

Table of Contents ix

List of Figures xi

List of Abbreviations xiii

Chapter 1 1

Introduction

The autonomic nervous system and cardiovascular regulation 2

The sympathetic nervous system 3

The parasympathetic nervous system 5

Sympathetic/parasympathetic nervous system interactions 6

Parasympathetic control of heart rate 7

Neurophysiology of cardiac vagal neurons 8

Cardiac vagal neurons in the nucleus ambiguus 9

Cardiac vagal neurons in the dorsal motor nucleus of the vagus 11

The paraventricular nucleus of the hypothalamus 12

Role of the paraventricular nucleus of the hypothalamus in controlling heart rate and generating/maintaining hypertension 17

Changes in autonomic function in obstructive sleep apnea patients and in models of obstructive sleep apnea following chronic intermittent hypoxia 18

Oxytocin in cardiovascular function 20

Optogenetics 22

Chemogenetics 26

Summary and specific aims 30

Chapter 2 **32**

Study 1: Visualization of oxytocin release in the brainstem upon photoactivation of ChR2-expressing fibers originating from parvocellular neurons in the paraventricular nucleus of the hypothalamus

Introduction 33

Materials and methods 34

Results 43

Conclusions from Study 1 57

Chapter 3 **58**

Study 2: Restoration of oxytocin neuron activity prevents hypertension caused by chronic intermittent hypoxia/hypercapnia

Introduction 59

Materials and methods 60

Results 67

Conclusions from Study 2 88

Chapter 4 **89**

Discussion

Study 1 Conclusions 90

Study 2 Conclusions 94

Future directions 103

Summary 103

References **105**

List of Figures

Figure 1. Simplified model of established and hypothesized descending PVN projections involved in cardiovascular regulation…… 14

Figure 2. Schematic depiction of the working of channelrhodopsin……... 24

Figure 3. Schematic depiction of the working of excitatory hM_3D_q DREADDs…… 28

Figure 4. PVN injection and brainstem slices…….. 37

Figure 5. Colocalization of ChR2-EYFP and OXT in brainstem fibers within the DMV…… 44

Figure 6. Characterization of OXT and vasopressin dose-response relationships of sniffer CHO cells…….. 47

Figure 7. Visualization of sniffer CHO cells and ChR2-expressing PVNfibers…….. 50

Figure 8. Oxytocin receptor activation…… 52

Figure 9. Effects of CIH/H on OXT receptor activation…….. 55

Figure 10. *In vitro* activation of PVN OXT neurons expressing excitatory DREADDs…… 69

Figure 11. Subpopulation-specific adenosine-associated viral vectors……... 72

Figure 12. Acute oxytocin neuron activation decreases resting blood pressure and heartrate……. 75

Figure 13. Activation of oxytocin neurons blunts the acute blood pressure responses to H/H…… 78

Figure 14. Chronic oxytocin neuron activation diminishes the development of hypertension and decreases heart rate with CIH/H……... 82

Figure 15. Activation of PVN OXT neurons during CIH/H exposure restores responses in OXT sensitive CHO cells…… 86

List of Abbreviations

AAV	adeno-associated virus
Ach	Acetylcholine
aCSF	Artificial cerebrospinal fluid
ANS	Autonomic nervous system
AVP	Arginine vasopressin
CHO	Chinese hamster ovarian
ChR2	Channelrhodpsin-2
CIH	Chronic intermittent hypoxia
CIH/H	Chronic intermittent hypoxia/hypercapnia
CNS	Central Nervous systems
CPAP	Continuous positive airway pressure
CVN	Cardiac vagal Neuron
DMV	Dorsal Motor Nucleus of the Vagus
DREADDs	Designer receptors exclusively activated by designer drugs
DVC	Dorsal Vagal Complex
EPSC	Excitatory post-synaptic current
GABA	Gamma-Aminobutyric Acid
GPCRs	G-protein coupled receptors
IML	Intermediolateral cell column of the spinal cord
IPSC	Inhibitory post-synaptic current
LH	Lateral Hypothalamus
nAChRs	Nicotinic acetylcholine receptors

NA	Nucleus Ambiguus
NMDG	*N*-methyl-D-glucamine
NTS	Nucleus of the Solitary Tract
OSA	Obstructive sleep apnea
OTA	Oxytocin antagonist
OXT	Oxytocin
PNS	Parasympathetic nervous system
PVN	Paraventricular Nucleus of the Hypothalamus
RVMM	Rostral ventromedial medulla
RVLM	Rostral ventrolateral medulla
SNA	Sympathetic nerve activity
SNS	Sympathetic nervous system

CHAPTER 1

Introduction

The autonomic nervous system and cardiovascular regulation

The autonomic nervous system (ANS) is responsible for maintaining homeostasis and regulating adaptation to challenges to the organism, and is divided into two distinct components, the sympathetic and parasympathetic systems. The cardiovascular system is regulated primarily by the ANS, but also by the endocrine system. Heart rate and blood pressure for example, are under neural control by mechanisms that include blood volume regulation by the kidney, as well as sympathetic activity that controls peripheral resistance in the arterioles and other vessels. Heart rate is controlled primarily by the levels of parasympathetic activity, and to a lesser extent, sympathetic activity. Preganglionic neurons important for the autonomic control of cardiovascular functions have their soma in autonomic motor nuclei such as the nucleus ambiguus (NA), the dorsal motor nucleus of the vagus nerve (DMV), and the intermediolateral cell column (IML). The NA and DMV nuclei are a part of the inhibitory parasympathetic branch, while the IML is a part of the excitatory sympathetic branch of the ANS that together balance neuronal input to organs in the body. Opposing actions of these autonomic branches of the ANS as well as the functioning of the target organs, achieve homeostasis and appropriate adaptation of the organism to the environment. Cardiac output for example, is regulated by both the sympathetic and parasympathetic limbs of the ANS and is determined by autonomic regulation of heart rate, myocardial contractility, and end-diastolic volume. Both parasympathetic and sympathetic activity regulate heart rate and myocardial contractility, while end-diastolic volume is determined by venous pressure,

which depends on sympathetically mediated alterations to blood volume and venous smooth muscle tone (Guyenet, 2006).

The sympathetic nervous system

Sympathetic nervous activity innervates almost all organs in the body and is traditionally associated with the fight or flight response (Loewy and Spyer 1990). During times of stress it is responsible for altering and adapting bodily functions such as heart rate and contractility, pupillary dilation, as well as vasoconstriction and vasodilation. Short preganglionic fibers originate from cells in the IML of the upper thoracic and lumbar regions of the spinal cord. These fibers exit the spinal cord through the ventral root at the same level of their somata, and synapse on many postganglionic neurons, often in the paravertebral ganglia (Guyton 1991b; Loewy and Spyer 1990). The postganglionic neurons then send long projections to innervate target tissues. The adrenal medulla however, is known to be directly innervated by preganglionic sympathetic fibers originating from the splanchnic nerve (Guyton 1991b; Loewy and Spyer 1990).

Sympathetic preganglionic neurons release acetylcholine (ACh), which binds to and activates nicotinic acetylcholine receptors (nAChRs) on the postganglionic neurons. Most postganglionic sympathetic neurons release norepinephrine as a neurotransmitter (Ganong 2005). Release of norepinephrine activates both alpha and beta adrenergic postsynaptic receptors on target organs (Ganong 2005). Alpha-adrenergic receptors, a class of G-protein coupled receptors (GPCRs), are responsible for mediating pupil dilation, vasoconstriction, bladder contractility, and insulin secretion (Boron and Boulpaep 2009). Activation of another class of GPCRs, beta-adrenergic receptors, evokes

vasodilation, increases in cardiac contractility and cardiac output, as well as stimulates insulin secretion (Large et al. 1997).

Sympathetic neurons in the stellate ganglion act as the dominant source of sympathetic input to the heart, and are activated by sympathetic preganglionic fibers originating from the IML, primarily at thoracic levels 1-4 (Jansen et al., 1995a; Jansen et al., 1995b). Transneuronal labeling studies from the stellate ganglion revealed IML input from three medullary regions: 1) the rostral ventromedial medulla (RVMM), 2) the rostral ventrolateral medulla (RVLM), and 3) the caudal raphe nuclei, with the greatest concentration of labeling located in the RVMM. Nuclei in the pons and midbrain including the A5 cell group, Kolliker-Fuse, the subcoeruleus, and the Edinger-Westphal are also possible sources of input to preganglionic sympathetic neurons. Finally, forebrain projections originating from both the paraventricular nucleus of the hypothalamus (PVN) and lateral hypothalamus (LH) are also known to project to sympathetic targets (Jansen et al., 1995b).

In addition to the structures mentioned above, the sympathetic network is also regulated by numerous types of sensory afferent information (Guyenet, 2006). Neurons in the IML for example, are directly innervated by spinal lamina I neurons, and influence an afferent visceral pathway. Additionally, input from medullary structures involving chemosensation such as the RVLM, have been reported and been shown to play an important role in the neural control of tonic and reflex cardiovascular activity (Guyenet, 2006; Dampney et al., 2003). The basal activity of presympathetic neurons that project to the spinal cord fire in rough accordance with the cardiac cycle and are thought to be a major determinant of the generation of sympathetic outflow (Yang et al., 2001). This

population of presympathetic RVLM neurons synapse directly onto preganglionic sympathetic neurons in the IML of the upper thoracic spinal cord (Guyenet, 2006). It has been shown that stimulation in vitro of Phox-2B neurons, a subpopulation of RVLM neurons, increased sympathetic nerve discharge and blood pressure (Abbot et al., 2009).

The parasympathetic nervous system

Parasympathetic activity is mainly concerned with the maintenance of bodily function at rest when an animal is under no stress. This includes conservation of oxygen, restoration of energy, facilitation of digestion, and absorption and secretion of waste (Freeman 2006; Patton and Howell 1989). This system helps to maintain a low heart rate and relatively normal blood pressure, facilitates bronchial constriction, and is generally complementary to the functions of the sympathetic system (Ganong 1979). The preganglionic parasympathetic fiber projections are extensive, as neurons originating in the medulla, pons, or midbrain nuclei synapse upon neurons in parasympathetic ganglia that are in close proximity to their target organ (Loewy and Spyer 1990). ACh is the primary neurotransmitter of both pre- and postganglionic parasympathetic neurons. When released by preganglionic neurons it subsequently binds to nAChRs on parasympathetic postganglionic neurons located near the target organ and excites these neurons, whereas ACh released from postganglionic neurons binds to muscarinic receptors on the target tissue (Ganong 1989), that often serve an inhibitory role.

The vast majority (~75%) of all parasympathetic fibers originate in the vagus (tenth) nerve. Descending nerve fibers from the vagus innervate mucous glands, the muscles of the pharynx, the esophagus, the stomach, and the gastrointestinal tract. Those

areas beyond the descending colon are controlled by sacral parasympathetic fibers. Vagal preganglionic fibers originating in the DMV regulate gastrointestinal motility and secretion, as well as endocrine and exocrine pancreatic secretion, while motor fibers extending from the NA innervate the soft palate, pharynx, esophagus, and larynx, which facilitates swallowing and vocalization (Loewy and Spyer 1990). In addition, the cell bodies of preganglionic cardiac neurons whose axons project to the cardiac ganglia and provide the dominant chronotropic influence on the heart originate within both the NA and DMV (Loewy and Spyer 1990).

Sympathetic/parasympathetic nervous system interactions

Multiple organs undergo innervation by both divisions of the autonomic nervous system. These two systems work in a complementary manner to achieve homeostasis. Pupil dilation, for example, occurs with sympathetic system activation while pupil constriction is mediated by the parasympathetic branch. Beat to beat regulation of heart rate is another example of how these two systems complement one another. Norepinephrine is released by sympathetic postganglionic neurons to accelerate the firing of cardiac pacemaker cells in the sinoatrial node and increase the activity of the heart (Guyton 1991a; Patton and Howell 1989). Conversely, parasympathetic postganglionic neurons hyperpolarize and decrease the firing rate of these pacemaker cells via ACh release and activation of muscarinic receptors in the sinoatrial node. Moreover, this release of ACh simultaneously slows the propagation of excitatory impulses through the atrioventricular fibers (Brooks et al. 1980). Sympathetic stimulation increases the

efficiency of the heart to pump, while parasympathetic innervation reduces the force of contraction.

Parasympathetic control of heart rate

Resting heart rate is primarily influenced by parasympathetic innervation of the heart. There is a tonic level of parasympathetic nerve firing in conscious and anesthetized animals such as dogs (Scher and Young, 1970), cats (Kunze, 1972), and rats (Coleman, 1980; Stornetta et al., 1987), and in humans (Katona et al., 1982; Pickering et al., 1972; Sullebarger et al., 1990), but little, if any, sympathetic activity at rest. In fact, if parasympathetic outflow is blocked by the muscarinic receptor antagonist, atropine, a significant increase in heart rate is observed. Blocking sympathetic activity however, with the beta adrenergic receptor antagonist, propranolol, causes minimal decreases in heart rate (Berne and Levy, 2001), suggesting parasympathetic activity dominates over sympathetic to influence resting heart rate (Levy and Zieske, 1969). Parasympathetic cardiac vagal nerve activity modulates the baroreflex-induced slowing of the heart in response to increases in arterial pressure. Additionally decreases in arterial pressure are coupled with baroreflex-induced tachycardia, increased sympathetic nerve activity, and decreased parasympathetic activity (Scher and Young, 1970; Spyer, 1981; Stornetta et al., 1987).

Cardiovascular diseases such as ventricular arrhythmias along with an increased risk for sudden cardiac death are associated with altered parasympathetic outflow (Hull et al., 1995). Cardiac vagal activity is also diminished in cardiovascular diseases including hypertension, congestive heart failure, diabetes, and coronary artery disease (Evrengul et

al., 2006; Ferguson et al., 1990; Mendelowitz, 1999; Motte et al., 2005). This blunting of parasympathetic activity is an independent predictor of mortality associated with chronic heart failure patients (Nishime et al., 2000). It has been suggested in patients who succumb to ischemia-induced arrhythmias as well as myocardial infarctions, that restoration of parasympathetic outflow may increase the likelihood of recovery (Townend and Littler, 1995; Vanoli et al., 1991). Additionally, in an animal model of myocardial ischemia, activation of parasympathetic neurons in the DMV reduced infarct size (Mastitskaya et al., 2012). These studies suggest that increasing and restoring parasympathetic function and/or cardiac vagal outflow, could potentially alleviate certain forms of cardiovascular disease.

Neurophysiology of cardiac vagal neurons

Brainstem premotor cardioinhibitory vagal neurons (CVNs) are responsible for mediating parasympathetic cardiac function and provide the major negative chronotropic influence on the heart. These neurons are principally located in the ventrolateral medulla in the NA and in the dorsal vagal complex (DVC) in the DMV (Loewy and Spyer 1990; Mendelowitz and Kunze 1991). Axons from CVNs travel within the vagus nerve and synapse upon postganglionic parasympathetic neurons in cardiac ganglia in the pericardial sac at the base of the heart (Mendelowitz, 1996; Stuesse, 1982; Wang et al. 2001b). These fibers subsequently innervate both the sinoatrial and atrioventricular nodes (Pardini et al. 1987; Rardon and Bailey 1983). Activation of CVNs regulates the beat-to-beat rhythm of the heart (Warner et al. 1986), and it has been proposed that

altering the firing properties of a single cardiac vagal neuron is sufficient to significantly change heart rate (Jordan et al. 1982; McAllen and Spyer 1978). Stimulation of the vagus nerve decreases heart rate and injection of the excitatory neurotransmitter glutamate into the NA has been shown to evoke a strong bradycardia (Machado and Brody 1988; Mills 1978).

In vivo studies have shown that CVNs are intrinsically silent and do not possess pacemaker-like activity. Upon injection of a small amount of depolarizing current however, CVNs fire with little delay and minimal spike frequency adaptation (Mendelowitz 1996; Rardon and Bailey 1983). These firing properties allow CVNs to follow synaptic activation for extended periods of time while adjusting to long-lasting modulatory inputs (Mendelowitz 1996).

While it is generally assumed that CVNs in the NA provide a greater contribution to the negative chronotropic parasympathetic activation of the heart than CVNs in the DMV (Loewy and Spyer, 1990), there is evidence that CVNs in the DMV also may play a cardioprotective role (Mastitskaya et al., 2012). The two following sections will highlight a number of important neurotransmitters involved in the synaptic pathways to CVNs in both the NA and DMV.

Cardiac vagal neurons in the nucleus ambiguus

Due to their normally silent nature, CVNs require synaptic input to fire action potentials. Several synaptically released neurotransmitters have been identified as important for excitatory or inhibitory activity in CVNs in the NA including glutamate, ATP, serotonin, ACh, glycine, and gamma-aminobutyric acid (GABA) (Jameson et al.,

2008a; Jameson et al., 2008b; Kamendi et al. 2008; Mendelowitz 1998; Neff et al. 1995; Neff et al. 1998a; Neff et al. 1998b; Wang et al. 2003). GABAergic neurotransmission is thought to be one of the most important endogenously active inhibitory inputs to CVNs (Wang et al. 2001a). Synaptic release of GABA can activate gabazine-sensitive $GABA_A$ receptors that mediate phasic currents, as well as picrotoxin-sensitive, gabazine-insensitive extrasynaptic receptors that facilitate tonic currents (Bouairi et al. 2006). Systematic mapping of GABA inputs to CVNs has revealed several brainstem areas with GABAergic neurons that have direct projections to CVNs including the nucleus of the solitary tract (NTS), RVLM, and lateral paragigantocellular nucleus (Dergacheva et al., 2010; Frank et al., 2009; Wang et al., 2001a).

Vasopressin (AVP) has been show to enhance the inhibitory GABAergic input to CVNs in the NA (Wang et al., 2002). There are only two major sources of AVP in the central nervous system (CNS), the PVN and the supraoptic nucleus (SON), suggesting the firing of CVNs can be modulated by descending hypothalamic projections from the PVN or SON that release AVP. Orexin, an additional hypothalamic neuropeptide, has been shown to increase inhibitory, and decrease excitatory synaptic pathways to CVNs (Dergacheva et al., 2005). Orexin not only activates GABAergic neurons in the brainstem with projections to CVNs, but likely facilitates GABAergic inputs to CVNs via its actions on presynaptic GABAergic terminals (Dergacheva et al., 2012).

The NTS, located in the DVC, receives a substantial fraction of the afferents from the cardiovascular system including sensory afferent input from arterial baroreceptors and chemoreceptors, and cardiac baroreceptors. A potential framework for the baroreceptor reflex pathway was proposed based upon work that has shown electrical stimulation of

the NTS results in glutamatergic mediated post-synaptic currents in CVNs (Neff et al., 1998b). Additionally, stimulation of trigeminal sensory afferents increases glutamatergic neurotransmission to CVNs providing a basis for the bradycardia that occurs upon activation of the diving reflex (Gorini et al., 2009).

Cardiac vagal neurons in the dorsal motor nucleus of the vagus

Neurotransmitters including GABA, glutamate, ACh, and endogenous opioids have been reported to produce inhibitory or excitatory currents in CVNs located in the DMV (Aicher et al., 2002; Evans et al., 2003; Neff et al., 1995; Wang et al., 2001b), with GABAergic inhibitory post synaptic currents (IPSCs) having higher frequencies in the DMV than in the NA (Wang et al., 2001b). CVNs in the DMV, like those in the NA, receive GABA(A), NMDA, and AMPA mediated currents from NTS neurons (Evans et al., 2003; Wang et al., 2001b), with stimulation of the vagus nerve resulting in GABAergic and glutamatergic currents (Evans et al., 2003).

More recent work has shown that the endogenous release of oxytocin (OXT), but not AVP, from PVN terminals in the DMV facilitates glutamatergic neurotransmission onto CVNs, postulating a role for OXT in the DVC to enhance parasympathetic regulation of heart rate (Pinol et al., 2012). The cardioprotective actions OXT may possess however, have not yet been thoroughly investigated.

Paraventricular nucleus of the hypothalamus

The PVN, a hypothalamic structure, serves as a major integrative site for autonomic and neuroendocrine homeostasis (Ferguson et al., 2008; Swanson and Sawchenko, 1983), as it receives robust afferent sensory input from cranial and spinal sensory nerves from multiple sites throughout the body (Rinaman, 2007). Nearly all areas of the CNS involved in cardiorespiratory function receive connections from the PVN (Kc et al., 2002, 2010; Luiten et al., 1985; Mack et al., 2002, 2007; Swansom and Kuypers, 1980; Swanson et al., 1981; Yeh et al., 1997), and via bidirectional interactions involving inhibitory and excitatory actions, the PVN contributes to maintenance of homeostasis (Kc and Dick, 2010).

The PVN borders the third ventricle, is composed of magno- (anterior, medial, and posterior regions) and parvocellular (periventricular, anterior, medial, dorsal, and lateral regions) regions, and the central and sensory inputs of the PVN determines its role in autonomic function. The magnocellular region contains mainly OXT and AVP cells with synaptic endings that terminate in the posterior pituitary and release OXT and AVP into the bloodstream. The parvocellular division however, expresses a vast number of neurotransmitters and neurohormones including OXT, AVP, dopamine, and corticotropin- and thyrotropin-releasing hormones. This area projects to many areas in the CNS and regulates many systems, including autonomic function (Kc and Dick, 2010).

A role for PVN projections to pre-sympathetic brainstem neurons has been well established, and PVN neurons have been found to have direct influence on sympathetic nerve activity (SNA) via parvocellular projections to the IML and RVLM (See Figure 1).

This influence on SNA is modulated directly via a pathway from the PVN to IML, indirectly via a PVN-RVLM connection, and both directly and indirectly via collaterals to the IML and RVLM (Badoer 2001; Card et al., 2006; Coote et al., 1998; Cruz et al., 2008). It has been proposed that projections from PVN neurons release the neurotransmitters AVP and glutamate to excite neurons in the RVLM (Yang et al., 2001). Additionally, axons projecting from these PVN neurons to the RVLM fire in association with the heartbeat interval (Chen and Toney, 2009). Furthermore, microinjections of AVP and OXT agonists into the RVLM cause increases in heart rate suggesting PVN neurons may modulate heart rate via projections to the RVLM (Kc et al., 2002; Mack et al., 2007).

There has been much less investigation regarding how the descending projections from parvocellular PVN neurons influence parasympathetic activity. Projections from the PVN however, have been shown to innervate the central gray matter, nucleus of the locus coeruleus, and parabrachial nucleus (Zheng et al., 1995), with dense axonal projections originating in the PVN observed in the regions of the brainstem where parasympathetic cardiac control originates, mainly the NA and the DMV (Geerling et al., 2010; Goncharuk et al., 2011; Saper et al., 1976; Ter Horst et al., 1984). After injection of the trans-synaptic pseudorabies virus in the heart, with spinal cord transection to prevent sympathetic pathway labeling, a robust population of neurons in the PVN was observed (Irnaten et al., 2001).

Figure 1 Simplified model of established and hypothesized descending PVN projections involved in cardiovascular regulation

Heart rate and contractility are regulated by both the sympathetic and parasympathetic branches of the autonomic nervous system, originating in the IML and in the DMV and NA, respectively. Early neuroanatomical studies established dense PVN innervation of DMV, NA, RVLM, and IML. The IML receives both direct, from the PVN, and indirect, relayed through the RVLM, innervation. PVN, paraventricular nucleus of the hypothalamus; DMV, dorsal motor nucleus of the vagus; NA, nucleus ambiguus; RVLM, rostral ventral lateral medulla; IML, intermediolateral column.

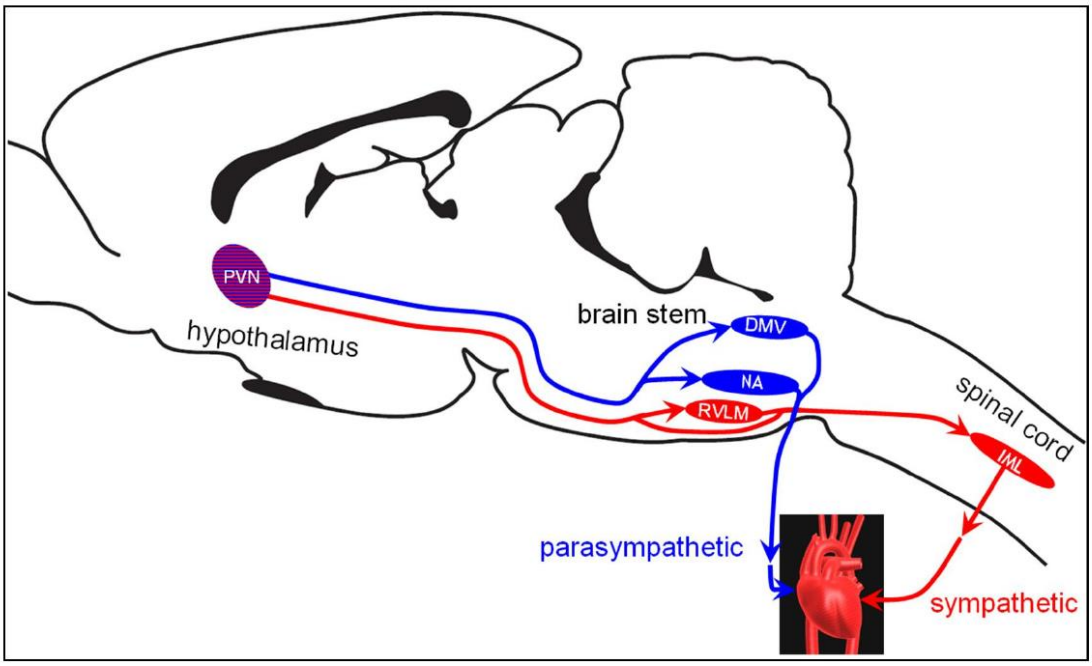
PVN
hypothalamus
brain stem
DMV
NA
RVLM
spinal cord
IML
parasympathetic
sympathetic

As mentioned earlier, pre-autonomic neurons in the PVN synthesize and release various neurotransmitters and neuropeptides including AVP and OXT. Both AVP fibers and the release of AVP has been observed in the DVC (Goncharuk et al., 2011), with AVP application to DMV neurons *in vitro* resulting in increases in heart rate (Mo et al., 1992). GABAergic neurotransmission to CVNs in the NA has been shown to be increased with AVP application, without any observed excitatory effect in CVNs (Wang et al., 2002). Conversely, studies have examined the projections from the PVN to CVNs in the DMV using the paired-pulse response paradigm to assess short-term plasticity of the PVN to CVN synapse. These studies showed AVP had no role in modulating the paired-pulse facilitation in this pathway, and additionally, the activation of PVN axons in the DMV did not alter GABAergic neurotransmission to CVNs. This absence of a modulatory effect of AVP on GABA IPSCs in CVNs in the DMV, may explain the contrasting findings observed in the NA (Pinol et al., 2012).

The most abundant neuropeptide found in descending PVN projections to the DVC is OXT (Sawchenko and Swanson, 1982). OXT fibers have been observed in the DMV (Voorn and Buijs, 1983; White et al., 1984; Dreifuss et al., 1992; Llewellyn-Smith et al., 2012; Rinaman, 1998) and the release of OXT has been shown in the DVC (Buijs and Van Heerikhuize, 1982; Landgraf et al., 1990). Furthermore, the membrane excitability of DMV neurons is altered with OXT application likely through activation of OXT receptors on DMV cells (Raggenbass and Dreifuss, 1992). OXT additionally, has also been reported to exert effects on cardiovascular regulation in the DVC; OXT projections from PVN to the DVC have been shown to improve reflex bradycardia and reduce exercise-induced tachycardia (Braga et al., 2000; Higa et al., 2002). OXT also

facilitates vagal afferent transmission to a subset of NTS neurons (Peters et al., 2008). Moreover, microinjection of OXT antagonist in the DVC suppressed PVN stimulation-induced bradycardia (Rogers and Hermann, 1986). These studies demonstrate that OXT influences vagal afferents and cardiac reflexes in NTS. Yet, until recently, it was unclear if there is a mechanism by which OXT modulates parasympathetic cardiac vagal neurons directly. Previous studies in our laboratory showed that OXT released in the DMV from synaptic terminals from PVN neurons facilitates glutamatergic neurotransmission to CVNs (Pinol et al., 2012). This work indicates a potential parasympathetic cardiac role of the PVN and the endogenous release of OXT from PVN synaptic terminals within the brainstem (Pinol et al., 2012). The role of the release of OXT from the PVN in cardiovascular diseases remains to be determined.

Role of PVN in controlling heart rate and generating/maintaining hypertension

In addition to its role in controlling autonomic function under normal conditions, the PVN is also important in regulating sympathetic and cardiovascular activity in response to hypoxic stress (Gan et al., 2012; Coleman et al., 2010). The PVN is an essential brain region targeted by chronic intermittent hypoxia (CIH), concomitant with the highly prevalent cardiovascular disease obstructive sleep apnea (OSA, see next section) (Coleman et al., 2010; Huang et al., 2007; Kc et al., 2010). Activity in neurons within the PVN that are critical for the cardiovascular responses to challenges such as stress and dehydration possess augmented activity with CIH. These neurons are involved

in the maintenance and/or generation of CIH induced hypertension (da Silva et al., 2011; Kc et al., 2010; Kc and Dick, 2010; Knight et al., 2011). Using FosB/ΔFosB as a marker of neuronal activation, CIH increased the activity of cells in the dorsal and medial parvocellular subdivisions through all rostral-caudal levels in the PVN, as well as the lateral parvocellular sub-region in the caudal PVN (Knight et al., 2011). After CIH, nitric oxide and NMDA signaling is reduced in nNOS neurons in the PVN, accompanied by an increase in blood pressure (Coleman, 2010). Additionally, the alterations in blood pressure, heart rate, and respiration that occurs with CIH have been postulated to involve pathways from the PVN to the RVLM, NTS, locus coeruleus, and spinal sympathetic preganglionic neurons (Kc et al., 2010; Pajolla, 2009; Sharpe, 2013). Similarly, PVN pathways to neurons in the NA and DVC, brainstem regions where parasympathetic cardiac control originates, are hypothesized to modulate brainstem autonomic function (Kc and Dick, 2010). Taken together, these data indicate that the activity of PVN neurons is altered with models of OSA, and leads to the generation of OSA induced hypertension.

Changes in autonomic function in obstructive sleep apnea patients and in models of obstructive sleep apnea following chronic intermittent hypoxia/hypercapnia

Patients with OSA experience repetitive complete or partial collapses of the upper airway during sleep, which causes an apnea and results in intermittent hypoxia and hypercapnia. These cycles of hypoxia and CO_2 retention alter the activity in both cardiac

parasympathetic (PNS) and sympathetic nervous system (SNS) activity leading to disruptions in heart rate (Azagra-Calero et al., 2012; Cutler et al., 2002; Loke et al., 2012; Pachikara and Mehra, 2011; Leung, 2009; Kufoy et al., 2012; Bradley and Floras, 2009). Upon termination of apneas, asphyxia causes a brief arousal from sleep, sympathetic activity increases, vagal tone decreases, and these autonomic changes lead to surges in blood pressure and heart rate (Loke et al., 2012; Leung, 2009; Bradley and Floras, 2009). These acute effects are thought to be the substrate for chronic long term changes in cardiovascular dysfunction that results in an increased risk of hypertension, daytime tachycardia, arrhythmias, myocardial ischemia, stroke, and cardiovascular mortality (Bradley and Floras, 2009).

Currently, continuous positive airway pressure (CPAP) therapy is the most common and successful treatment for OSA, however this treatment is only modestly effective, with mean blood pressure reductions of ~2 mmHg. Although CPAP improves the survival and quality of life, it is not well tolerated by all patients with OSA and its use is often discontinued. Thus, other avenues of treatment are crucial to mitigate the adverse cardiovascular effects caused by OSA.

Exposure to CIH during the sleeping period of animals mimics the repetitive episodes of hypoxia that occur in humans with OSA. Similar to what is observed in patients with OSA, data from animal models provide strong evidence that animals exposed to CIH experience decreased baroreflex sensitivity, increased blood pressure and sympathetic activity, and diminished parasympathetic activity to the heart (Carlson et al., 1996; Bonsignore et al., 2006, 2002; Lai et al., 2006; Narkiewicz and Somers, 2003; Parish and Somers, 2004; Balachandran et al., 2012). While CIH decreases baroreflex

control of heart rate, it also enhances baroreceptor afferent function as well as the heart rate responses upon stimulation of the vagus nerve suggesting that impairment with CIH occurs not in the sensory or efferent premotor fibers, but instead within the brainstem (Yan et al., 2009).

Oxytocin in cardiovascular function

In addition to the classic peripheral effects of OXT on uterine contraction and milk ejection in females, the role of centrally released OXT has been shown to have a diverse range of CNS functions in both males and females. The effects of OXT on the behavioral responses to anxiety and stress have been extensively studied in both humans and non-humans. OXT has been shown to have strong anti-stress responses that promote bonding, trust, cooperation, and relaxation (McCall and Singer, 2012). More recently however, the role of centrally released OXT in regulating autonomic responses to stress as well as its role as a cardiovascular hormone, has garnered more attention (Higa et al., 2002; Michelini et al; 2003; Ring et al., 2006). In non-human mammalian species, for example, OXT release causes acute and long-term decreases in heart rate and blood pressure via peripheral and central actions in the brainstem, heart, and vessels (Grewen and Light, 2011). Conversely, blocking central OXT release has been shown to increase heart rate and blood pressure responses in rats after acute stress (Grewen and Light, 2011). Recent work has indicated OXT could be especially beneficial to modulate sympathetic and parasympathetic activity balance in response to stress (Higa et al., 2002; Gamer and Buchel, 2012). OXT for example, alters baroreceptor reflex control of heart

rate by increasing vagal outflow to slow heart rate, while blocking OXT release prevents reflex bradycardia during baroreceptor activation (Higa et al., 2002).

The anti-stress and anxiolytic properties of OXT imply that it modulates sympathetic and parasympathetic tone. In response to stress, OXT alters baroreceptor reflex control of heart rate by increasing vagal outflow to slow heart rate. Conversely, blocking OXT release prevents reflex bradycardia during the loading of baroreceptors (Higa, 2002). While the mechanisms responsible for OXT modulating heart rate remain to be determined, there are several nuclei that receive projections thought to be involved in the beneficial slowing of the heart under stressful situations. These nuclei include the NT, DMV, the RVLM, and the NA, all of which are involved in autonomic regulation (Stauss, 2003).

In the human population, higher OXT plasma levels have been linked to lower blood pressure and have been shown to regulate stress-induced tachycardia (Grewen and Light, 2011), while intranasal administered OXT has positive effects on anxiety and stress responses and specifically increases parasympathetic and decreases sympathetic cardiac control (Norman et al., 2011). Particularly relevant to the hypotheses put forth in this proposal, a recent study showed that intranasal administered OXT was sufficient to prevent the increased stress and anxiety in response to inhalation of 7.5% CO_2 in healthy volunteers (de Oliveira et al., 2012).

Optogenetics

In order to identify and assess the targets and responses of long-range synaptic pathways within the CNS, electrical stimulation of neurons and fibers *in* vivo has been utilized for many years. While many studies have used this approach, it possesses several insurmountable inherent obstacles such as limited control over the spread and spatial resolution of stimulation, confounding stimulation of a heterogeneous population of neurons or axons within the stimulated regions, unpredictable effectiveness of stimulation that depends on different thresholds for fibers and neurons within the region, and the potential for tissue damage. The inability to apply pharmacological agents *in vivo* in highly localized areas surrounding the target neuron receiving long-range projections is also hindered by this approach (Cruikshank et al., 2010).

Approaches developed over the last 20 years using *in vivo* electrophysiology have overcome some of these limitations permitting tight control over the external and internal milieu surrounding cells, and allowing more precise stimulation and electrophysiological recordings from neurons. The examination of pathways *in vitro* however, are limited by these approaches and therefore many important long-range projections to neurons cannot be studied.

Approaches using optogenetic techniques overcomes many of these obstacles. Optogenetics affords highly selective stimulation of homogenous neuronal populations as well as activation of synapses originating from neurons distant from the neuron of interest, while retaining the high degree of control and precision afforded *in vitro* (Fenno et al., 2011). This approach utilizes heterologous expression of the microbial opsin

channelrhodopsin-2 (ChR2), a light-activated cation channel that is ubiquitously inserted into the plasma membrane of cells (Nagel et al., 2003). Membrane depolarization of cell bodies, dendrites, and axons of neurons that express ChR2 is achieved with brief (millisecond scale) blue light pulses, and allows for excitation of specific compartments of the plasma membrane including presynaptic terminals distant from the soma (See Figure 2) (Petreanu et al., 2007).

Many studies have used optogenetics to examine the neurophysiology of distant synapses by driving ChR2 expression using different viral vectors (Cruikshank et al., 2010; Varga et al., 2009), as well as transgenic mice (Ren et al., 2011). Other studies have utilized viral vectors to drive ChR2 expression in the plasma membrane of distal synaptic terminals (Pinol et al., 2012).

Figure 2 Schematic depiction of the working of channelrhodopsin

Blue light (473nm) illumination opens the channelrhodopsin cation channel, thereby increasing the conductance for small positively charged ions. Increases in positively charged particles in the cell then depolarizes the cellular membrane and when the membrane potential becomes sufficiently depolarized (e.g. from -65 to -40 mV), a neuron can fire an action potential. If the action potential is generated in or near the presynaptic terminal, it can lead to neurotransmitter release.

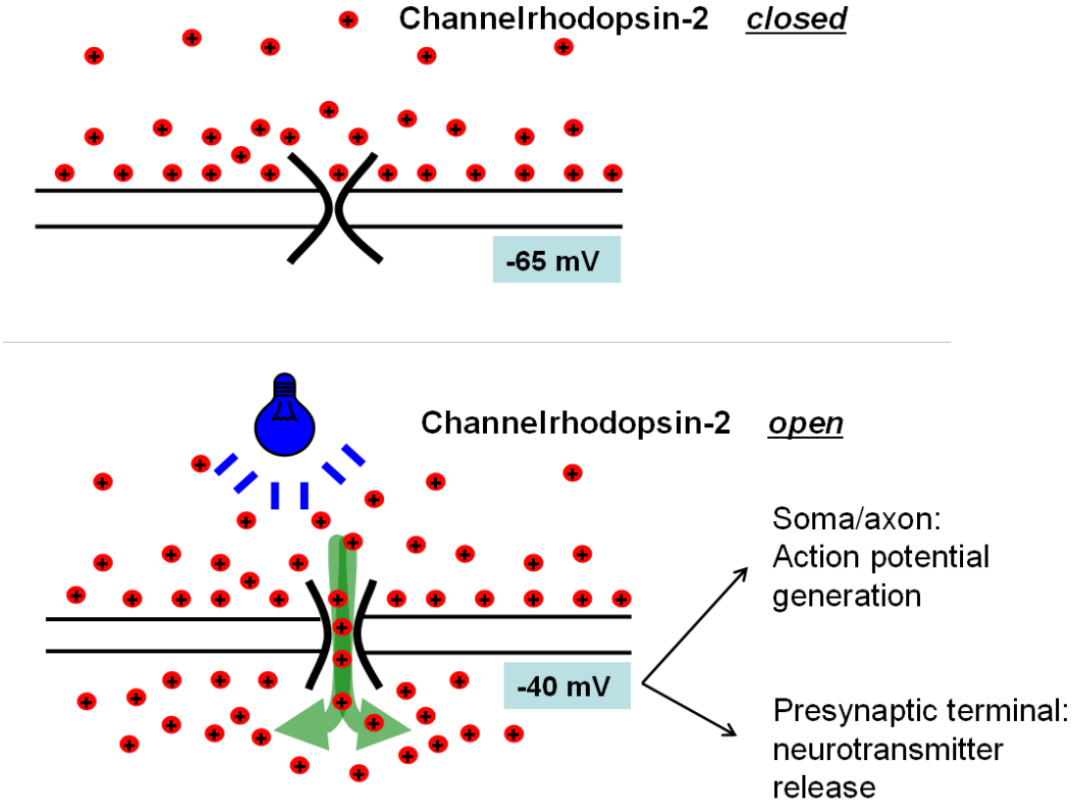
Channelrhodopsin-2 closed
-65 mV
Channelrhodopsin-2 open
-40 mV
Soma/axon:
Action potential
generation
Presynaptic terminal:
neurotransmitter
release

Chemogenetics

While the development of optical approaches to visualize and manipulate neuronal activity has proved to be an invaluable tool to decipher neuronal networks and brain functions, there are limitations to these approaches which include a degree of invasiveness when used *in vivo*, populations of neurons in the brain that are inaccessible to light, and a need for a high level of technological expertise. In order to overcome the limitations of optogenetics, Roth and colleagues developed **d**esigner **r**eceptors **e**xclusively **a**ctivated by **d**esigner **d**rugs (DREADDs) to noninvasively control neuronal signaling and activity in mammalian brains, and examine how specific populations of neurons and local circuits contribute to health and disease (Alexander et al., 2009; Sternson and Roth, 2014).

Derived from human muscarinic receptors (Armbruster et al., 2007; Conklin et al., 2008; Pei et al., 2008), DREADDs allow for precise spatiotemporal control of GPCR signaling *in vivo* (Sternson and Roth, 2014). These designer GPCRs contain two-point mutations of highly conserved amino acids resulting in a high insensitivity to ACh (the endogenous agonist) and a high potency and efficacy to clozapine-N-oxide (CNO) that is otherwise biologically inert and crosses the blood-brain-barrier **(**Sternson and Roth, 2014**;** Armbruster et al., 2007; Nawaratne et al., 2008). The excitatory G_q (hM_3D_q) DREADDs are used to activate neurons as CNO activation causes neuronal depolarization and burst firing (Alexander et al., 2009; Atasoy et al., 2012). Designer receptors G_i (hM_4D_i) conversely are used to inhibit neurons with CNO inducing neuronal hyperpolarization and silencing (5D: Armbruster et al., 2007; Atasoy et al., 2012).

DREADDs are packaged into viral vectors (See Figure 3), or expressed in transgenic mice, to increase or decrease the activity of specific populations of neurons *in vivo* by expression of the excitatory or inhibitory hM_3D_q and hM_4D_i DREADDs, respectively (Ferguson and Neumaier, 2012). Advantages of utilizing DREADDs over other approaches such as optogenetics include noninvasive control of neuronal signaling (Sternson and Roth, 2014), ability to examine widely dispersed neurons (Garner et al., 2012), neurons out of range for optogenetic studies can be examined (Vrontou et al., 2013), and use for long-term studies (Farrell et al., 2013) as the effects after a single injection of CNO last hours (Alexander et al., 2009).

The selective expression and activation of DREADDs has been used to increase or decrease the activity of specific populations of neurons *in-vivo* by expression of the excitatory or inhibitory hM_3D_q and hM_4D_i DREADDs, respectively, in neurons essential for memory formation, appetite and feeding, sleep/wake states, and other behaviors (Alexander et al., 2009; Armbruster et al., 2007; Sasaki et al., 2011; Krashes et al., 2011; Nawaratne et al., 2008; Rogan and Roth, 2011; Ferguson et al., 2011; Dong et al., 2010; Ferguson and Neumaier, 2012). Use of this technology will greatly increase our understanding of neuronal control and signaling in both healthy and disease states.

Figure 3 Schematic depiction of the working of excitatory hM_3D_q DREADDs

In the Cre-dependent system, two adeno-associated viruses are injected into a specific brain region: the first a double-floxed inverted AAV, and the second a cell-type specific Cre- expressing AAV. After cell-type specific Cre-induced recombination, the DREADDs are flipped into the correct orientation, and with CNO injection G-protein signaling is expressed in defined cell populations (Adapted from Zhu and Roth, 2014).

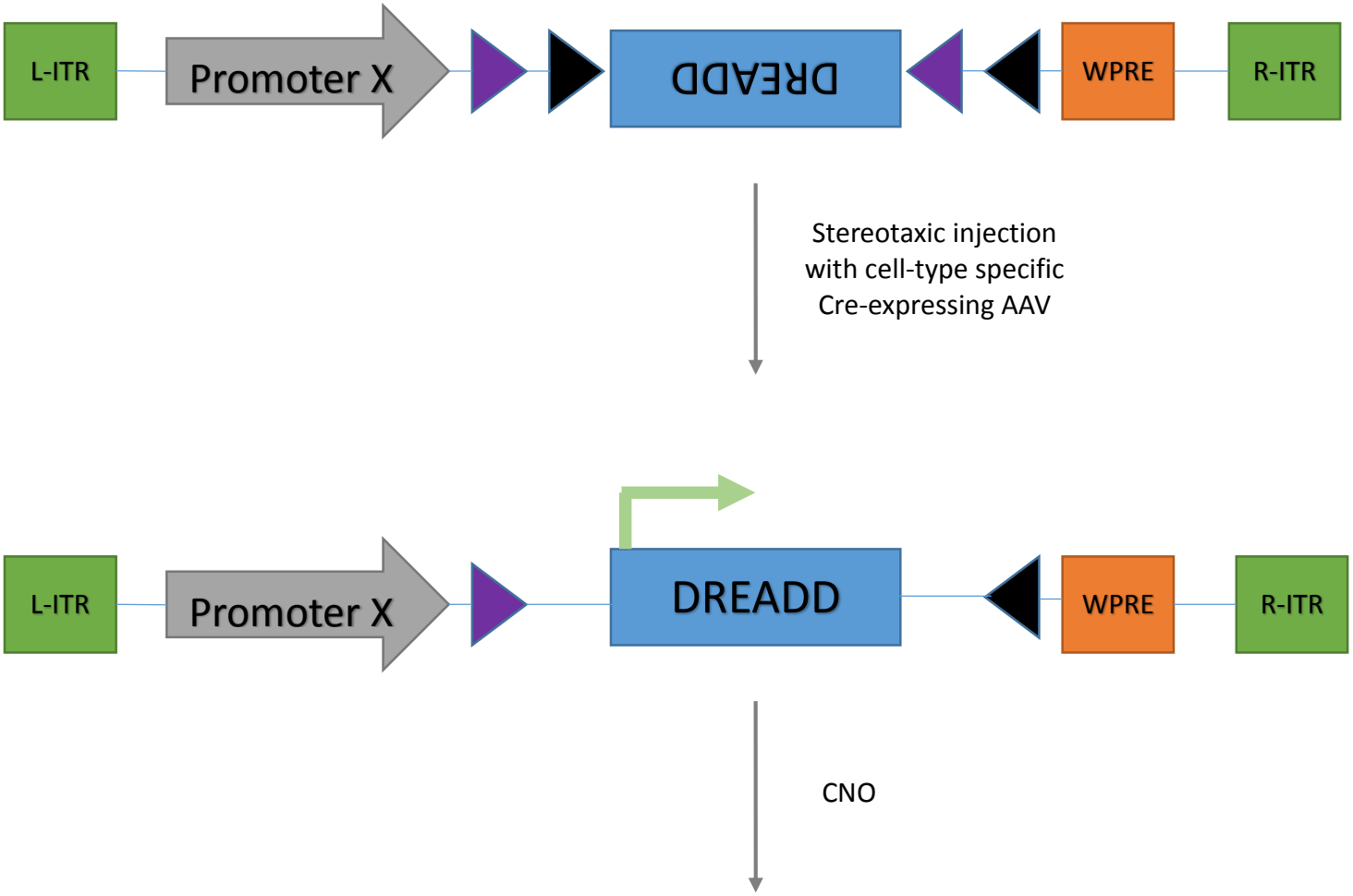
L-ITR
Promoter X
DREADD
WPRE
R-ITR
Stereotaxic injection
with cell-type specific
Cre-expressing AAV
L-ITR
Promoter X
DREADD
WPRE
R-ITR
CNO
Activation of G-protein signaling in specific cell populations

Summary and specific aims

As stated previously, recent work has revealed photoactivation of ChR2 containing PVN fibers elicited paired-pulse facilitation of glutamatergic neurotransmission to CVNs and this enhancement was diminished after application of the OXT receptor antagonist, OTA, suggesting this excitatory pathway is facilitated by endogenous OXT release from these synaptic terminals. Additionally, work from our lab showed that the paired-pulse facilitation of the excitatory post-synaptic currents (EPSCs) that occur in unexposed rats is significantly blunted in animals exposed to chronic intermittent hypoxia/hypercapnia (CIH/H) (Dergacheva et al., 2014). In Chapter 2, I test the hypothesis that PVN fibers in brainstem slices directly release OXT onto CVNs, and the release of OXT from PVN fibers onto CVNs is diminished with CIH/H. To investigate the release of OXT onto CVNs from PVN fibers we engineered and dispersed within the brainstem sniffer Chinese Hamster Ovarian (CHO) cells highly sensitive to oxytocin. These sniffer CHO cells were stably transfected to express the human recombinant OXT receptor, and calcium changes within these cells could be visualized as these cells also express the red fluorescent calcium indicator, R-GECO1. We dispersed these sniffer CHO cells onto brainstem tissue containing ChR2-expressing PVN fibers and CVNs, and assessed the intracellular calcium changes upon photostimulation of ChR2-containing fibers.

In Chapter 3, I describe the other aim of this study which tested the hypothesis that selective activation of PVN OXT neurons would decrease resting heart rate and blood pressure in conscious telemetry instrumented animals, blunt the acute responses to hypoxia/hypercapnia (H/H), and diminishe the development of hypertension with CIH/H.

In order examine if restoration of OXT neuron activity would prevent the adverse cardiovascular effects of CIH/H in vivo, we selectively activated PVN OXT neurons utilizing viral expression of excitatory hM_3D_q DREADDs within the PVN OXT neurons in animals implanted with telemetry devices to monitor blood pressure and heart rate.

CHAPTER 2

Study 1: Visualization of oxytocin release in the brainstem upon photoactivation of ChR2-expressing fibers originating from parvocellular neurons in the paraventricular nucleus of the hypothalamus

Introduction

The PVN plays an important role in controlling cardiovascular function both via release of hormones from the pituitary and additionally via its descending pathways to the brainstem and spinal cord. Neuroanatomical studies suggest that PVN neurons project to CVNs that are essential in parasympathetic control of the heart in the NA and DMV, but little is known how these projections influence parasympathetic activity.

OXT, a neuropeptide released from the PVN, is most commonly known due to the classic effects of the hormone on uterine contraction and milk ejection. Recent work however, has suggested OXT can act as a neuromodulator upon synaptic release from parvocellular neurons originating in the PVN. Targets of PVN neurons include the parasympathetic neurons in the brainstem that generate parasympathetic activity to the heart. Recent studies using optogenetic stimulation of the PVN neurons that express ChR2 revealed a direct pathway from these PVN neurons to brainstem parasympathetic CVNs. Photoactivation of ChR2 containing PVN fibers elicited paired-pulse facilitation of glutamatergic neurotransmission to CVNs and this enhancement was diminished after application of the OXT receptor antagonist, OTA, suggesting this excitatory pathway is facilitated by endogenous OXT release from these synaptic terminals (Pinol et al., 2014). Additional data from our lab that showed the paired-pulse facilitation of the EPSCs that occurs in unexposed rats is significantly blunted in animals exposed to CIH/H (Dergacheva et al., 2014). However, it remains to be determined if this blunted response is due to decreased OXT release. In this chapter, I test this hypothesis by elucidating the conditions required for OXT release from PVN fibers, and examine if the release of OXT from PVN neurons onto CVNs is diminished with CIH/H, an animal model of OSA. To

conduct these experiments, we engineered and dispersed within the brainstem sniffer CHO cells highly sensitive to oxytocin. These sniffer CHO cells were stably transfected to express the human recombinant OXT receptor, and calcium changes within these cells could be visualized as these cells also express the red fluorescent calcium indicator, R-GECO1.

Material and methods

Lentiviral vector plasmids

Lentiviral plasmids pLenti-Syn-hChR2(H134R)-EYFP-WPRE, packaging plasmid pCMV-_R8.74, and envelope plasmid pMD2.G were all kindly provided by K. Deisseroth (Stanford University, Stanford, CA).

Viral vectors

The pLenti-Syn-hChR2(H134R)-EYFP-WPRE plasmid was transformed into MAX Efficiency Stbl3 Competent Cells for amplification (Invitrogen/Life Technologies, Grand Island, NY). Plasmids pMD2.G and pCMV- R8.74 were transformed into DH5 cells for amplification and all plasmids were purified using a Maxiprep kit (Qiagen, Valencia, CA). VSVg pseudotyped lentivirus particles were produced according to standard protocols (Pinol et al., 2012; Szulc et al., 2006). Briefly, we transfected 8-24 1500 mm plates of 60-80% confluent HEK 293T cells with 37.5 μg pLenti, 33 μg pCMV-_R8.74 and 18 μg pMD2.G using 2.5 M $CaCl_2$ and 2x HBSS for transfection. Cells were cultured in Dulbecco's modified Eagle's medium (DMEM), 10% FBS (Gibco, Invitrogen), 1% L-glutamine (Invitrogen) and 1% Pen/Strep (Invitrogen). Eight hours

after the transfection, plates were washed with incubation medium and replaced with 13 ml medium. Twenty-four hours after transfection, sodium butyrate was added to the plates in a final concentration of 5 mM. The virus was harvested 48 hr after the transfection and the supernatant was spun for 15 min at 1500 x g and filtered through a 0.22 μm PES bottle top filter. The supernatant then was concentrated by ultracentrifuging for 2 hr at 20,000 rpm using 38.5 ml thinwall tubes and a Beckmann SW-28 rotor. Viral particles were then resuspended in 1- 2 ml PBS and pooled into one 10 ml thick wall tube for a second 2 hr spin at 20,000 rpm in an ultracentrifuge. The final viral vector pellet was resuspended in 35 – 100 μl of PBS and stored in 4 μl aliquots at – 80° C. The viral titer was determined by counting infected HEK 293T cells using FACS (Ramezani and Hawley, 2002). All batches of virus had a titer between 2 x 10^8 and 1 x 10^9 transducing units (TU) per ml.

Oxytocin receptor-expressing CHO cells

CHO cells were transfected with pcDNA3.1+ containing human OXT receptor cloned in at EcoRI (5′) and XhoI (3′) (plasmid obtained from Missouri S&T cDNA Resource Center) using lipofectamine, and stable over-expression was achieved by genetcin (500 μg/ml) selection. OXT receptor-expressing CHO cells were then plated and transiently transfected to also express the red fluorescent genetically encoded calcium indicator (R-GECO1; plasmid kindly donated by Robert Campbell, University of Alberta, Canada; Addgene plasmid 32444) (Zhao Y et al., 2001) with Fugene 6.

Stereotactic injections

Neonatal Sprague Dawley rats (postnatal day 4 or 5) were anesthetized by hypothermia and mounted in a stereotactic apparatus with a neonatal adapter (Stoelting, Wood Dale, IL). A midline incision exposed the skull and a small burr hole was made to position a pulled calibrated pipette (VWR, Radnor PA) with a thin tip (inner diameter <30 μm) containing viral vector at the following coordinates: 1.5 – 1.95 mm posterior (depending on the distance between bregma and lambda) and 0.3 mm lateral relative to bregma. The pipette tip was lowered 5.15 – 5.25 mm from the dorsal surface of the brain and 90-100 nl of viral vector was injected at a visually monitored rate of 60 nl per min. The pipette was left in place for 10 min, prior to slow retraction. The incision was closed using surgical glue, antibiotic ointment was applied to closed incisions and animals were warmed up on a heating pad before being returned to their nest. The stereotactic PVN coordinates of postnatal day five rat pups were based on those used in (Valenstein et al., 1969) and verified after each experiment for accuracy of the injection sites (see Figure 4).

Air or chronic intermittent hypoxia/hypercapnia exposure

Juvenile rats (3-4 weeks old) that previously underwent stereotaxic injections were transferred to commercial atmosphere controlled chambers in their cages. Using a commercial chamber with computer controlled atmospheric gas control (Biospherix, Ltd), rats were kept in cages with normal bedding and unrestricted food and water during CIH/H. Bioactive gas sensors in the chambers monitored oxygen and CO_2 concentrations and exchanged these gases within the chamber until the defined set points were reached. CIH/H exposure was be performed by

Figure 4 PVN injection and brainstem slices

1) A lentiviral vector expressing ChR2-EYFP was injected into the PVN of p5 pups. 2) A coronal medullary slice was cut containing the dorsal motor nucleus of the vagus, cardiac vagal neurons, and PVN axons expressing ChR2-EYFP.

1. ChR2-EYFP lentiviral vector

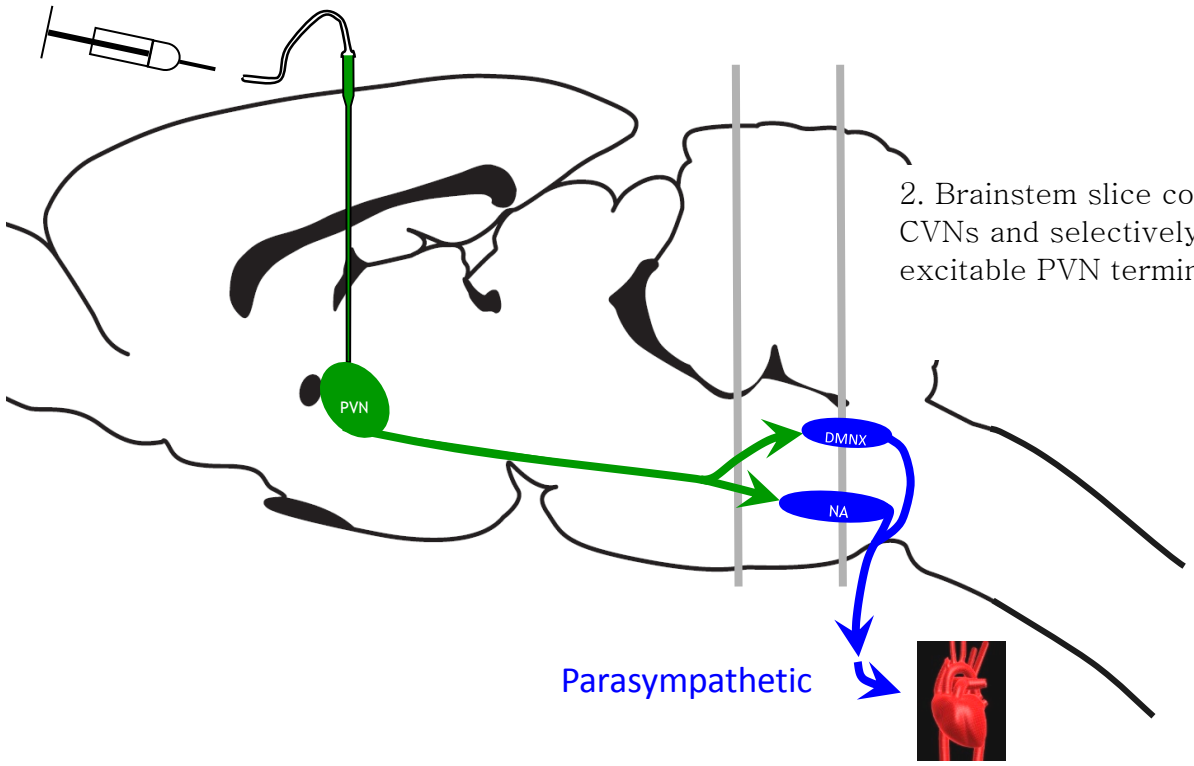

2. Brainstem slice containing CVNs and selectively excitable PVN terminals

cycling between room air (21% O_2, 79% N_2) and mild hypoxia/hypercapnia (6% O_2, 5% CO_2, 89% N_2) 10 times each hour, 8 hr each day, for 21 days. Each CIH/H cycle had 4 phases each of 90 sec: 1) room air was changed to H/H, 2) H/H was maintained, 3) the chamber was returned to room air, and 4) room air was maintained. The animals were exposed to CIH/H for 8 hr during the light phase and to normal air during the remaining 16 hr. Control animals were exposed to normal air (21% O_2 + 79% N_2) and placed adjacent to the chambers during the exposure period to undergo similar handling, general lab conditions, and background noise as the CIH/H group.

During each apnea, patients experience oxygen desaturations coupled with arterial CO_2 increases of ~9 mm Hg (Gislason et al., 1989; Sanders et al., 1994; Iber et al., 1986). Conversely, CIH exposure in mice causes hyperventilation ultimately decreasing arterial CO_2 (Kanagy, 2009). While the differences between CIH and CIH/H models of OSA however, have shown to be minor with regards to inducing hypertension, increasing sympathetic nerve activity, and impairing cardiac function, CIH/H exposure may more closely mimic what is seen in patients with OSA (Troncoso Brindeiro et al., 2007; Cooper et al., 2005; Kanagy et al., 2001; McGuire and Bradford, 2001). The increased arterial CO_2 ~9 mm Hg during apneas in patients is best mimicked by an inspired CO_2 of ~5% during hypoxic events (Gislason et al., 1989, Hare et al., 2003).

Slice preparation

To obtain brainstem slices containing the DMNV and ChR2-expressing PVN fibers (see Figure 4), rats between P21 and P35 were anesthetized, euthanized, and transcardially perfused with ice-cold glycerol-based artificial cerebrospinal fluid (aCSF)

(252 mM glycerol, 1.6 mM KCl, 1.2 mM NaH_2PO_4, 1.2 mM $MgCl_2$, 1.2 mM $CaCl_2$, 18 mM $NaHCO_3$, 11 mM glucose, 1.0 mM pyruvic acid and 1.0 mM ascorbic acid, perfused with 95% O_2 and 5% CO_2, pH = 7.4) to achieve exsanguination. The brain was carefully removed and brainstem slices (330 μm for confocal microscopy experiments, 200 μm for immunohistochemistry) were obtained using a vibratome (all in the glycerol based aCSF), as well as forebrain slices (300 μm for injection site verification) containing the PVN. Slices were allowed to recover for 15 min at 32 ºC in an *N*-methyl-D-glucamine (NMDG)-based aCSF (110 mM NMDG, 2.5 mM KCl, 1.2 mM NaH_2PO_4, 25 mM $NaHCO_3$, 25 mM glucose, 0.5 mM $CaCl_2$ and 10 mM $MgSO_4$; pH = 7.4, perfused with 95% O_2 and 5% CO_2,), before being transferred to 22–24°C aCSF (125 mM NaCl, 3 mM KCl, 2 mM $CaCl_2$, 26 mM $NaHCO_3$, 5 mM glucose, and 5 mM HEPES, perfused with 95% O_2 and 5% CO_2, pH = 7.4) in which experiments were performed.

Calcium imaging in oxytocin receptor-expressing CHO cells

Visualization of CHO cells expressing the OXT receptor and calcium indicator, as well as ChR2-containing PVN fibers, was performed on a confocal microscope system consisting of an upright Zeiss Axio Examiner Z1 microscope, with a W Plan Apocromat 20x/1.0 objective, equipped with Carl Zeiss 710 confocal hardware. Z-series spectral image sets were used to produce two channel image sets representing ChR2-EYFP fibers and OXT receptor-expressing CHO cells, by applying off-line a linear spectral un-mixing protocol. For calcium imaging in the CHO cells, images measuring 128×128 pixels were taken at 2.3 zoom factor with bi-directional scanning. Thus the pixel measured 1.44 μm, providing sufficient cellular and temporal resolution. Images were obtained every 76 milliseconds and analyzed offline.

Selectivity, affinity, and responsiveness of the OXT receptor-expressing CHO cells was examined using the dose-response relationship of these cells to both OXT and AVP. Plated CHO cells expressing the OXT receptor and the calcium indicator were perfused with aCSF (125 mM NaCl, 3 mM KCl, 2 mM $CaCl_2$, 26 mM $NaHCO_3$, 5 mM glucose, and 5 mM HEPES, perfused with 95% O_2 and 5% CO_2, pH = 7.4). Doses of oxytocin acetate salt (Bachem, Torrence, CA) or [Arg^8]-vasopressin acetate salt (Sigma-Aldrich, St. Louis, MO) were added to the perfusate 10 minutes apart at concentrations of 0.1 nm, 0.3 nm, 1 nm, 3 nm, 10 nm, 30 nm, and 100 nm.

To study the activation of oxytocin receptors upon optogenetic activation of ChR2-expressing PVN fibers in the DMNV, OXT receptor-expressing CHO cells were pipetted onto the DVC of brain stem slices from animals previously injected with pLenti-Syn-hChR2(H134R)-EYFP-WPRE into the PVN. OXT receptor-expressing CHO cells within the boundaries of the DMV and in close apposition to ChR2-containing PVN fibers (7.5 ± 0.5 µm) were used for experiments.

Immunohistochemistry and imaging

Slices processed for immunohistochemistry of ChR2-expressing axons and synaptic terminals in the brain stem were visualized after the experiments upon placing the brainstem tissue in 10% formalin then mounting and cover slipping the tissue with Prolong anti-fade mounting medium (Invitrogen, Eugene, OR). In PVN containing slices, the injection site was examined to assess whether the viral vector had spread to adjacent brain regions. If the viral vector injection spread outside of the PVN, the experiments from this animal were discarded.

To determine the co-localization of ChR2-EYFP and OXT in PVN fibers within the DMV, immunohistochemistry was utilized to co-localize OXT and viral expression of EYFP. Slices were soaked overnight in 10% formalin and were processed for OXT and EYFP using the following primary antibodies (overnight incubation at 22-24ºC): rabbit anti-OXT antibody (1:15000 dilution; Peninsula Laboratories, Inc., San Carlos, CA) and mouse anti-GFP/EYFP (1:500 dilution; Abcam, Cambridge, MA). As secondary antibodies we used goat anti-rabbit Alexa Fluor 405 and chicken anti-mouse Alexa Fluor 488 (all 1:200 dilution and 4 hr incubation at 22-24 ºC; Life Technologies, Carlsbad, CA).

Low magnification pictures were generated using an inverted Motic AE31 microscope. Brainstem slices were used for confocal microscopy. Stack images (12 – 80 μm; collapsed into 2D images) and tile scans were collected with the 20x and 63x objective of the Zeiss 710 confocal system and composed with Volocity software. For colocalization analysis, we used a 60 μm z-stack image of every other 100 μm for offline analysis. ChR2-EYFP fibers were counted and examined positive for OXT.

Statistical analysis

CHO cell experiments

Changes in fluorescent intensity were analyzed and presented as percent of control fluorescence. Fluorescent intensity in CHO cells was grouped into 0.5 sec bins for a total of 10 bins with the 3rd bin (time 0) representing the time point of ChR2-expressing PVN fiber activation. Results are presented as percent control and statistically compared with data from the same experiment using a one-way ANOVA with repeated-

measures analysis of variance followed by Bonferroni's multiple comparison test. For those experiments comparing CHO cell responses in unexposed brainstem tissue to CIH/H exposure and independent samples, Student's *t* test (unpaired) was used. Data with $p < 0.05$ were considered significant. Software used for statistical analysis of the data included Graphpad Prism 4.01 (Graphpad Software, San Diego, CA), Microcal Origin 7.0 (OriginLabs Corp, Nothhampton, MA) and Microsoft Excel (Microsoft Corp., Redmond, WA).

Results

Colocalization of ChR2-EYFP and OXT in brainstem fibers within the DMNV

The presence of ChR2-expressing PVN fibers in the DMNV was visualized by injecting into the PVN a lentiviral vector driving ChR2-EYFP expression by a synapsin promoter. Immunohistochemical analysis on brainstem slices containing both the DMV and ChR2-expressing PVN fibers confirmed that 56.0 ± 3.7% of ChR2-EYFP PVN fibers in the DMV are positive for OXT (Figure 5).

OXT receptor activation

CHO cells expressing both OXT receptors and the red fluorescent calcium indicator, R-GECO1, were utilized to detect the synaptic release of OXT from PVN fibers in the DMV. The dose-response relationship in the CHO cells was first examined to test the sensitivity of these engineered CHO cells to both OXT and AVP.

Figure 5 Colocalization of ChR2-EYFP and OXT in brainstem fibers within the DMV

Confocal image of immunohistochemical staining for ChR2 and OXT in the DMV from an animal injected with the Syn-ChR2-EYFP lentiviral vector. Colocalization of ChR2-EYFP and OXT in brainstem fibers within the DMV is shown in orange (scale bar represents 28 μm). 56.0 ± 3.7% of ChR2-EYFP PVN fibers in the DMV are positive for OXT.

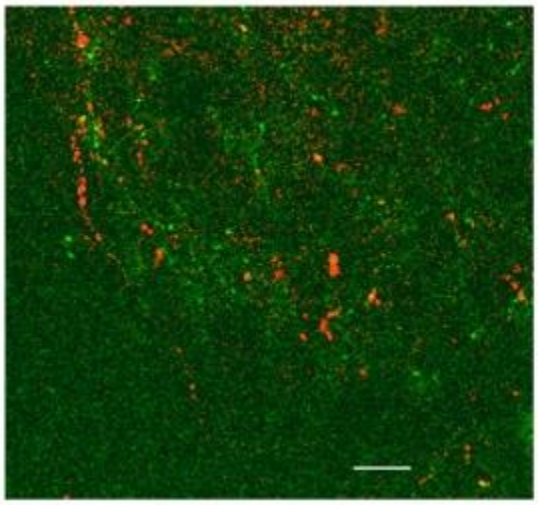

Independent applications of either OXT or AVP in a dose-dependent manner showed that the OXT receptor-expressing CHO cells are considerably more sensitive and responsive to OXT than AVP (Figure 6). The half maximal response (EC-50) of the sniffer CHO cells for OXT occurred at a concentration of 1.5 nM, whereas the EC-50 for AVP was 12.1 nM. Responses to OXT were additionally more robust than that for AVP; at the concentration (1 μM) at which OXT maximally activates the CHO cells, AVP evoked a blunted response of only 24 ± 5% of the OXT response.

Figure 6 Characterization of OXT and vasopressin dose-response relationships of sniffer CHO cells

CHO cells expressing an OXT receptor and an R-GECO Calcium indicator are considerably more sensitive and responsive to OXT than vasopressin with a half maximal response (EC-50) for OXT of 1.5 nM, and an EC-50 for vasopressin of 12.1 nM. Responses to OXT were considerably more robust than that for vasopressin; at the concentration (1 μM) at which OXT maximally activates these cells, vasopressin evoked a blunted response of only 24 ± 5% of the OXT response.

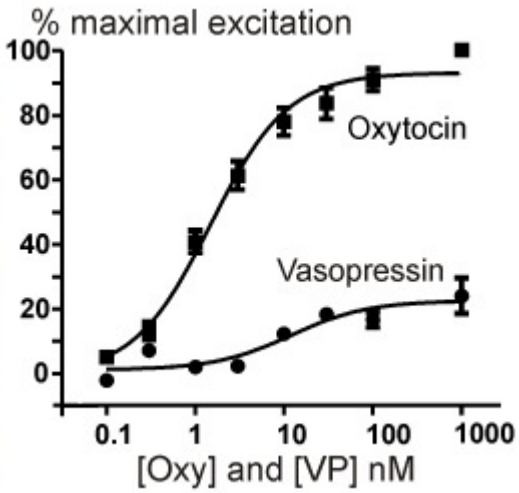
% maximal excitation
100
80
60
40
20
0
Oxytocin
Vasopressin
0.1
1
10
100
1000
[Oxy] and [VP] nM

Release of OXT from PVN fibers in the DMNV

To examine how the release of OXT from ChR2-expressing PVN fibers alters the intracellular calcium levels in the OXT receptor-expressing CHO cells, the cells were deposited onto the surface of the DVC of brainstem slices in close apposition to CVNs and ChR2-expressing PVN fibers (Figure 7). Only CHO cells inside the boundaries of the DMV and within 7.5 ± 0.5 μm from ChR2-expressing PVN fibers were used for experiments. Optogenetic stimulation of ChR2-expressing PVN fibers evoked large, reproducible, and transient increases in calcium (average increases of 13.0 ± 0.04% from baseline during first second; n = 9; $*p < 0.05$; one-way ANOVA with repeated measures) within the CHO cells (Figure 8A). In order to determine if the photostimulation-elicited increases in calcium in the CHO cells upon PVN fiber activation were due to the release of OXT from PVN fibers, the OXT receptor antagonist, OTA, was applied (10 μM). Upon PVN fiber activation, OTA application abolished the increases in intracellular calcium in the OXT-sensitive CHO cells (control: 21.0 ± 0.05%; OTA: 4.6 ± 0.02%; n = 7; one-way ANOVA with repeated measures; Figure 8B). While the release of AVP upon photoactivation of ChR2-containing PVN fibers in the DMV in this experimental paradigm cannot be ruled out, these results indicate that the intracellular calcium changes observed in these engineered CHO cells is most likely due to the synaptic release of OXT and activation of oxytocin receptors in the CHO cells that surround CVNs.

Figure 7 Visualization of sniffer CHO cells and ChR2-expressing PVN fibers

Confocal images showing OXT receptor-expressing CHO cells (red) deposited onto brainstem tissue in close apposition to ChR2-expressing PVN fibers (green) in the DMV (3-D reconstruction; top down view (left) and side view (right)).

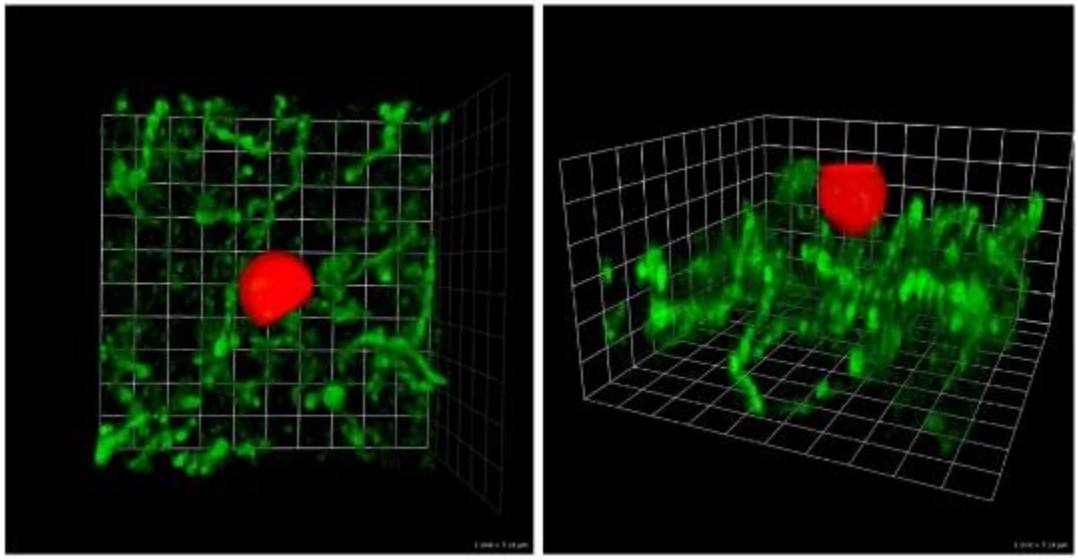

Figure 8 Oxytocin receptor activation

(A) Optogenetic stimulation of PVN fibers evokes large, reproducible, and transient increases in calcium in OXT sensitive CHO cells. Repeated stimulations (5 min apart) of ChR2 axons in the DMV increased calcium in OXT receptor-expressing CHO cells. Representative multiple responses of one CHO cell (top), and quantitative bar charts (bottom) depict the average responses in CHO cells after repeated stimulations (n = 9; $*p < 0.05$; one-way ANOVA with repeated measures). (B) Calcium increases in OXT receptor-expressing CHO cells is abolished by application of the OXT receptor antagonist, OTA. Representative trace of one CHO cell (top), and quantitative bar charts (bottom) depict average control increases in control conditions and in the presence of OTA in CHO cells (n = 7; $*p < 0.05$; one-way ANOVA with repeated measures).

A

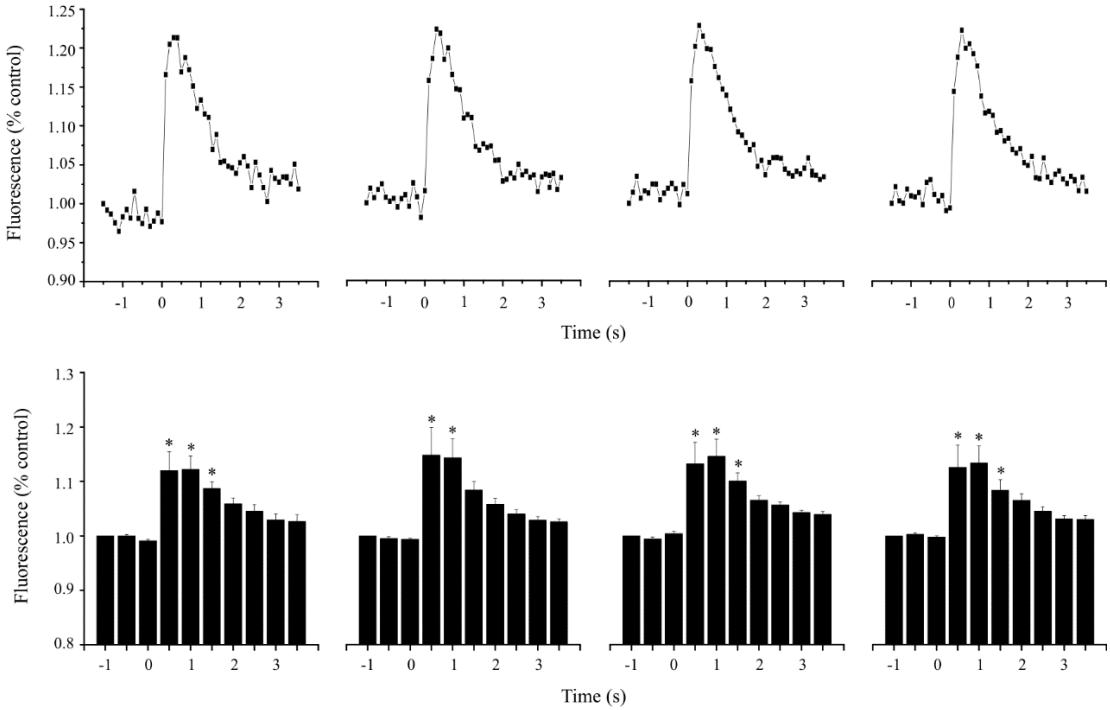
Fluorescence (% control)
Time (s)
Fluorescence (% control)
Time (s)

B

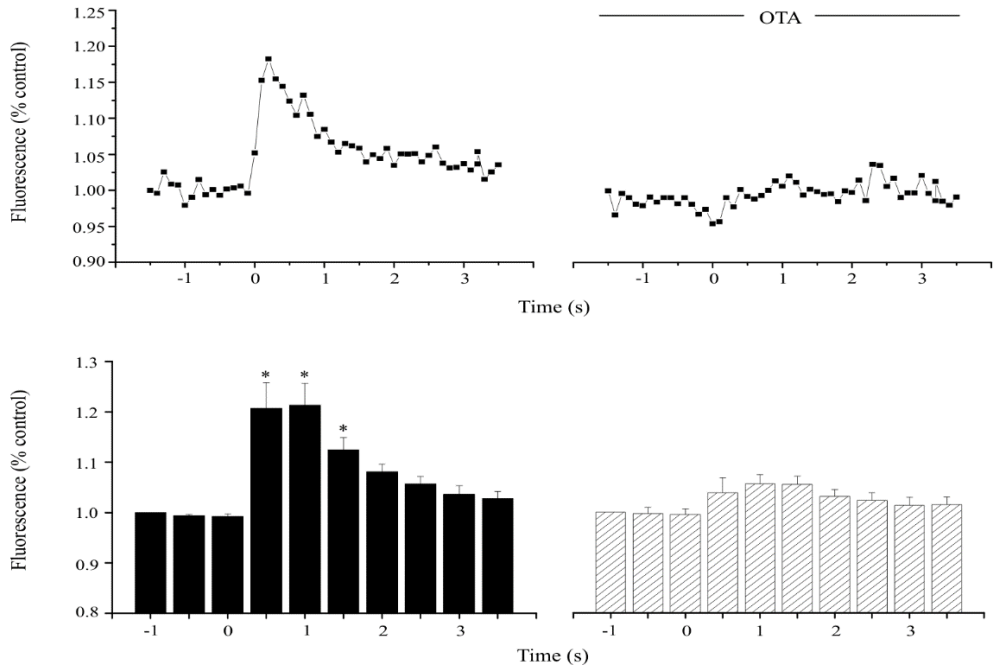
OTA
Fluorescence (% control)
Time (s)
Fluorescence (% control)
Time (s)

The effects of CIH/H on OXT receptor activation

In order to examine if the release of OXT is altered with CIH/H, the responses in CHO cells expressing OXT receptors and the calcium indicator, RGECO1, were examined in brainstem slices from unexposed and CIH/H exposed animals. Photoactivation of ChR2-containing PVN fibers in the DMV of brainstem slices from unexposed animals evoked large, reproducible, and transient increases in intracellular calcium levels in OXT-sensitive CHO cells (average increases of 15.0 ± 0.02% from baseline during first second; n = 14; $p < 0.05$; one-way ANOVA with repeated measures; Figure 9, bottom left). CHO cell responses upon PVN fiber stimulation in brainstem slices from animals exposed to CIH/H was significantly decreased compared to responses in unexposed animals (average increases of 9.1 ± 0.01% from baseline during first second; n = 16; $*p < 0.05$; unpaired *t*-test; Figure 9, bottom right) indicating that the release of OXT from PVN fibers in the DMV is reduced following CIH/H exposure.

Figure 9 Effects of CIH/H on OXT receptor function

The calcium increases in OXT sensitive CHO cells upon photoactivation of PVN fibers in the DMNV are significantly decreased when compared with air controls. Representative responses from CHO cells deposited onto brainstem tissue taken from animals exposed to air control (top left) and CIH/H (top right). Quantitative bar charts depict the percent control fluorescence of CHO cell responses in brainstem tissue taken from animals exposed to air (bottom left; n = 14) and CIH/H (bottom right; n = 16). *p < 0.05; unpaired t test.

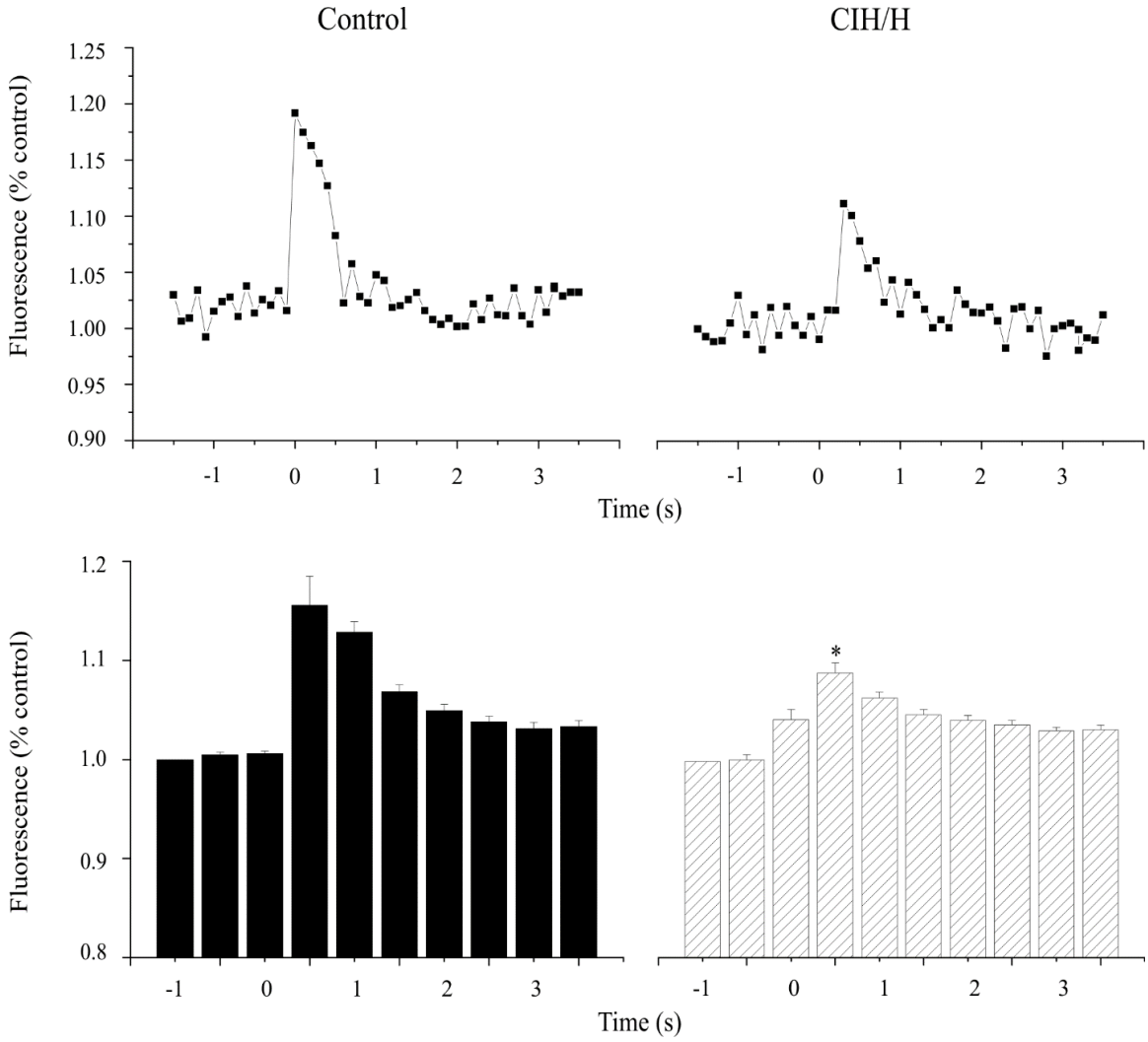
Control
CIH/H
Fluorescence (% control)
1.25
1.20
1.15
1.10
1.05
1.00
0.95
0.90
-1
0
1
2
3
Time (s)
Fluorescence (% control)
1.2
1.1
1.0
0.9
0.8
*
-1
0
1
2
3
Time (s)

Conclusions from Study 1

Recent studies using optogenetic stimulation of the PVN neurons that express ChR2 revealed a direct pathway from PVN neurons to brainstem parasympathetic CVNs. Photoactivation of ChR2-containing PVN fibers elicited paired-pulse facilitation of glutamatergic neurotransmission to CVNs and this enhancement was diminished after application of the OXT receptor antagonist, OTA, suggesting this excitatory pathway is facilitated by endogenous OXT release from these synaptic terminals. Recently published data from our lab also showed the paired-pulse facilitation of the EPSCs that occurs in unexposed rats is significantly blunted in animals exposed to CIH/H (Dergacheva et al., 2014). The results of my first study support and extend the hypothesis that excitation of parvocellular PVN fibers releases OXT at their brainstem CVN targets, and this approach can be used as a highly sensitive assay for endogenous OXT release from PVN synapses. I additionally showed that the release of OXT onto CVNs upon photoactivation of PVN fibers was blunted in animals exposed to 21 days of CIH/H.

These data provide direct evidence that the release of OXT from PVN fibers activates OXT receptors on sniffer CHO cells in close proximity to CVNs, and this release is diminished with exposure to CIH/H. As stated previously, parasympathetic activity is diminished in a number or cardiovascular diseases including OSA and hypertension. Restoring OXT function that is lost in animals exposed to CIH/H, could potentially restore parasympathetic activity to the heart and serve as a promising new therapeutic approach to inhibit the progression of such cardiovascular diseases.

CHAPTER 3

Study 2: Restoration of oxytocin neurons activity prevents hypertension caused by chronic intermittent hypoxia/hypercapnia

Introduction

Recent work from our lab, as well as the results presented in Study 1, reveal a direct pathway from PVN neurons to brainstem parasympathetic CVNs as photoactivation of ChR2-containing PVN fibers elicited paired-pulse facilitation of glutamatergic neurotransmission to CVNs and this enhancement was diminished after application of the OXT receptor antagonist, OTA (Pinol et al., 2014). In addition, as shown in Study 1, excitation of parvocellular PVN fibers releases OXT at the brainstem DMV targets to activate OXT-sensitive CHO cells, and the release of OXT is blunted after 21 days CIH/H, a model of OSA.

Daytime tachycardia and hypertension are associated with OSA one primary, yet poorly understood disease that causes stress to the cardiovascular system. OXT, a conserved neuropeptide secreted from the PVN, blunts the cardiovascular responses to stress. When an organism is stressed, OXT projections from the PVN to areas in the brainstem modulate the baroreceptor reflex and increase vagal outflow to the heart resulting in decreased blood pressure and heart rate. The work in chapter 3 will utilize DREADDs to test if selective activation of PVN OXT neurons: 1) decreases resting heart rate and blood pressure, 2) blunts the acute responses to H/H, and 3) mitigates the hypertension caused by CIH/H. In order to test this hypothesis and activate OXT neurons in the PVN, two viral vectors were injected into the PVN in male rats: one expressing Cre recombinase under an OXT promoter and the second expressing a double-floxed excitatory hM_3D_q DREADDs. Male rats serving as controls were injected with the double-floxed DREADDs viral vector but without the Cre virus, and, as expected, these animals did not have any expression of DREADDs. Animals from both groups were

implanted with a wireless telemetry device to monitor arterial blood pressure and EKG activity. Animals received daily injections of clozapine-N-oxide to activate PVN OXT neurons and the effects on resting heart rate and blood pressure, and after an 8 hr exposure of CIH/H were analyzed.

Methods and Materials

Adenosine-associated viral vectors

A rat minimal oxytocin promoter element from -530 bp to +33 relative to the origin of transcription of the oxytocin gene (UCSC genome browser on rat Nov. 2004 assembly; chr3:118,193,690 to 118,194,252) was synthesized de novo and flanked by multiple cloning sites (Genscript, Piscataway, NJ) (Chu and Zingg, 1999; Richard and Zingg, 1991). We had produced the rAAV1-OXT-Cre using the OXT promoter fragment in the following way (MIT, Viral Gene Transfer Core): pFB-AAV-oxytocin promoter cre was created by cloning the oxytocin promoter into V032 by excising the oxytocin promoter/pUC57 with XbaI (5') and AgeI (3') and cloning it into V032 cut with SpeI (5') and AgeI (3'). Then Cre was added by cutting Cre out of pBS185 with XhoI (5') and MluI-blunt (3') and moving it into pFB-AAV-OXT cut with XhoI (5') and Asp718-blunt (3'). To achieve robust and highly selective expression of DREADDs in PVN OXT neurons, the reporter viral vector co-injected with AAV-OXT-Cre was AAV2-hSyn-DIO-$hM_3D(G_q)$-mCherry (UNC, Gene Therapy Center, Vector Core Services). Expression of these Cre-dependent vectors will only be initiated in neurons selectively expressing Cre

as they contain silencing double-floxed inverse open reading frames (Zhu and Roth, 2014).

Stereotactic injections

Neonatal Sprague Dawley male rats (postnatal day 4 or 5) were anesthetized by hypothermia and mounted in a stereotactic apparatus with a neonatal adapter (Stoelting, Wood Dale, IL). A midline incision exposed the skull and a small burr hole was made to position a pulled calibrated pipette (VWR, Radnor PA) with a thin tip (inner diameter <30 μm) containing viral vectors rAAV1-OXT-Cre and AAV2-hSyn-DIO-hM$_3$D(G$_q$)-mCherry at a 1:2 ratio for DREADDs-expressing animals, and AAV2-hSyn-DIO-hM$_3$D(G$_q$)-mCherry only for sham animals at the following coordinates: 1.5 – 1.95 mm posterior (depending on the distance between bregma and lambda) and 0.3 mm lateral relative to bregma. The pipette tip was lowered 5.15-5.25 mm from the dorsal surface of the brain and 20 nl of viral vector was injected at a visually monitored rate of 60 nl per minute. The pipette was left in place for 10 min, prior to slow retraction. The incision was closed using surgical glue, antibiotic ointment was applied to closed incisions and animals were warmed up on a heating pad before being returned to their nest. The stereotactic PVN coordinates of postnatal day five rat pups were based on those used in previously published studies (Valenstein et al., 1969) and verified after each experiment for accuracy of the injection sites.

Telemetry implantation

For animals in which blood pressure and heart rate were obtained, male Sprague–Dawley rats, 3–4 weeks of age, were anaesthetized using isoflurane (2–4%) and a

wireless HD-X11 pressure transmitter was implanted (Data Sciences International, St Paul, MN). Radiotelemetry allows for non-invasive and long-term monitoring of blood pressure and ECG in freely moving animals (Rowan III et al., 2007). The pressure catheter was inserted into the abdominal aorta to sense arterial pressure, and two biopotential leads were implanted to detect EKG activity. This device receives information from both the pressure catheter and biopotential leads and transmits the data to an electronic module. All rats with telemetry devices were allowed 7–14 days to recover from transmitter implantation surgery before any measurements were recorded. Blood pressure and heart rate were recorded via radio-frequency signals obtained through the Ponemah data acquisition system (Data Sciences International). Baseline recordings of blood pressure and heart rate were obtained for 3 days prior to CIH/H exposure in both groups. Prior to, and during, the 28 day CIH/H exposure period daily baseline recordings of blood pressure and heart rate were recorded in all animals.

Animal acclimation and daily DREADDs activation

In order to acclimate animals to human handling, male rats were handled daily beginning one week after stereotaxic injections. One- two weeks after telemetry implantation, DREADDs receptors were activated daily by intraperitoneal (IP) injection of CNO (1.0 mg/kg). To investigate the effects of CNO on resting blood pressure and heart rate in both DREADDs-expressing and sham animals, 3 days prior to CIH/H exposure (control days) baseline blood pressure and heart rate values were recorded for a 20 min period before CNO injection. Animals from each group then received an IP injection of CNO, blood pressure and heart rate were recorded for 1 hr, and the animals then underwent exposure to air for 8 hr to achieve acclimation to the chambers. During

the 21 days of CIH/H exposure, baseline recordings of blood pressure and heart rate were obtained before CNO injection, recorded for 1 hr post CNO injection, and for the entire duration of CIH/H exposure.

Chronic intermittent hypoxia/hypercapnia exposure

Juvenile male rats (3-4 weeks old) that previously underwent stereotaxic injections and were implanted with telemetry devices were transferred to commercial atmosphere controlled chambers in their cages with free access to food and water. This system (Oxycycler model A84, Biospherix, NY) allowed for the monitoring and independent control of oxygen, carbon dioxide, and nitrogen. The animals inside the chambers were exposed to repetitive cycles of 3 min of mild H–H (6% O_2 + 5% CO_2 + 89% N_2) followed by 3 min of normoxia (21% O_2 + 79 % N_2), repeated 10/per hr, 8 hr per day for 3 weeks. The animals were exposed to CIH/H for 8 hr during the light phase and to normal air during the remaining 16 hr.

Slice preparation and electrophysiology

For forebrain slice electrophysiology and immunohistochemistry (after 21 days CIH/H exposure), rats between P21 and P35 or P52-66 respectively, were anesthetized, euthanized, and transcardially perfused with ice-cold glycerol-based aCSF (252 mM glycerol, 1.6 mM KCl, 1.2 mM NaH_2PO_4, 1.2 mM $MgCl_2$, 1.2 mM $CaCl_2$, 18 mM $NaHCO_3$, 11 mM glucose, 1.0 mM pyruvic acid and 1.0 mM ascorbic acid, perfused with 95% O_2 and 5% CO_2, pH = 7.4) to achieve exsanguination. The brain was carefully removed and forebrain slices containing the PVN (400 μm for electrophysiology, 200 μm for immunohistochemistry) were obtained using a compresstome. Slices were allowed to recover for 15 min at 32 ºC in an NMDG-based aCSF (110 mM NMDG, 2.5 mM KCl,

1.2 mM NaH_2PO_4, 25 mM $NaHCO_3$, 25 mM glucose, 0.5 mM $CaCl_2$ and 10 mM $MgSO_4$; pH = 7.4, perfused with 95% O_2 and 5% CO_2,), before being either transferred to 22–24°C aCSF (125 mM NaCl, 3 mM KCl, 2 mM $CaCl_2$, 26 mM $NaHCO_3$, 5 mM glucose, and 5 mM HEPES, perfused with 95% O_2 and 5% CO_2, pH = 7.4) in which electrophysiology experiments were performed, or to 10% formalin for immunohistochemistry.

Electrophysiology experiments were performed on a Zeiss AxioPlan using a 40× water immersion objective. Identified PVN neurons expressing mCherry were imaged with differential interference contrast optics, infrared illumination, and infrared-sensitive video detection cameras to gain better spatial resolution. Patch pipettes were filled with a solution at pH 7.3 consisting of K^+-gluconic acid (150 mM), HEPES (10 mM), EGTA (10 mM), $MgCl_2$ (1 mM), and $CaCl_2$ (1 mM) to isolate for excitatory currents. Identified PVN neurons expressing mCherry were recorded in current-clamp configuration with no current injection. After a 5 min baseline recording, CNO (10 μm; Enzo Life Sciences, Farmingdale, NY) was included in the perfusate to examine its effects on spontaneous action potential firing. Current-clamp whole-cell recordings were made with an Axopatch 200B and pClamp 9 software (Axon Instruments, Union City, CA, USA).

Immunohistochemistry and imaging

Slices processed for immunohistochemistry of mCherry-expressing cell bodies in the PVN were visualized after the brain slices were taken upon placing the brainstem tissue in 10% formalin then mounting and cover slipping the tissue with Prolong anti-fade mounting medium (Invitrogen, Eugene, OR). In PVN containing slices, the injection site was examined to assess whether the viral vector had spread to adjacent

brain regions. If the viral vector injection spread outside of the PVN, the experiments from this animal were discarded. The injection site was also examined in sham animals although as expected, viral expression was not detected in any sham animals.

To determine the co-localization of mCherry and OXT in PVN cell bodies, immunohistochemistry was utilized to co-localize OXT and viral expression of mCherry. Slices were soaked overnight in 10% formalin and were processed for OXT and mCherry using the following primary antibodies (overnight incubation at 22-24ºC): rabbit anti-OXT antibody (1:15000 dilution; Peninsula Laboratories, Inc., San Carlos, CA) and mouse anti-mCherry (1:1000 dilution; Clontech Laboratories, Inc., Mountain View, CA). As secondary antibodies we used goat anti-rabbit Alexa Fluor 405 and goat anti-mouse Alexa Fluor 633 (all 1:200 dilution and 4 hr incubation at 22-24 ºC; Life Technologies, Carlsbad, CA).

Low magnification pictures were generated using an inverted Motic AE31 microscope. Brainstem slices were used for confocal microscopy. Stack images (12 – 80 μm; collapsed into 2D images) and tile scans were collected with the 20x and 63x objective of the Zeiss 710 confocal system and composed with Volocity software. For colocalization analysis, we used a 60 μm z-stack image of every other 100 μm for offline analysis.

Statistical Analysis

Electrophysiology experiments

Changes in the action potential firing frequency were determined using the MiniAnalysis version 6.0.3 software (Synaptosoft, Decatur, GA). Action potential firing

frequency was grouped into 5 min bins for a total of 12 bins with the 2nd bin representing the start of CNO application. Results are presented as means ± SE and statistically compared with control data from the same experiment using a one-way ANOVA with repeated-measures analysis of variance followed by Bonferroni's multiple comparison test for all experiments. Data with $p < 0.05$ were considered significant.

In vivo experiments

To examine the effects of CNO on mean arterial blood pressure and heart rate over the 21 days of CIH/H exposure, values were recorded before and after CNO injection on control days prior to CIH exposures, and days 1, 3, 6, 9, 12, 15, 18, and 21 of CIH/H. Changes within the groups of DREADDs-expressing animals and the sham animals were statistically analyzed by one-way ANOVA with repeated-measures analysis of variance followed by Bonferroni's multiple comparison test. Data with $p < 0.05$ were considered significant. Comparisons between the groups of DREADDs-expressing animals and the sham animals were statistically analyzed by two-way ANOVA with repeated-measures analysis of variance followed by Bonferroni's multiple comparison test. Data with $p < 0.05$ were considered significant.

For acute H/H evoked responses in mean arterial blood pressure and heart rate during CIH/H exposure, the values recorded during the last 30 sec of normoxia, as well as H/H of each cycle during the 8 hr CIH/H exposure of days 1, 3, 6, 9, 12, 15, 18, 21 were averaged for each animal. A paired Student's *t* test was used to test the significance within each group of either DREADDs-expressing animals or sham animals, while independent samples (unpaired) Student's *t* test was used to access the significant

differences between the two groups of animals. Data with $p < 0.05$ were considered significant.

To examine the chronic changes in mean arterial blood pressure and heart rate over the 21 day CIH/H exposure, values recorded before each CIH/H exposure on control days, day 1, 3, 6, 9, 12, 15, 18, and 21. Changes within the DREADDs-expressing animals and the sham animals were statistically analyzed by one-way ANOVA with repeated-measures analysis of variance followed by Bonferroni's multiple comparison test. To examine the statistical changes in mean arterial blood pressure and heart rate between the two groups of animals, a two-way ANOVA with repeated-measures analysis of variance (two-way ANOVA) followed by Bonferroni's multiple comparison test was used. Data with $p < 0.05$ were considered significant.

Software used for all statistical analysis of the data included Graphpad Prism 4.01 (Graphpad Software, San Diego, CA), Microcal Origin 7.0 (OriginLabs Corp, Nothhampton, MA) and Microsoft Excel (Microsoft Corp., Redmond, WA).

Results

In vitro activation of excitatory DREADDs in PVN neurons

Prior to in vivo activation of PVN OXT neurons using the DREADDs approach, the responses upon activation of DREADDs in PVN OXT neurons were assessed in vitro. Forebrain slices containing the PVN were taken from animals (P21-35) previously injected with rAAV1-OXT-Cre and AAV2-hSyn-DIO-hM$_3$D(G$_q$)-mCherry, and PVN neurons expressing mCherry were studied using the whole-cell patch clamp method. The

action potential firing frequency of DREADDs-expressing PVN neurons significantly increased within 5 min of CNO application (from 0.19 ± 0.05 Hz to 0.75 ± 0.14 Hz; n = 7; *$p < 0.05$; one-way ANOVA; Figure 10). These experiments indicate that the combination of viral vectors rAAV1-OXT-Cre and AAV2-hSyn-DIO-hM$_3$D(G$_q$)-mCherry drives expression of excitatory DREADDs in PVN neurons, and activation of these receptors by CNO application significantly increases the firing of these PVN neurons.

Figure 10 ***In vitro*** **activation of PVN OXT neurons expressing excitatory DREADDs**

Representative action potential traces (top) recorded under current-clamp configuration from a PVN OXT neuron expressing mCherry before CNO (top left) and post CNO (top right) indicating excitatory DREADDs activation with CNO application. Quantitative bar charts depict the frequency of action potentials before and after CNO application in 7 PVN neurons expressing mCherry. $*p < 0.05$; one-way ANOVA.

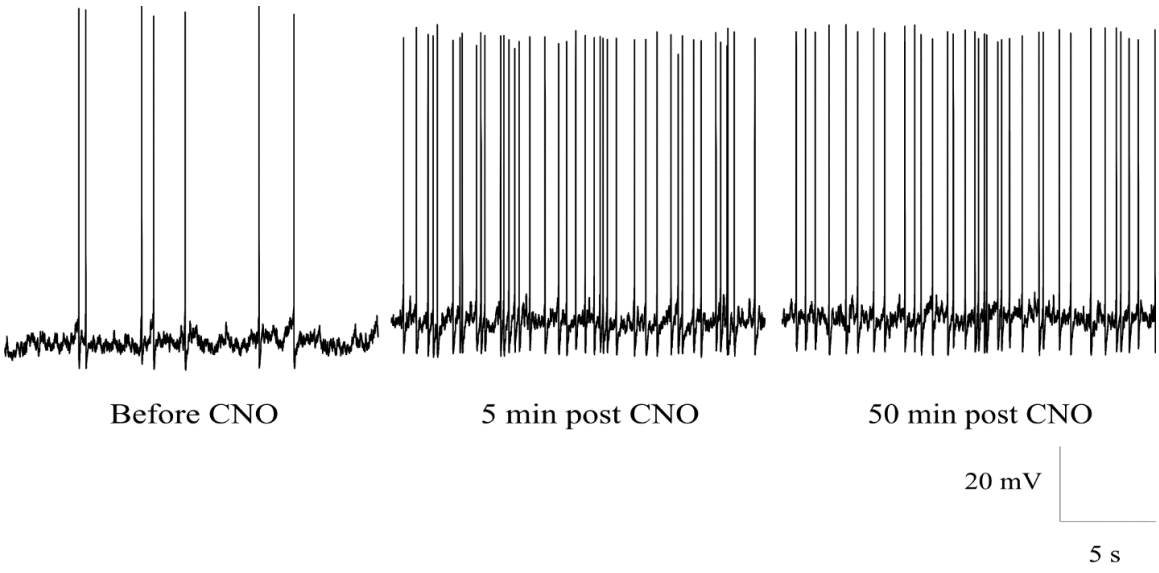
Before CNO
5 min post CNO
50 min post CNO
20 mV
5 s

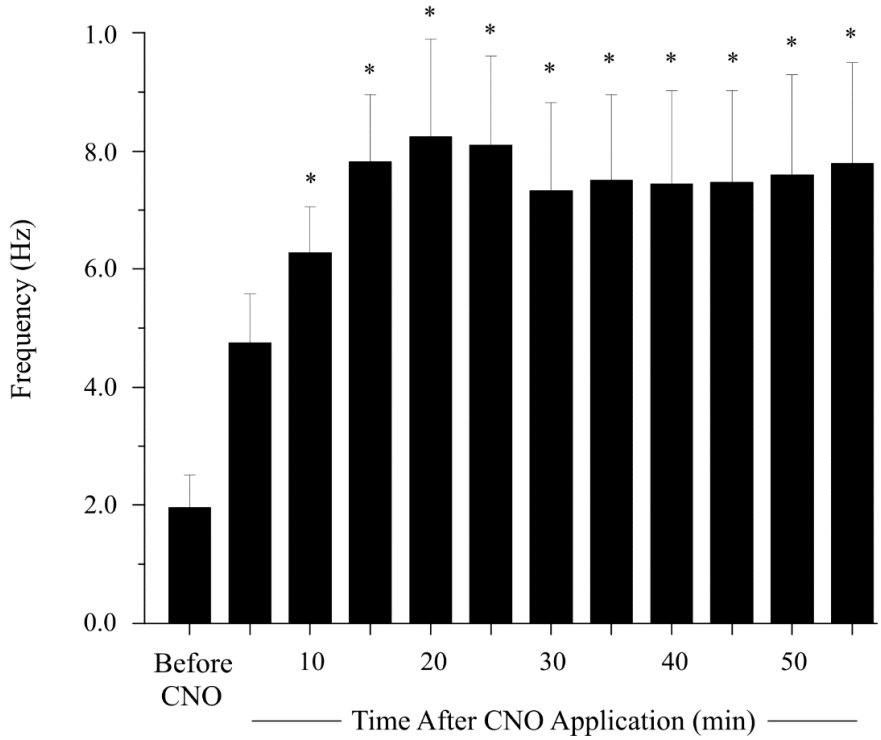
Frequency (Hz)
1.0
8.0
6.0
4.0
2.0
0.0
Before CNO
10
20
30
40
50
Time After CNO Application (min)

Excitatory DREADDs expression in the PVN

To examine the alterations that occur in blood pressure and heart rate upon selective activation of PVN OXT neurons two viral vectors in combination with the Cre/lox system were used. In this approach, one viral vector expresses Cre under a specific promoter (OXT promoter fragment) and the other is a Cre dependent vector expressing excitatory $hM_3D(G_q)$ DREADDs under a strong promoter (synapsin). For this intersectional viral vector approach an AAV vector that expresses Cre under the 563 bp OXT promoter fragment was designed and combined with a Cre-dependent reporter viral vector for stereotaxic injections into the PVN. Serotypes 2, 5, and 8 of the Cre-dependent viral vector AAV-hSyn-DIO-$hM_3D(G_q)$-mCherry were tested for expression specificity in PVN OXT neurons. Serotypes 5 and 8 of the reporter virus was found to drive expression in a large number of neurons that did not stain immunopositive for OXT (data not shown). This potential lack of specificity with these serotypes discouraged any additional experiments with these viral vectors. Immunohistochemical analysis of serotype 2 however, confirmed that a large fraction (83.0 ± 2.1 %) of neurons infected with $hM_3D(G_q)$-mCherry were co-localized with OXT, and that this viral combination elicited high (83.0%) selectivity for DREADDs expression in PVN OXT neurons (Fig 11).

Figure 11 Subpopulation-specific adenosine-associated viral vectors

Viral vectors AAV-OXT-Cre and AAV2-hSyn-DIO-hM$_3$D(G$_q$)-mCherry expresses mCherry in OXT neurons in the PVN. Confocal images of immunohistochemical staining of individual neurons in the PVN of an animal injected with OXT-Cre and hSyn-DIO-hM$_3$D(G$_q$)-mCherry AAV vectors for OXT expression in green (A), mCherry localized to the cell membrane in red (B), and the merged image shown in orange (C). Scale bar is 32 µm.

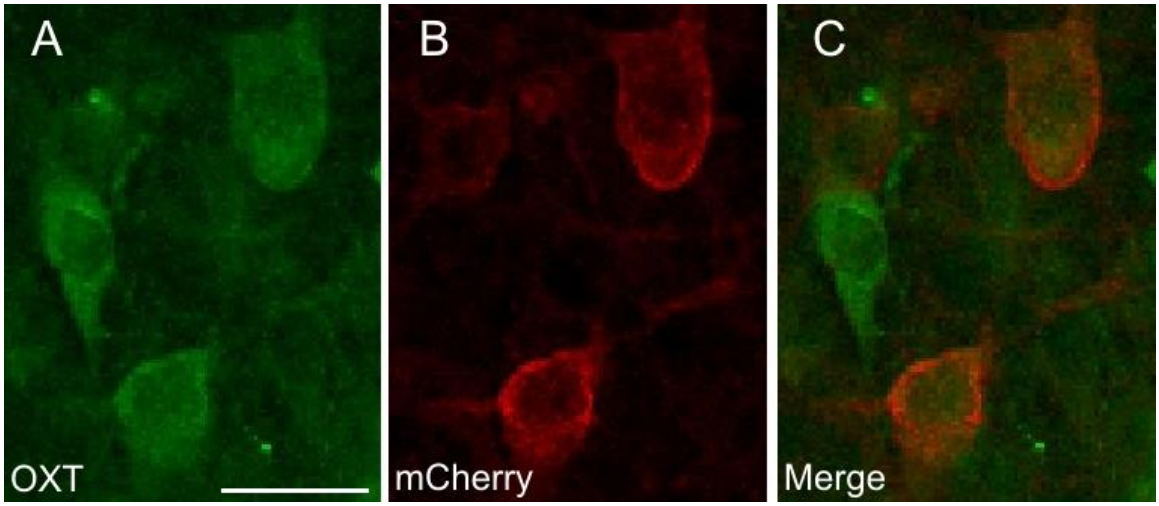
A
B
C
OXT
mCherry
Merge

In vivo activation of DREADD in PVN OXT neurons

Acute oxytocin neuron activation decreases resting blood pressure and heart rate

To examine any potential effects of CNO administration on mean arterial blood pressure and heart rate in animals without DREADDs, expression experiments were conducted on sham animals. These sham animals had surgeries and injections identical to those in the OXY group of animals, with the exception that the rAAV1-OXT-Cre virus was injected without the AAV2-hSyn-DIO-h$M_3D(G_q)$-mCherry virus. In this sham group of animals injections of CNO did not significantly change mean arterial blood pressure (102.0 ± 3.3 mm Hg before CNO, 100.0 ± 3.2 mm Hg after CNO; n = 7; $p > 0.05$; paired *t* test; Figure 12A) or heart rate (394.0 ± 10.4 beats/min before CNO, 389.0 ± 9.8 beats/min after CNO; n = 7; $p > 0.05$; paired *t* test; Figure 12B).

We next examined the effects of activating PVN OXT neurons throughout 21 days of CIH/H exposure. Values were recorded before and after CNO injections on 3 control days immediately prior to CIH/H exposures, and on days 1, 3, 6, 9, 12, 15, 18, and 21 of CIH/H. After CNO injection to activate OVN OXT neurons these DREADDs-expressing animals experienced a significant decrease in mean arterial blood pressure (104.0 ± 2.6 mm Hg before CNO to 93.0 ± 1.7 mm Hg after CNO; n = 8; $^{+}p < 0.05$; paired *t* test; Figure 12A) and heart rate (416.0 ± 7.1 beats/min before CNO to 362.0 ± 10.5 beats/min after CNO; n = 8; $^{+}p < 0.05$; paired *t* test; Figure 12B).

Figure 12 Acute oxytocin neuron activation decreases resting blood pressure and heart rate

(A) Changes in resting mean arterial blood pressure before and after CNO injection. Mean arterial blood pressure in DREADDs expressing animals was significantly decreased 45 min after CNO injection (n = 8; $^{+}p < 0.05$, one-way ANOVA). In sham animals, CNO injection did not significantly change mean arterial blood pressure (n = 7; one-way ANOVA). (B) Heart rate changes in response to CNO injection. 45 min after CNO injection, heart rate in DREADDs expressing was significantly decreased (n = 8; $^{+}p < 0.0001$, one-way ANOVA), while CNO injection did not significantly change heart rate in sham animals (n = 7; one-way ANOVA). The values for both mean arterial blood pressure (A) and heart rate (B) represent the averages of each recorded 20 min prior to CNO injection and 45 min after CNO injection on control days.

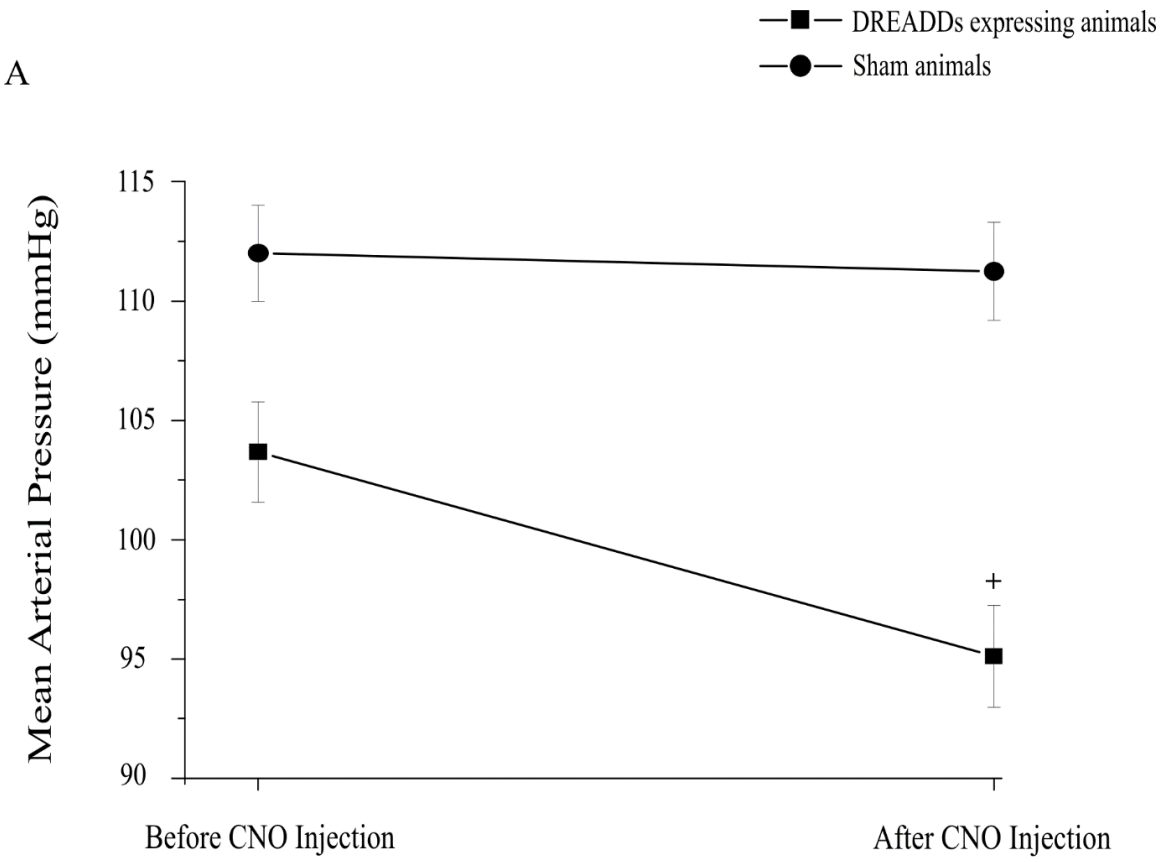
DREADDs expressing animals
Sham animals
A
Mean Arterial Pressure (mmHg)
115
110
105
100
95
90
+
Before CNO Injection
After CNO Injection

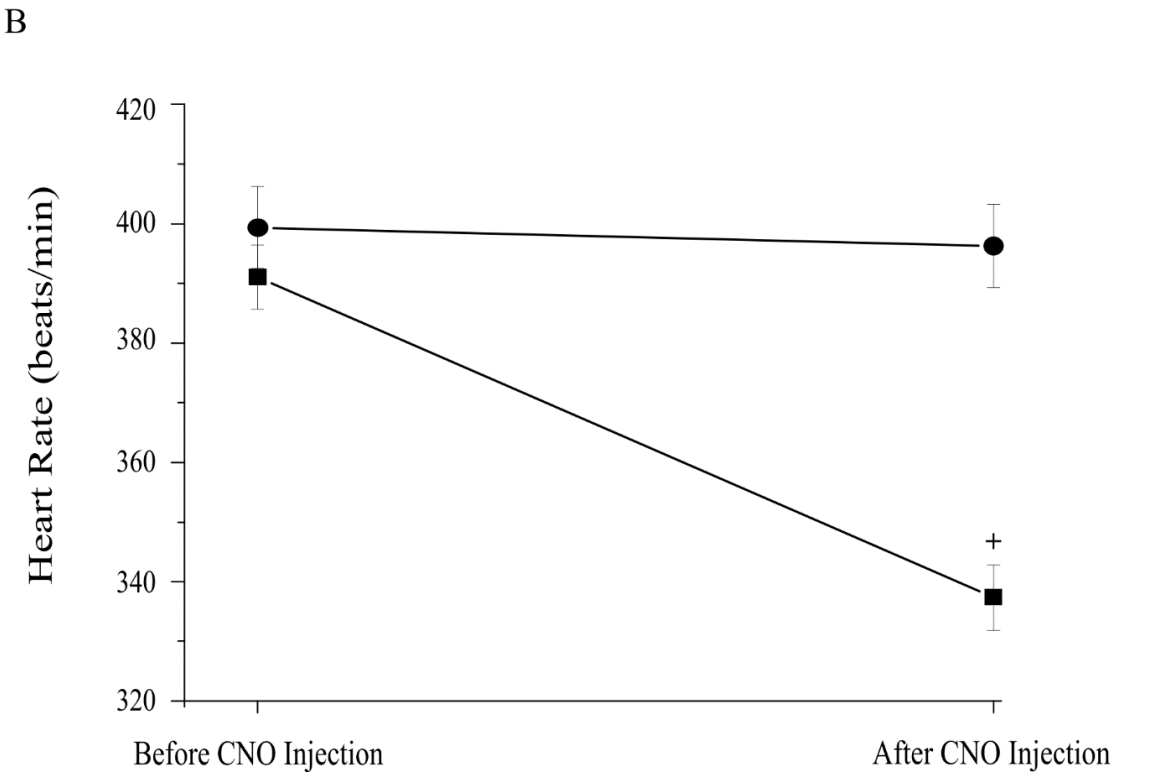
B
Heart Rate (beats/min)
420
400
380
360
340
320
+
Before CNO Injection
After CNO Injection

Activation of oxytocin neurons blunts the acute responses to H/H

To test if PVN OXT neuron activation alters the blood pressure and heart rate changes to acute exposures to H/H, the responses from sham animals were compared to the responses from animals with PVN OXT neurons activated. Changes in blood pressure and heart rate evoked by H/H were assessed by comparing the values of mean arterial blood pressure and heart rate during the last 30 sec of normoxia to the last 30 sec of H/H in each cycle during the 8 hr CIH/H exposure of days 1, 3, 6, 9, 12, 15, 18, 21 of CIH/H. Both groups of animals similarly experienced a significant decrease in heart rate during H/H (In sham animals, 384.0 ± 10.0 beats/min in normoxia to 279.0 ± 10.7 beats/min in H/H; n = 7; $^{+}p < 0.05$; paired *t* test; In DREADDs-expressing animals, 361.0 ± 7.0 beats/min in normoxia to 305.0 ± 9.7 beats/min in H/H; n = 8; $^{+}p < 0.05$; paired *t* test; Figure 13B). The decrease in heart rate evoked by H/H was not significantly different in sham and PVN OXT neuron activated animals. Both groups of animals experienced significant increases in mean arterial blood pressure in response to H/H (sham animals, mean arterial blood pressure increased from 113.0 ± 2.1 mm Hg in normoxia to 124.0 ± 2.7 mm Hg in H/H; n = 7; $^{+}p < 0.05$; paired *t* test; DREADDs animals, mean arterial blood pressure increased from 110.0 ± 1.8 mm Hg in normoxia to 115.0 ± 2.7 mm Hg in H/H; n = 8; $^{+}p < 0.05$; paired *t* test; Figure 13A). Interestingly however, the increase in mean arterial blood pressure in the DREADDs- expressing animals was significantly blunted compared to sham animals (Increases of 11 mm Hg in sham animals compared to increases of 5 mm Hg in DREADDs-expressing animals; n = 7 sham and 8 DREADDs-expressing; $*p < 0.05$; unpaired *t* test; Figure 13A).

Figure 13 Activation of oxytocin neurons blunts the acute blood pressure responses to H/H

(A) Acute changes in mean arterial blood pressure in response to normoxia and H/H. Both DREADDs expressing and sham animals experienced significant increases in mean arterial blood pressure during H/H (n = 8; $^{+}p < 0.05$, Student's paired *t* test; n = 7 $^{+}p < 0.05$, Student's paired *t* test, respectively), however the increase in mean arterial blood pressure in DREADDs expressing animals was significantly reduced compared to sham animals ($*p < 0.05$, unpaired *t* test). (B) Acute changes in heart rate in response to normoxia and H/H. During H/H, both DREADDs expressing and sham animals experienced significant decreases in heart rate (n = 8; $^{+}p < 0.05$, Student's paired *t* test; n = 7 $^{+}p < 0.05$, Student's paired *t* test, respectively), and while not statistically significant, the bradycardia in DREADDs expressing animals in response to H/H was blunted compared to sham animals. The values for both mean arterial blood pressure (A) and heart rate (B) represent the averages recorded during the last 30 sec of normoxia as well as H/H, of each cycle during the 8 hr CIH/H exposure on days 1, 3, 6, 9, 12, 15, 18, and 21.

A

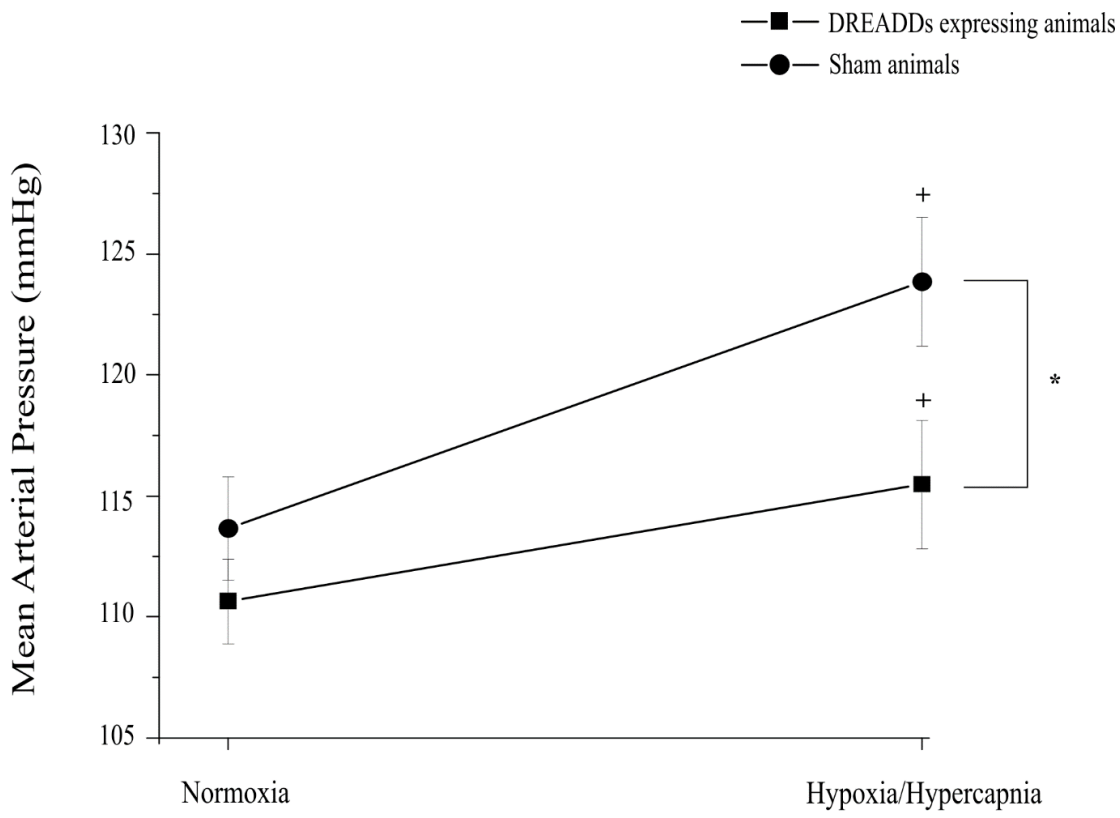
DREADDs expressing animals
Sham animals
Mean Arterial Pressure (mmHg)
130
125
120
115
110
105
+
+
*
Normoxia
Hypoxia/Hypercapnia

B

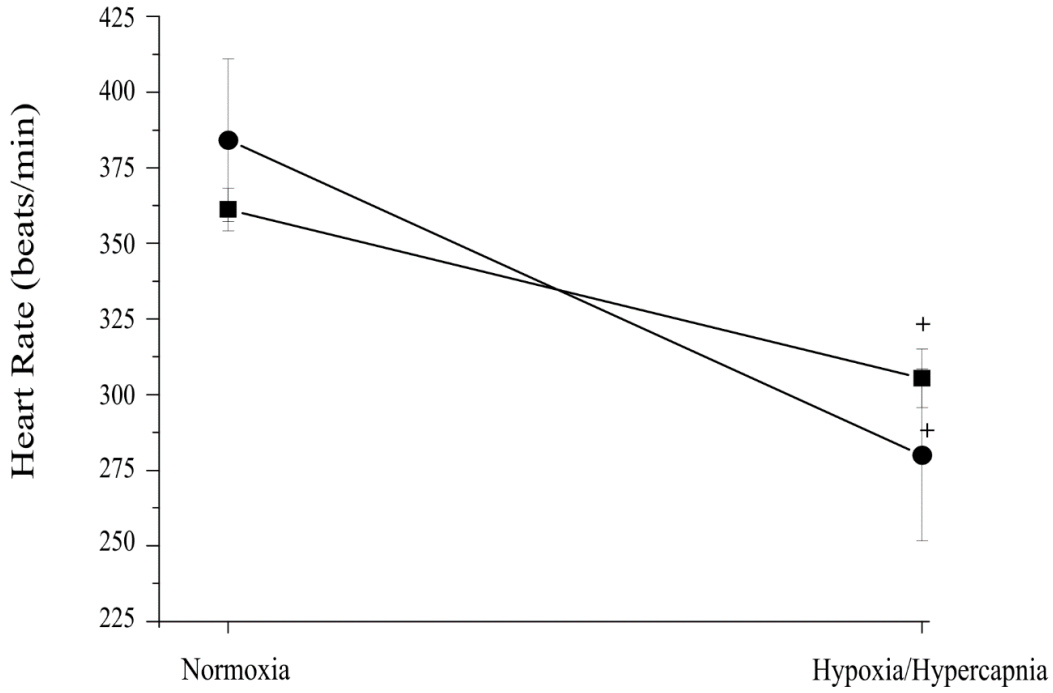
Heart Rate (beats/min)
425
400
375
350
325
300
275
250
225
+
+
Normoxia
Hypoxia/Hypercapnia

Chronic oxytocin neuron activation diminishes the development of hypertension and decreases heart rate with CIH/H

To test if activation of PVN OXT neurons alters the changes in mean arterial blood pressure and heart rate that occur with CIH/H blood pressure and heart rate were examined before and throughout 21 days of CIH/H exposure in sham and DREADDs-expressing animals. Sham animals experienced no significant changes in heart rate after 3 weeks of CIH/H exposure (from 394.0 ± 10.3 beats/min on control days to 379.0 ± 15.4 beats/min on day 21; n = 7; $p > 0.05$; one-way ANOVA; Figure 14B), while DREADDs-expressing animals experienced a significant decrease in heart rate despite CIH/H exposure (from 416.0 ± 7.1 beats/min on control days to 369.0 ± 11.1 beats/min on day 21; n = 8; $^{+}p < 0.01$; one-way ANOVA; Figure 14B).

After 3 weeks of CIH/H, mean arterial blood pressure increased to hypertensive levels in sham animals (from a mean arterial blood pressure of 102.0 ± 3.3 mm Hg on control days to 120 ± 0.5 mm Hg on day 21; n = 7; $^{+}p < 0.01$; one-way ANOVA; Figure 14A). Interestingly, DREADDs-expressing animals experienced no significant changes in mean arterial blood pressure with 21 days of CIH/H exposure (from a mean arterial blood pressure of 104.0 ± 2.6 mm Hg on control days to 103.0 ± 3.0 mm Hg on day 21; n = 8; $p > 0.05$; one-way ANOVA; Figure 14A). Animals in the sham group experienced significant increases in mean arterial blood pressure from days 12 through days 21, whereas the increase in mean arterial blood pressure was prevented in the DREADDs-expressing group (Day 12: mean arterial blood pressure in sham group of 117.0 ± 4.1 mm Hg, mean arterial blood pressure in DREADDs-expressing group of 105.0 ± 2.6 mm Hg; Day 15: mean arterial blood pressure in sham group of 118.0 ± 2.6 mm Hg, mean arterial

blood pressure in DREADDs-expressing group of 105.0 ± 3.1 mm Hg; Day 18: mean arterial blood pressure in sham group of 122.0 ± 1.1 mm Hg, mean arterial blood pressure in DREADDs-expressing group of 104.0 ± 2.9 mm Hg; Day 21: mean arterial blood pressure in sham group of 120.0 ± 0.5 mm Hg, mean arterial blood pressure in DREADDs-expressing group of 103.0 ± 3.0 mm Hg; n = 7 sham animals and 9 DREADDs-expressing animals; *$p < 0.01$; two-way ANOVA; Figure 14A).

Figure 14 Chronic oxytocin neuron activation diminishes the development of hypertension and decreases heart rate with CIH/H

(A) Changes in mean arterial blood pressure from control days to day 21 of CIH/H exposure. Mean arterial pressure in sham animals significantly increased from day 9 to day 21 compared to control day and reached hypertensive levels by day 12 (n = 7; $^{+}p < 0.05$, one-way ANOVA). Mean arterial pressure did not significantly increase in DREADDs expressing animals over the 21 days of CIH/H exposure compared to control days (n = 8; one-way ANOVA). Mean arterial blood pressure significantly increased in sham animals compared to DREADDs expressing animals from day 12 to day 21 ($*p < 0.05$, two-way ANOVA with repeated measures). (B) Changes in heart rate from control days to day 21 of CIH/H. Heart rate was significantly decreased in DREADDs expressing animals on day 21 compared to control days (n = 8; $^{+}p < 0.05$, one-way ANOVA), while heart rate in sham animals did not significantly change over the 21 days of CIH/H exposure (n = 7; one-way ANOVA). The values for both mean arterial blood pressure (A) and heart rate (B) represent averages of each recorded for 20 min during exposure to air in days prior to and during CIH/H exposures.

A

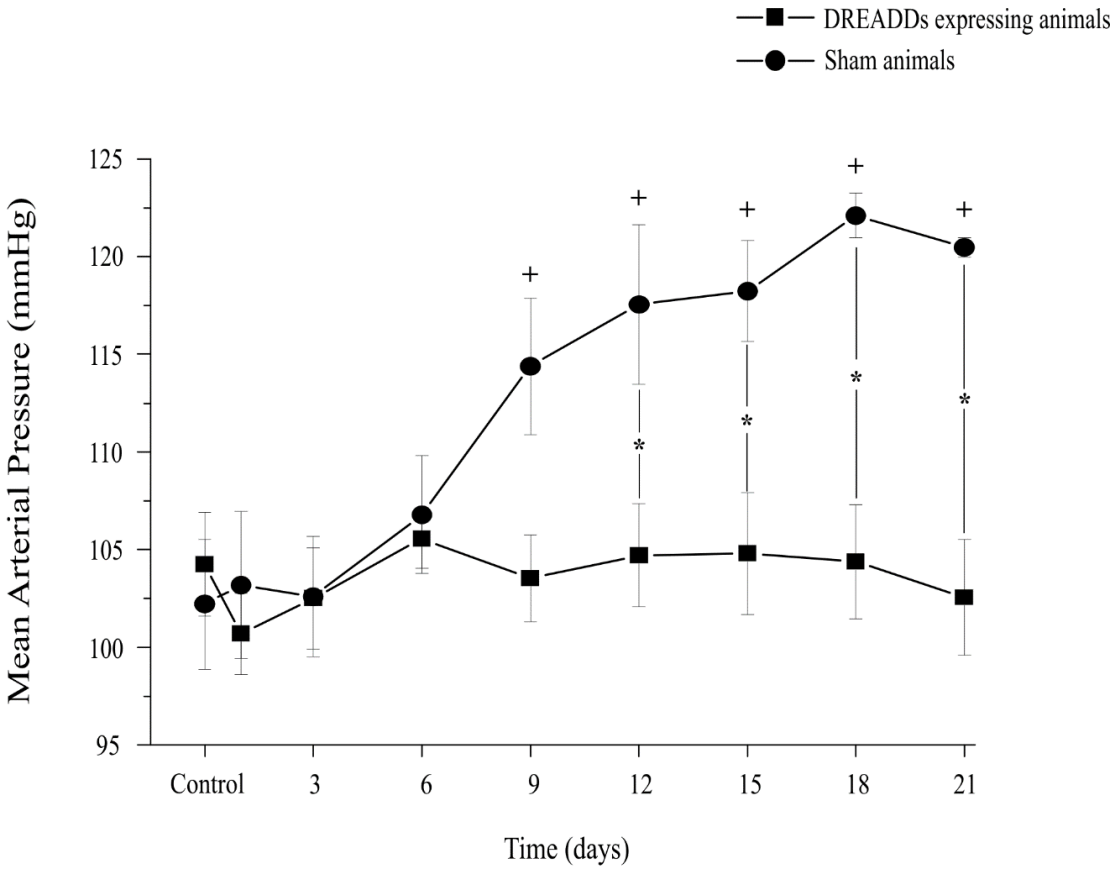
DREADDs expressing animals
Sham animals
Mean Arterial Pressure (mmHg)
125
120
115
110
105
100
95
Control
3
6
9
12
15
18
21
Time (days)
+
*

B

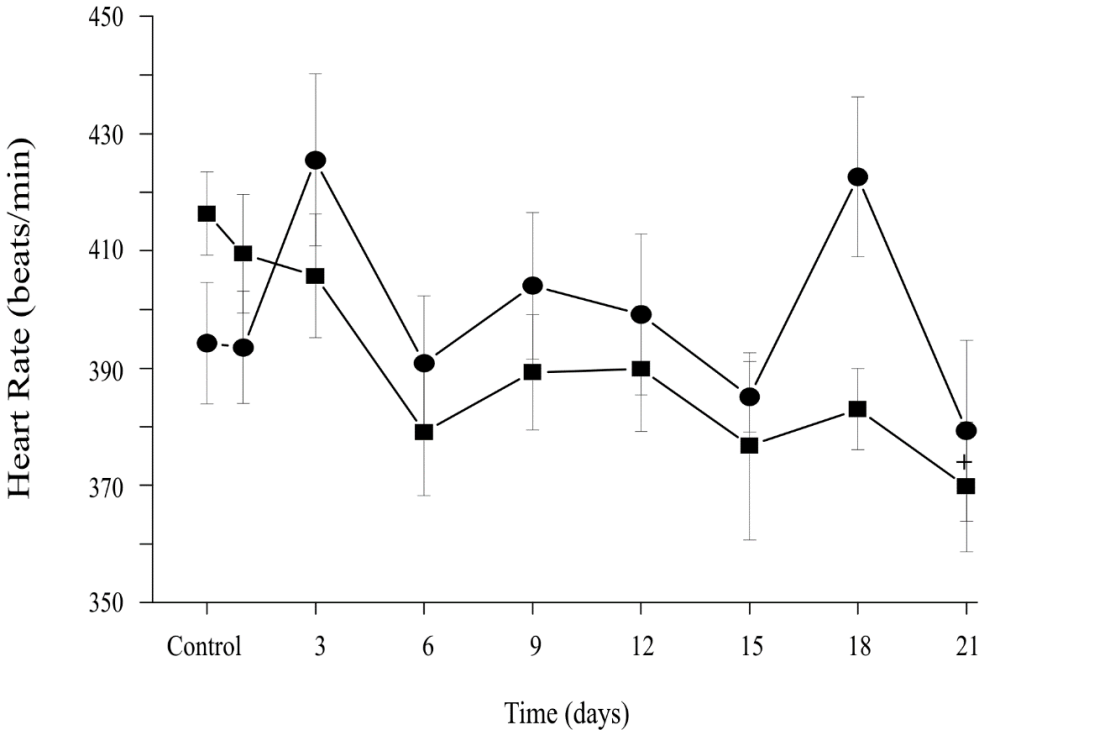
Heart Rate (beats/min)
450
430
410
390
370
350
Control
3
6
9
12
15
18
21
Time (days)
+

The effects of CIH/H on OXT receptor activation

In order to examine if the release of OXT from PVN fibers is altered with CIH/H, the responses in sniffer CHO cells (CHO cells expressing OXT receptors and the calcium indicator, RGECO1) were examined in brainstem tissue from unexposed sham and CIH/H exposed animals. Photoactivation of ChR2-containing PVN fibers in the DMV of brainstem slices from unexposed animals evoked large, reproducible, and transient increases in intracellular calcium levels in OXT-sensitive sniffer CHO cells (average increases of 21.1 ± 0.02% from baseline during first second; n = 14; $*p < 0.05$; one-way ANOVA with repeated measures; Figure 15, bottom left). CHO cell responses upon PVN fiber stimulation in brainstem slices from animals exposed to CIH/H was significantly decreased (average increases of 8.1 ± 0.01% from baseline during first second; n = 16; $*p < 0.05$; one-way ANOVA with repeated measures; Figure 15, bottom middle) compared to responses in unexposed animals ($^{+}p < 0.05$; one-way ANOVA; Figure 15, bottom middle). These results indicate the release of OXT from PVN fibers in the DMV is reduced following CIH/H exposure. To examine if restoration of OXT neuron function during CIH/H could restore responses in OXT-sensitive CHO cells, PVN OXT neurons were activated daily before and during CIH/H by daily injections of CNO to activate DREADDs receptors in PVN OXT neurons. In treatment animals with chronic activation of OXT neurons the responses in sniffer OXT-sensitive CHO cells upon photostimulation of ChR2-containing PVN fibers in the DMV were restored and not significantly different from responses in air exposed control animals (average increases of 23.4 ± 0.03% from baseline during first second; n = 17; $*p < 0.05$; one-way ANOVA with repeated measures; Figure 15, bottom right). These restored responses in the

treatment group were significantly increased compared to CIH/H exposed animals ($^{+}p < 0.05$; one way ANOVA; Figure 15, bottom right). These data indicate that the release of OXT onto parasympathetic CVNs is diminished with CIH/H, but that this release can be restored with chronic PVN OXT neuron activation.

Figure 15 Activation of PVN OXT neurons during CIH/H exposure restores responses in OXT sensitive CHO cells.

The calcium increases in OXT sensitive CHO cells upon photoactivation of PVN fibers in the DMV are significantly decreased with CIH/H when compared with sham air exposed animals and in treatment animals in which OXT neurons have been activated daily during CIH/H. Representative responses from CHO cells deposited onto brainstem tissue taken from animals exposed to air (top left), CIH/H (top middle), and CIH/H with daily OXT neuron activation (top right). Quantitative bar charts depict the percent control fluorescence of CHO cell responses in brainstem tissue taken from animals exposed to air (bottom left; n = 14), CIH/H (bottom middle; n = 16), and CIH/H with daily OXT neuron activation (bottom right; n = 17). $^{*}p < 0.05$; one-way ANOVA with repeated measure. $^{+}p < 0.05$; *one*-way ANOVA.

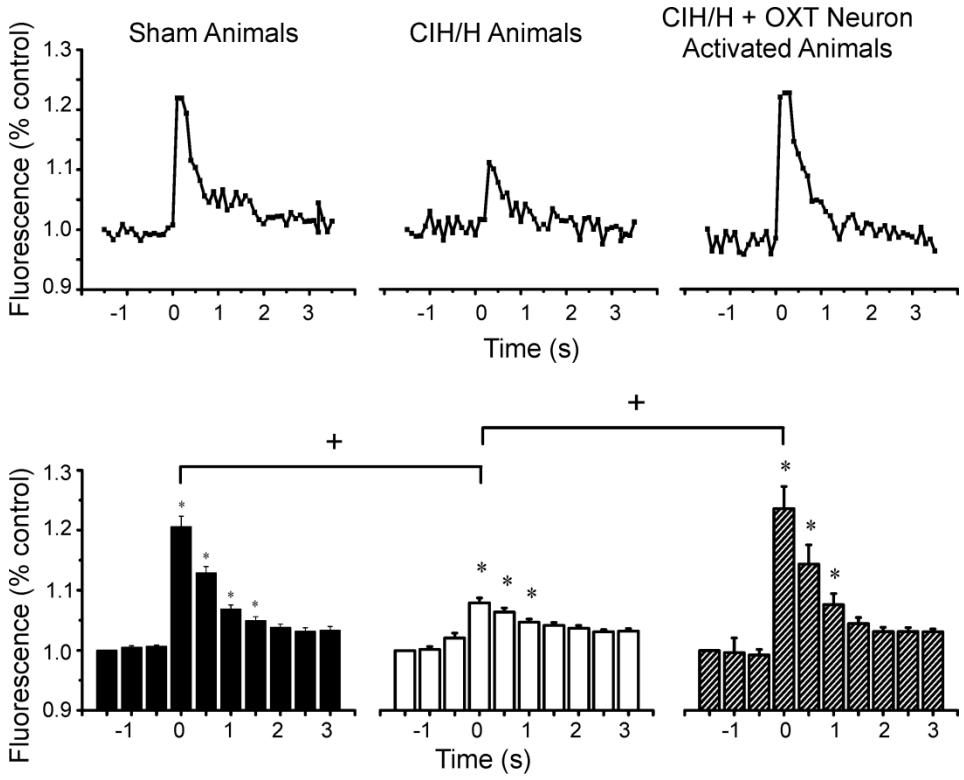
Sham Animals
CIH/H Animals
CIH/H + OXT Neuron Activated Animals
Fluorescence (% control)
1.3
1.2
1.1
1.0
0.9
-1
0
1
2
3
Time (s)
+
+
*

Conclusions from Study 2

In Study 1 (Chapter 2) we demonstrated that excitation of parvocellular PVN fibers releases OXT at brainstem CVN targets and the release of OXT is diminished following CIH/H exposure. This led us to test the hypothesis that restoring OXT neuron activity could be beneficial in blunting the adverse consequences of CIH/H, which was tested in Study 2 (Chapter 3). Our findings in Study 2 suggest that selective chronic activation of PVN OXT neurons has many beneficial effects, including decreasing resting blood pressure and heart rate, blunting the acute responses in blood pressure to H/H, and perhaps most importantly, chronic PVN OXT neuron activation prevented the elevations in blood pressure and heart rate that occur with CIH/H. The results in Study 2 not only establish a role for PVN OXT neurons in cardiovascular homeostasis in both control and disease conditions, but also identify a promising target to restore cardiac vagal activity, reduce sympathetic activity, and reduce adverse cardiovascular changes that occur in diseases such as OSA.

CHAPTER 4

Discussion

Conclusions

The work in this dissertation not only establishes the role of PVN OXT neurons in cardiovascular homeostasis, but also identifies promising targets to reduce the adverse cardiovascular changes associated with cardiovascular diseases such as OSA. This study has three major conclusions: 1) excitation of parvocellular PVN fibers releases OXT at parasympathetic brainstem targets, 2) the release of OXT is diminished following CIH/H exposure, and 3) chronic PVN OXT neuron activation decreases resting heart rate and blood pressure, blunts increases in blood pressure with H/H, and prevents the development of hypertensions with CIH/H, an animal model of OSA.

Study 1 Conclusions

Release of OXT from PVN fibers in the DMV

Recent work from our lab has shown that OXT receptor activation facilitates the excitatory neurotransmission from the PVN to CVNs with paired-pulse facilitation and enhancement of bursting patterns of stimulations. In the paired-pulse stimulation paradigm, OXT release from the first stimulation increased the amplitude of the second response, and this facilitation of the second response was abolished by application of the OXT receptor antagonist, OTA. Additionally, this direct OXT receptor mediated modulation in the neurotransmission to CVNs from the hypothalamic PVN nucleus is selective for this synaptic connection, and does not occur upon non-selective activation of glutamatergic synapses to CVNs (Pinol et al., 2014). The fact that optogenetic stimulation of PVN axons releases OXT is supported by the findings presented in Study 1

(Chapter 2), as this release of OXT from PVN fibers onto CVNs evoked large, reproducible, and transient increases in calcium in sniffer CHO cells highly sensitive to OXT, and application of the OXT receptor antagonist OTA, abolished these increases in intracellular calcium in the OXT-sensitive CHO cells.

The pathway from PVN to CVNs likely influences the activity of CVNs that are the dominant parasympathetic input to the heart. This work indicates that there are PVN OXT neurons that project to the DMV to regulate autonomic control. Indeed, studies have shown that OXT has cardioprotective qualities and can modulate reflex control of heart rate at the level of the DVC (Llewellyn-Smith et al., 2012). Additional studies have found that brainstem administration of OXT and OXT antagonists alter autonomic control of the heart, OXT release in the DVC after exercise contributes to the vagally-modulated blunting of the post-exercise tachycardic response, and OXT facilitates the baroreflex bradycardia (Rogers and Hermann, 1987; Higa et al., 2002; Michelini, 2001). The data presented here along with previous studies from our lab are consistent with these *in vivo* results, and provide evidence for endogenous release of OXT onto CVNs in the DMV. Overall, our data from Study 1 are consistent with, and extend, the postulated role for OXT in the DVC to enhance parasympathetic regulation of heart rate and OXT being cardioprotective.

Strong neuronal promoter (Synapsin) lentiviral approach

While the use of the strong neuronal promoter fragment synapsin 1 elicited robust expression of ChR2-EYFP in PVN fibers in brainstem slices and as our data shows, optogenetic stimulation of these fibers increased calcium levels in OXT-sensitive sniffer

CHO cells, a disadvantage to this approach is the lack of selectivity in driving expression of ChR2 with a nearly ubiquitous neuronal promoter. As such, while our immunohistochemistry results show that the majority (~55%) of ChR2-expressing PVN fibers in the brainstem slices stained positive for OXT, we cannot completely rule out the possibility that AVP instead of, or with OXT, is released from these PVN fibers to activate OXT receptors. There are however, several results that indicate a high level of specificity for only inducing OXT release upon optogenetic stimulation of PVN descending pre-autonomic axons in our experiments. The amount of lentivirus we injected (90-100 nl) was relatively low: other studies that have used this lentiviral vector typically injected larger volumes such as 0.3 – 2 µl (Cruikshank et al., 2010), and we additionally verified the injection site of each animal used for these studies and excluded animals that had neurons labeled outside of the PVN. Moreover, the sniffer CHO cells expressing OXT receptors are ~8 fold more sensitive and responsive to OXT than AVP, and the responses in the sniffer CHO cells were abolished with the OXT receptor antagonist, OTA. While the release of AVP upon photoactivation of ChR2-containing PVN fibers in the DMNV in this experimental paradigm cannot be ruled out, our results indicate that the intracellular calcium changes observed in these engineered CHO cells is due to the activation of OXT receptors, most likely via the synaptic release of OXT.

Oxytocin release is blunted with CIH/H

Our results from Study 1 indicate that the release of OXT from PVN fibers activates OXT receptors on sniffer CHO cells in close proximity to CVNs, and this release is diminished with exposure to 21 days of CIH/H, which is associated with the

highly prevalent cardiovascular disease, OSA (Coleman et al., 2010; Huang et al., 2007; Kc and Dick, 2010). These results extend recently published data from our lab that showed the paired-pulse facilitation of the EPSCs that occurs in unexposed rats is significantly blunted in animals exposed to CIH/H (Dergacheva et al., 2014). The diminished paired-pulse facilitation in CIH/H animals suggests impaired presynaptic transmitter release from PVN synaptic terminals. This impaired synaptic function may be due to alterations in neuromodulation by co-released peptides, neurotransmitter synthesis, vesicular accumulation or release properties, including impaired expression of ChR2 or diminished photostimulation of ChR2 in CIH/H animals. The results from Study 1 indicate OXT release is altered by CIH/H, and may explain the absence of paired-pulse facilitation from the PVN to CVNs in animals exposed to CIH/H (Dergacheva et al., 2014), as endogenous OXT release has been shown to mediate this paired-pulse facilitation (Pinol et al., 2014).

Several studies have indicated that the PVN is one of the major targets of CIH (Coleman et al., 2010; Huang et al., 2007; Kc et al., 2010). Activity in neurons within the PVN that are critical for the cardiovascular responses to challenges such as stress and dehydration are not impaired, but rather possess augmented activity with CIH and are involved in the maintenance and/or generation of CIH induced hypertension (da Silva et al., 2011; Kc et al., 2010; Kc and Dick, 2010; Knight et al., 2011). Using FosB/ΔFosB as a marker of neuronal activation, CIH increased the activity of cells in the dorsal and medial parvocellular subdivisions through all rostral-caudal levels in the PVN, as well as the lateral parvocellular subregion in the caudal PVN (Knight et al., 2011). Both nitric oxide and NMDA signaling are reduced in nNOS neurons in the PVN after CIH, and this

is accompanied by an increase in blood pressure (Coleman et al., 2010; Huang et al., 2007). Additionally, CIH causes increases in AVP-mediated PVN neurotransmission to the RVLM, the pathway thought to be involved in the alterations in blood pressure, heart rate, and respiration that occurs with CIH (Kc et al., 2010). Additionally, the alterations in blood pressure, heart rate, and respiration that occurs with CIH has been postulated to involve pathways from the PVN to the RVLM, NTS, locus coeruleus, and spinal sympathetic preganglionic neurons (Kc et al., 2010; Pajolla, 2009; Sharpe, 2013). Similarly, PVN pathways to neurons in the NA and DVC, brainstem regions where parasympathetic cardiac control originates, are hypothesized to modulate brainstem autonomic function (Kc and Dick, 2010). Taken together with the results from Study 1, these data indicate that the activity of PVN OXT neurons are altered in models of OSA, and along with diminished parasympathetic activity and augmented sympathetic activity, may lead to the generation of OSA induced hypertension.

Study 2 Conclusions

The effects of OXT neuron activation on resting blood pressure and heart rate

In Study 2 (Chapter 3) we examined the *in vivo* effects of selectively activating PVN OXT neurons using viral expression of excitatory hM_3D_q DREADDs in OXT neurons within the PVN. Until recently, OXT, has been known for its pivotal role on uterine contraction and milk ejection in females however, the role of centrally released OXT has been shown to have a diverse range of CNS functions in both males and females. There is much evidence suggesting OXT may be involved in the regulation of

the cardiovascular system by direct peripheral and indirect central actions (Petersson et al., 1996; Braga et al., 2000; McCann et al., 2002). OXT projections from the PVN as well as OXT receptors, have been found in areas of the brainstem known to regulate cardiovascular, behavioral, and neuroendocrine responses to stress (Sawchenko and Swanson, 1982; Sofroniew and Schrell, 1981), and the content of OXT in the PVN and brainstem has been shown to be augmented in spontaneously hypertensive rats (Mohring et al., 1983; Morris et al., 1985). Additionally, it has been suggested that centrally released OXT is cardioprotective and blocks the increases in blood pressure and heart rate during sudden stress (Wsol et al., 2009). The mechanisms by which OXT exerts its effects on cardiovascular system however, remains to be elucidated.

Many studies have examined the role of OXT in the regulation of resting blood pressure and heart rate, but the results of these studies have been inconsistent. Reports utilizing acute intracerebroventricular injection and/or infusion of OXT in rats showed no effect on resting blood pressure or heart rate (Wsol et al., 2009; Feuerstein et al., 1984). Similarly, central administration of OXT has been shown to have no effect on resting blood pressure and heart rate (Higa et al., 2002). Conversely, OXT activation of cardiovascular neurons in the DVC results in increases in baroreflex bradycardia and decreases in exercise-induced tachycardia (Michelini, 2001; Higa et al., 2002) by activation of neurons in the NTS (Braga et al., 2000), while blocking OXT receptors in the brain increases the cardiovascular responses to stress. Moreover, chronic intracerebroventricular injections of OXT significantly decreased resting blood pressure in rats (Petersson and Uvna-Moberg, 2007) and intracisternal injections of OXT in anesthetized rats elicited significant pressor responses with no changes in heart rate. The

data surrounding the role of OXT in the regulation of heart rate and blood pressure remain controversial, probably in part due to the differences in previous studies in which OXT receptors were activated with different doses, types of neurons affected, locations of application, and presence of anesthesia. In my study I did not administer OXT receptor agonists, but rather used the DREADDs approach to selectivity increase the firing of OXT neurons, increasing the activity in these PVN OXT neurons. We have shown selective activation of PVN OXT neurons decreases resting blood pressure and heart rate. These data indicate that PVN OXT neurons can play a significant role in cardiovascular regulation under resting conditions.

OXT neuron activation blunts the acute responses to H/H

Our results indicate that PVN OXT neuron activation significantly blunts the increases in blood pressure in response to H/H, and has little to no effect on the H/H-induced bradycardia. Exposure to acute H/H in animals, corresponding to apneas in humans, induces sympathetic and parasympathetic activation, which results in increases in blood pressure and decreases in heart rate, respectively (Ferreira et al., 2015). In humans, obstructive apnea is known to activate both sympathetic output, leading to vasoconstriction, and parasympathetic cardiac vagal activation, resulting in bradycardia (Dempsey et al., 2010). Animal studies have shown hypoxia causes changes in pH and gas concentrations and in response, the chemoreflex mediates sympathetic increases in blood pressure and parasympathetic activity mediated reductions in heart rate (Braga *et al*. 2008). A recent study from our lab additionally revealed acute H/H *in vitro* resulted in inhibition of GABAergic and glycinergic neurotransmission to CVNs in

brainstem slices from adult animals. These data suggest that the reductions in GABAergic and glycinergic transmission due to hypoxia relieves the inhibition on CVNs and increases parasympathetic activity to the heart resulting in bradycardia (Dyavanapalli et al., 2014).

The results in Study 2 indicate PVN OXT neuron activation has little to no effect on the evoked bradycardia in response to acute H/H. These results are not entirely surprising as studies have observed attenuation of pressor-induced bradycardia by blocking OXT receptors in the NTS/DMV, as well as intravenous OXT receptor injections completely blocking reflex bradycardia (Higa et al., 2002; Russ and Walker, 1994). These data indicate that OXT projections to the NTS/DMV facilitate bradycardic responses. Taken together with data from our lab showing OXT release excites CVNs in the DMV (Pinol et al., 2014), we might expect that parasympathetic cardiac vagal neurons are maximally excited by H/H, and accompanying OXT neuron activation could not provide any further increase in parasympathetic activity.

Similar to our results indicating that PVN OXT neuron activation blunts the increases in blood pressure with H/H, many studies have examined the effects of OXT on blood pressure, and such activation has been shown to buffer the effects of stress on the cardiovascular system resulting in hypotensive properties (Japundzic-Zigone, 2013). The blood pressure responses to acute stress for example, have been shown to be increased in OXT knockout mice (Bernatova et al., 2004), and central application of OXT receptor antagonists enhanced blood pressure increases to stress (Wsol et al., 2008). In humans, OXT administered in women to induce uterine contractions during labor was shown to decrease blood pressure, and this hypotensive effect was due to decreases in total

vascular resistance despite compensatory increases in heart rate, stroke volume, and cardiac output (Thomas, 2007; Archer et al., 2008). Overall, our data strengthen the argument that OXT blunts the severity and duration of stress-induced alterations in cardiovascular homeostasis.

Chronic OXT neuron activation decreases resting heart rate despite CIH/H

Our data indicate that after 21 days of chronic OXT neuron activation, DREADDs-expressing animals experience a significant decrease, compared to control days, in resting heart rate despite CIH/H exposure. OXT knockout mice have been reported to exhibit higher heart rates than wild-type controls, indicating the loss of OXT function increases resting heart rate (Japundzic-Zigon). Investigations that have examined the effects of OXT in exercise-trained rats have also observed that the release of OXT opposes the exercise-induced tachycardic response by reducing vagal withdrawal (Higa et al., 2002; Braga et al., 2000; Michelini, 2003). Additionally, data examining the effects of OXT on exercise and baroreflex control indicate central OXT projections to the NTS/DMV area provide an important mechanism to modulate heart rate control under stressful conditions, augmenting vagal outflow and resulting in a beneficial slowing of the heart rate. Conversely, OXT has not been observed to influence sympathetic outflow to the heart and does not appear to modulate the tachycardic responses to decreases in pressure (Higa et al., 2002). It is also important to note that in humans, plasma OXT has been related with lower cardiovascular activity in response to stress, and lactating women have been observed to have greater parasympathetic control of the heart (Grewen and Light, 2011; Altemus et al., 2001). Taken together with the data presented in Study 2,

these data indicate the importance of OXT as a central cardiovascular modulatory peptide. The associations between OXT and lower heart rate could be due to decreases in sympathetic activity, increases in parasympathetic activity, or to OXT having direct effects on OXT receptors in cardiac tissue (Grewen and Light, 2011).

OXT neuron activation diminishes the development of hypertension

Many studies have examined the role of OXT in hypertension. In rodents, hypertension alters mRNA and OXT receptor density, decreasing OXT mRNA expression in the hypothalamus and reducing OXT receptor density within the NTS (Higa-Taniguchi et al., 2009). Furthermore, OXT administration has been reported to have antihypertensive effects in spontaneously hypertensive male rats, and when administered postnatally, leads to blood pressure decreases in adulthood (Petersson et al., 1997). These hypotensive qualities of OXT were shown as daily peripheral administration of exogenous OXT for 5 days in rats resulted in decreases in blood pressure lasting at least 2 months (Holst et al., 2002). Additionally, OXT administration blunts the increases in blood pressure caused by electrical stimulation of the mesencephalic ventricular formation in male rats (Versteeg et al., 1982). Our data agree with previous studies that OXT is hypotensive, as chronic activation of PVN OXT neurons diminishes the development of hypertension with CIH/H.

The mechanism by which OXT decreases blood pressure is not currently known. It has been suggested however, that the long-lasting reductions in blood pressure may be mediated by the CNS, as elevated OXT concentrations in the CSF were found in rats injected with OXT (Petersson, 2002). It has also been hypothesized that OXT may

decrease blood pressure through inhibition of sympathetic preganglionic neurons (Yamashita et al., 1987; Kannan et al., 1998). Since OXT projections have been observed in a number of brain regions including the LC, NTS, DMV, RVLM, and IML (Buijs et al., 1982; Sofroniew et al., 1983), it is likely that the effects of OXT on blood pressure are modulated by these targets in the CNS.

Perspectives of in vivo studies

It is important to point out that we conducted only unilateral injections of the viruses into the PVN. The stimulation produced by activating OXT neurons in one PVN nucleus is sufficient to reduce resting blood pressure and heart rate, blunt the increases in blood pressure in response to H/H, and diminish the development of hypertension with CIH/H, thus providing evidence for the strong cardioprotective qualities of OXT. While we did observe in DREADDs-expressing animals a significant decrease in resting heart rate after 21 days of CIH/H exposure, this modest response in heart rate could be due to the limitations of unilateral activation of PVN OXT neurons. In other words, activating OXT neurons in both PVN nuclei could have induced greater changes in the vagal control of the heart, as injections of OXT directly into the NTS/DMV facilitates slowing of the heart and increases bradycardic responses (Higa et al., 2002), and OXT knockout mice have increased resting heart rates (Japundzic-Zigon, 2013).

Additionally, our sham animals do not experience the increases in resting heart rate with CIH/H associated with observed daytime tachycardia in patients with OSA. The heart rate changes following CIH however, are known to be less reproducible among animal models. Indeed, both significant increases or no changes in heart rate have been

observed with CIH exposure: no changes in heart rate was observed after 5 weeks CIH (Chen et al., 2005), however, 90 days CIH exposure caused significant increases in heart rate (Min et al., 2007). It appears that longer exposure periods of CIH may be required to induce adverse changes in heart rate.

Clinical use of OXT

Several questions concerning the cardiovascular effects of OXT remain to be answered, including the importance of OXT in promoting positive effects in cardiovascular diseases. Many studies conducted in the past two decades have expanded the classical roles of OXT on uterine contraction and milk ejection to include social behavior and cardiovascular regulation. Intranasal administration of OXT in humans has been shown to modulate several socio-cognitive and socio-emotional behaviors, reducing the responses to stress, having anxiolytic actions, and generating trust (Gamer and Buchel, 2012; Neurmann et al., 2013). More pertinent to the topics of this work, evidence suggests that both endogenous and exogenous OXT modulates ANS processes (Churchlan and Winkielma, 2012). A double blind placebo-controlled study showed that intranasal administration of OXT was sufficient to enhance the heart rate responses to pictures of facial expression, with the presentation of various facial expressions having no effect on sympathetic activity, but rather heart rate changes were solely due to alterations in parasympathetic activity (Gamer and Buchel, 2012). Additionally, intranasal administration of OXT was shown to increase the high frequency component of heart rate variability, which reflects parasympathetic activity (Norma et al., 2012).

We confirm in the studies presented here that OXT seems to directly enhance parasympathetic activity, so one could propose the use of intranasal administration of OXT to treat cardiovascular diseases in which there is a reduction in vagal innervation such as OSA. There is still much debate about the possible ways that intranasal OXT increases brain OXT concentrations (Churchland and Winkielman, 2012). There has been no evidence to confirm if nasal delivery of OXT increases brain OXT concentrations via diffusion or alternatively, activates OXT neurons. Regardless of the mechanism of increased OXT levels with intranasal administration, it may be a possible way to increase parasympathetic tone to the heart.

Based upon the results presented in Study 2, OSA patients could potentially benefit from intranasal OXT administration. Currently, continuous positive airway pressure (CPAP) therapy is the most common and successful treatment for OSA with mean blood pressure reductions of ~2 mmHg. Although CPAP improves the survival and quality of life, it is not well tolerated by all patients with OSA and its use if often discontinued. Thus, other avenues of treatment are crucial to mitigate the adverse cardiovascular effects caused by the disease. Intranasal OXT administration in these patients might serve as an alternative therapy, potentially by increasing parasympathetic activity and thus reducing or preventing the development of the adverse cardiovascular consequences such as hypertension and daytime tachycardia, documented in patients with this sleep disorder. The work presented in this dissertation has served as the foundation for designing a clinical study that will test whether intranasal oxytocin administration can blunt the adverse cardiorespiratory events that occur during apneas in patients with OSA.

Future Directions

Our studies have focused on establishing a role of OXT neurons in obstructive sleep apnea mediated cardiovascular disease. The results of this dissertation show that OXT is released at brainstem CVN targets and that this release is blunted with CIH/H exposure. Our results additionally indicate that selective activation of OXT neurons in the PVN decreases resting blood pressure and heart rate, and prevents the elevations in blood pressure and heart rate that occur after 21 days of CIH/H. The work presented here however, lacks a defined mechanism of action. To overcome this limitation, one could potentially activate subpopulations of PVN OXT neurons and examine the physiological effects of doing so. It would also be interesting to examine the effects of OXT neuron activation in animals already experiencing the adverse cardiovascular consequences associated with models of OSA, as it is unknown if OXT neuron activation could reverse the elevated blood pressure and heart rate after an animal has been exposed to 21 days of CIH/H and has already generated hypertension due to CIH/H.

Summary

Our data provide evidence that OXT is released onto CVNs in the DMV upon photoactivation of synaptic terminals from PVN neurons, and that 21 days of CIH/H exposure diminishes this release of OXT. This work additionally shows that chronic activation of PVN OXT neurons decreases resting blood pressure and heart rate, blunts the acute responses in blood pressure to H/H, and finally blocks the development of hypertension in animals exposed to CIH/H. While more studies need to be completed to determine the mechanisms by which OXT positively effects blood pressure and heart

rate, this work indicates that the release of OXT and activation of PVN OXT neurons is cardioprotective as excitation of parvocellular PVN fibers releases OXT at brainstem CVN targets, and selective activation of OXT neurons in the PVN decreases resting blood pressure and heart rate, and prevents the elevations in blood pressure and heart rate that occur after 21 days of CIH/H.

References

Aicher SA, Mitchell JL, Mendelowitz D. Distribution of mu-opioid receptors in rat visceral premotor neurons. Neuroscience, 2002; 115: 851-60. Berne RM, Levy MN. Cardiovascular physiology. 8th ed. Mosby: St. Louis, 2001.

Alexander GM, Rogan SC, Abbas AI, Armbruster BN, Pei Y, Allen JA, Nonneman RJ, Hartmann J, Moy SS, Nicolelis MA, McNamara JO, Roth BL. Remote control of neuronal activity in transgenic mice expressing evolved G protein-couple receptors. Neuron. 2009; 63: 29-39.

Altemus M, Redwine LS, Leong YM, Frye CA, Porges SW, Carter CS. Responses to laboratory psychosocial stress in postpartum women. Psychosom. Med. 2001; 63: 814–21.

Archer TL, Knape K, Liles D, Wheeler AS, Carter B. The hemodynamics of oxytocin and other vasoactive agents during neuraxial anesthesia for cesarean delivery: findings in six cases. International Journal of Obstetrics Anesthesia. 2008; 17: 247–54.

Armbruster BN, Li X, Pausch MH, Herlitze S, Roth BL. Evolving the lock to fit the key to create a family of G protein-coupled receptors potently activated by an inert ligand. Proc Natl Acad Sci U S A. 2007; 104: 5163–68.

Atasoy D, Betley JN, Su HH, Sternson SM. Deconstruction of a neural circuit for hunger. Nature. 2012; 488: 172–77.

Azagra-Calero E, Espinar-Escalona E, Barrera-Mora JM, Llamas-Carreras JM, Solano-Reina E. Obstructive sleep apnea syndrome (OSAS): Review of the literature. Medicina oral, patologia oral y cirugia buccal. 2012; 17:e925-929.

Badoer E. Hypothalamic paraventricular nucleus and cardiovascular regulation. Clin. Exp. Pharmacol. Physiol. 2001; 28:95–99.

Balachandran JS, Bakker JP, Rahangdale S, Yim-Yeh S, Mietus JE, Goldberger AL, Malhotra A. Effect of mild, asymptomatic obstructive sleep apnea on daytime heart rate variability and impedance cardiography measurements. The American journal of cardiology. 2012; 109: 140-45.

Bernatova I, Rigatto KV, Key MP, Morris M. Stress-induced pressor and corticosterone response in oxytocin-deficient mice. Exp. Physiol. 2004; 89: 549–57.

Bonsignore MR, Parati G, Insalaco G, Marrone O, Castiglioni P, Romano S, Di Rienzo M, Mancia G, Bonsignore G. Continuous positive airway pressure treatment improves baroreflex control of heart rate during sleep in severe obstructive sleep apnea syndrome. American journal of respiratory and critical care medicine. 2002; 166: 279-286.

Bonsignore MR, Parati G, Insalaco G, Castiglioni P, Marrone O, Romano S, Salvaggio A, Mancia G, Bonsignore G, Di Rienzo M. Baroreflex control of heart rate during sleep in severe obstructive sleep apnoea: effects of acute CPAP. The European respiratory journal: official journal of the European Society for Clinical Respiratory Physiology. 2006; 27: 128-35.

Boron WF, and Boulpaep EL. Medical physiology : a cellular and molecular approach. Philadelphia, PA: Saunders/Elsevier, 2009, p. xii, 1337 p.

Bouairi E, Kamendi H, Wang X, Gorini C, Mendelowitz D. Multiple types of GABAA receptors mediate inhibition in brain stem parasympathetic cardiac neurons in the nucleus ambiguus. J Neurophysiol. 2006; 96: 3266-72.

Bradley TD, Floras JS. Obstructive sleep apnoea and its cardiovascular consequences. Lancet. 2009; 373: 82-93.

Braga DC, Mori E, Higa KT, Morris M, Michelini LC. Central oxytocin modulates exercise induced tachycardia. Am J Physiol Regul Integr Comp Physiol. 2000; 278: R1474-82.

Braga VA, Burmeister MA, Sharma RV, Davisson RL. Cardiovascular responses to peripheral chemoreflex activation and comparison of different methods to evaluate baroreflex gain in conscious mice using telemetry. Am J Physiol Regul Integr Comp Physiol. 2008; 295: R1168–74.

Brooks CM, Koizumi K, Taleisnik S, Ferreyra Moyano H, Beltramino C, Deis RP, and Prilusky J. Sensory control of the hypothalamus and the neuroendocrine system. Acta physiologica latino americana 30: 159-170, 1980.

Buijs RM, Van Heerikhuize JJ. Vasopressin and oxytocin release in the brain--a synaptic event. Brain Res. 1982; 252: 71-6.

Card JP, Sved JC, Craig B, Raizada M, Vazquez J, Sved AF. Efferent projections of rat rostroventrolateral medulla C1 catecholamine neurons: Implications for the central control of cardiovascular regulation. J Comp Neurol. 2006; 499:840–859.

Carlson JT, Hedner JA, Sellgren J, Elam M, Wallin BG. Depressed baroreflex sensitivity in patients with obstructive sleep apnea. American journal of respiratory and critical care medicine. 1996; 154:1490-96.

Chen L, Einbinder E, Zhang Q, Hasday JC, Balke W, Scharf SM. Oxidative Stress and Left Ventricular Function with Chronic Intermittent Hypoxia in Rats. American Journal of Respiratory and Critical Care Medicine. 2005; 172: 915-20.

Chen QH, Toney GM. Excitability of paraventricular nucleus neurones that project to the rostral ventrolateral medulla is regulated by small-conductance Ca2+-activated K+ channels. J Physiol. 2009; 587: 4235-47.

Chu K, Zingg HH. Activation of the mouse oxytocin promoter by the orphan receptor RORalpha. J Mol Endocrinol. 1999; 23: 337-46.

Churchland PS, Winkielman P. Modulating social behavior with oxytocin: how does it work? What does it mean? Hormones and behavior, 2012; 61: 392-9. Coleman TG. Arterial baroreflex control of heart rate in the conscious rat. Am J Physiol. 2012; 238: H515-20.

Coleman CG, Wang G, Park L, Anrather J, Delagrammatikas GJ, Chan J, Zhou J, Iadecola C, Pickel VM. Chronic intermittent hypoxia induces NMDA receptor-dependent plasticity and suppresses nitric oxide signaling in the mouse hypothalamic paraventricular nucleus. The Journal of Neuroscience. 2010; 30:12103-12.

Conklin BR, Hsiao EC, Claeysen S, Dumuis A, Srinivasan S, Forsayeth JR, Guettier JM, Chang WC, Pei Y, McCarthy KD, et al. Engineering GPCR signaling pathways with RASSLs. Nat Methods. 2008; 5: 673–78.

Cooper VL, Pearson SB, Bowker CM, Elliott MW, Hainsworth R. Interaction of chemoreceptor and baroreceptor reflexes by hypoxia and hypercapnia - a mechanism for promoting hypertension in obstructive sleep apnoea. The Journal of physiology. 2005; 568: 677-87.

Coote JH, Yang Z, Pyner S, Deering J. Control of sympathetic outflows by the hypothalamic paraventricular nucleus. Clin. Exp. Pharmacol. Physiol. 1998; 25:461–463.

Cruikshank SJ, Urabe H, Nurmikko AV, Connors BW. Pathway-specific feedforward circuits between thalamus and neocortex revealed by selective optical stimulation of axons. Neuron. 2010; 65: 230-45.

Cruz JC, Bonagamba LG, Machado BH, Biancardi VC, Stern JE. Intermittent activation of peripheral chemoreceptors in awake rats induces Fos expression in rostral ventrolateral medulla-projecting neurons in the paraventricular nucleus of the hypothalamus. Neuroscience. 2008; 157:463–472.

Cutler MJ, Hamdan AL, Hamdan MH, Ramaswamy K, Smith ML. Sleep apnea: from the nose to the heart. The Journal of the American Board of Family Practice / American Board of Family Practice. 2002; 15:128-141.

Dampney RA, Horiuchi J, Tagawa T, Fontes MA, Potts PD, Polson JW. Medullary and supramedullary mechanisms regulating sympathetic vasomotor tone. Acta Physiol Scand. 2003; 177(3): 209-18.

Dempsey SC, Veasey BJ, Morgan CP, O'Donnell. Pathophysiology of sleep apnea. Physiol Rev, 2010; 90: 47–112.

Dergacheva O, Wang X, Huang ZG, Bouairi E, Stephens C, Gorini C, Mendelowitz D. Hypocretin 1 (Orexin A) Facilitates Inhibitory and Diminishes Excitatory Synaptic Pathways to Cardiac Vagal Neurons in the Nucleus Ambiguus. J Pharmacol Exp Ther. 2005.

Dergacheva O, Wang X, Lovett-Barr MR, Jameson H, Mendelowitz D. The lateral paragigantocellular nucleus modulates parasympathetic cardiac neurons: a mechanism for rapid eye movement sleep-dependent changes in heart rate. J Neurophysiol. 2010; 104: 685-94.

Dergacheva O, Bateman R, Byrne P, Mendelowitz D. Orexinergic modulation of GABAergic neurotransmission to cardiac vagal neurons in the brain stem nucleus ambiguus changes during development. Neuroscience. 2012; 209: 12-20.

Dergacheva O, Dyavanapalli J, Pinol R, Mendelowitz D. Chronic intermittent hypoxia and hypercapnia inhibit the hypothalamic paraventricular nucleus neurotransmission to parasympathetic cardiac neurons in the brain stem. Hypertension. 2014; 64: 597-603.

Dong S, Allen JA, Farrell M, Roth BL. A chemical-genetic approach for precise spatio-temporal control of cellular signaling. Molecular bioSystems. 2010; 6:1376-80.

Dreifuss JJ, Dubois-Dauphin M, Widmer H, Raggenbass M. Electrophysiology of oxytocin actions on central neurons. Ann N Y Acad Sci. 1992; 652: 46-57.

Dyavanapalli J, Jameson H, Dergacheva O, Jain V, Alhusayyen M, Mendelowitz D. Chronic intermittent hypoxia–hypercapnia blunts heart rate responses and alters neurotransmission to cardiac vagal neurons. The Journal of Physiology. 2014; 592: 2799–811.

Evans C, Baxi S, Neff RA, Venkatesan P, Mendelowitz D. Synaptic activation of cardiac vagal neurons by capsaicin sensitive and insensitive sensory neurons. Brain Res. 2003; 979: 210-5.

Evrengul H, Tanriverdi H, Kose S, Amasyali B, Kilic A, Celik T, Turhan H. The relationship between heart rate recovery and heart rate variability in coronary artery disease. Annals of noninvasive electrocardiology: the official journal of the International Society for Holter and Noninvasive Electrocardiology, Inc, 2006; 11: 154-62.

Farrell MS, Roth BL. Pharmacosynthetics: reimagining the pharmacogenetic approach. Brain Res. 2013; 1511: 6–20.

Fenno L, Yizhar O, Deisseroth K. The development and application of optogenetics. Annu Rev Neurosci. 2011; 34: 389-412.

Ferguson DW, Berg WJ, and Sanders JS. Clinical and hemodynamic correlates of sympathetic nerve activity in normal humans and patients with heart failure: evidence from direct microneurographic recordings. Journal of the American College of Cardiology. 1990; 16: 1125-34.

Ferguson AV, Latchford KJ, Samson WK. The paraventricular nucleus of the hypothalamus - a potential target for integrative treatment of autonomic dysfunction. Expert Opin Ther Targets. 2008; 12: 717-27.

Ferguson SM, Eskenazi D, Ishikawa M, Wanat MJ, Phillips PE, Dong Y, Roth BL, Neumaier JF. Transient neuronal inhibition reveals opposing roles of indirect and direct pathways in sensitization. Nature neuroscience. 2011; 14: 22-24.

Ferguson SM, Neumaier JF. Grateful DREADDs: Engineered receptors reveal how neural circuits regulate behavior. Neuropsychopharmacology, 2012; 37: 296-312.

Ferreira CB, Schoorlemmer GH, Rossi MV, Takakura AC, Barna BF, Moreira TS, Cravo SL. Brainstem areas activated by intermittent apnea in awake unrestrained rats. Neuroscience. 2015; in press.

Feuerstein G, Zerbe RL, Faden AI. Central cardiovascular effects of vasotocin, oxytocin and vasopressin in conscious rats. J Pharmacol Exp Ther. 1984; 228: 348–53.

Frank JG, Jameson HS, Gorini C, Mendelowitz D. Mapping and identification of GABAergic neurons in transgenic mice projecting to cardiac vagal neurons in the nucleus ambiguus using photo-uncaging. J Neurophysiol. 2009; 101: 1755-60.

Freeman R. Assessment of cardiovascular autonomic function. Clinical neurophysiology: official journal of the International Federation of Clinical Neurophysiology. 2006; 117: 716-30.

Gamer M, Buchel C. Oxytocin specifically enhances valence-dependent parasympathetic responses. Psychoneuroendocrinology. 2012; 37: 87-93.

Gan XB, Liu TY, Xiong XQ, Chen WW, Zhou YB, Zhu GQ. Hydrogen sulfide in paraventricular nucleus enhances sympathetic activity and cardiac sympathetic afferent reflex in chronic heart failure rats. 2012; PloS One. 7:e50102.

Ganong WF. The nervous system. Los Altos, Calif.: Lange Medical Publications, 1979, p. 243 p.

Ganong WF. Physiology : a study guide. Norwalk, Conn: Appleton & Lange, 1989, p. iv, 218 p.

Ganong WF. Review of Medical Physiology. San Francisco: Lange Medical Books/McGraw-Hill, 2005.

Garner AR, Rowland DC, Hwang SY, Baumgaertel K, Roth BL. Generation of a synthetic memory trace. Science. 2012; 335: 1513–16.

Geerling JC, Shin JW, Chimenti PC, Loewy AD. Paraventricular hypothalamic nucleus: axonal projections to the brainstem. J Comp Neurol. 2010; 518: 1460-99.

Gislason T, Sandhagen B, Boman G. Transcutaneous CO2 monitoring in adults with sleep-related breathing disorders. Upsala journal of medical sciences. 1989; 94: 171-81.

Goncharuk VD, Buijs RM, Jhamandas JH, Swaab DF. Vasopressin (VP) and neuropeptide FF (NPFF) systems in the normal and hypertensive human brainstem. J Comp Neurol. 2011; 519: 93-124.

Gorini C, Jameson HS, Mendelowitz D. Serotonergic modulation of the trigeminocardiac reflex neurotransmission to cardiac vagal neurons in the nucleus ambiguus. J Neurophysiol. 2009; 102: 1443-50.

Grewen KM, Light KC. Plasma oxytocin is related to lower cardiovascular and sympathetic reactivity to stress. Biological psychology. 2011; 87: 340-49.

Guyenet PG. The sympathetic control of blood pressure. Nat Rev Neurosci. 2006; 7: 335-46.

Guyton AC. Blood pressure control--special role of the kidneys and body fluids. Science. 1991a; 252: 1813-1816.

Guyton AC. Textbook of Medical Physiology. Philadelphia, PA: W.B. Saunders, 1991b.

Hare GM, Kavanagh BP, Mazer CD, Hum KM, Kim SY, Coackley C, Barr A, Baker AJ. Hypercapnia increases cerebral tissue oxygen tension in anesthetized rats. Canadian journal of anaesthesia = Journal canadien d'anesthesie. 2003; 50: 1061-68.

Higa KT, Mori E, Viana FF, Morris M, Michelini LC. Baroreflex control of heart rate by oxytocin in the solitary-vagal complex. Am J Physiol Regul Integr Comp Physiol. 2002; 282: R537-45.

Higa-Taniguchi, K. T., Felix, J. V. C. and Michelini, L. C. Brainstem oxytocinergic modulation of heart rate control in rats: effects of hypertension and exercise training. Experimental Physiology. 2009; 94: 1103–13.

Holst S, Uvnas-Moberg K, Petersson M. Postnatal oxytocin treatment and postnatal stroking of rats reduce blood pressure in adulthood. Autonomic Neuroscience. 2002; 99: 85–90.

Huang J, Tamisier R, Ji E, Tong J, Weiss WJ. Chronic intermittent hypoxia modulates nNOS mRNA and protein expression in the rat hypothalamus. Respir Physiol Neurobiol. 2007; 158: 30-38.

Hull SS, Jr., Vanoli E, Adamson PB, De Ferrari GM, Foreman RD, Schwartz PJ. Do increases in markers of vagal activity imply protection from sudden death? The case of scopolamine. Circulation. 1995; 91: 2516-9.

Iber C, Davies SF, Chapman RC, Mahowald MM. A possible mechanism for mixed apnea in obstructive sleep apnea. Chest. 1986; 89: 800-05.

Irnaten M, Neff RA, Wang J, Loewy AD, Mettenleiter TC, Mendelowitz D. Activity of cardiorespiratory networks revealed by transsynaptic virus expressing GFP. J Neurophysiol. 2001; 85: 435-8.

Jameson HS, Pinol RA, Kamendi H, Mendelowitz D. ATP facilitates glutamatergic neurotransmission to cardiac vagal neurons in the nucleus ambiguus. Brain Res. 2008a; 1201: 88-92.

Jameson HS, Pinol RA, Mendelowitz D. Purinergic P2X receptors facilitate inhibitory GABAergic and glycinergic neurotransmission to cardiac vagal neurons in the nucleus ambiguus. Brain Res. 2008b; 1224: 53-62.

Jansen AS, Nguyen XV, Karpitskiy V, Mettenleiter TC, Loewy AD. Central command neurons of the sympathetic nervous system: basis of the fight-or-flight response. Science. 1995a; 270: 644-6.

Jansen AS, Wessendorf MW, Loewy AD. Transneuronal labeling of CNS neuropeptide and monoamine neurons after pseudorabies virus injections into the stellate ganglion. Brain Res. 1995b; 683: 1-24.

Japundzic-Zigon N. Vasopressing and oxytocin in control of the cardiovascular system. Current Neuropharmacology. 2013; 11: 218-30.

Jordan D, Khalid ME, Schneiderman N, and Spyer KM. The location and properties of preganglionic vagal cardiomotor neurones in the rabbit. Pflugers Arch. 1982; 395: 244-250.

Kamendi HW, Cheng Q, Dergacheva O, Frank JG, Gorini C, Jameson HS, Pinol RA, Wang X, and Mendelowitz D. Recruitment of excitatory serotonergic neurotransmission to cardiac vagal neurons in the nucleus ambiguus post hypoxia and hypercapnia. Journal of neurophysiology. 2008; 99: 1163-1168.

Kanagy NL, Walker BR, Nelin LD. Role of endothelin in intermittent hypoxia-induced hypertension. Hypertension. 2001; 37: 511-15.

Kanagy NL. Vascular effects of intermittent hypoxia. ILAR journal / National Research Council, Institute of Laboratory Animal Resources. 2009; 50: 282-88.

Kannan H, Niijima A, Yamashita H. Effects of stimulation of the hypothalamic paraventricular nucleus on blood pressure and renal sympathetic nerve activity. Brain Res. Bull. 1998; 20: 779-83.

Katona PG, McLean M, Dighton DH, Guz A. Sympathetic and parasympathetic cardiac control in athletes and nonathletes at rest. J Appl Physiol. 1982; 52: 1652-7.

Kc P, Haxhiu MA, Tolentino-Silva FP, Wu M, Trouth CO, Mack SO. Paraventricular vasopressin-containing neurons project to brain stem and spinal cord respiratory related sites. Respir. Physiol Neurobiol. 2002; 133:75–88.

Kc P, Dick TE. Modulation of cardiorespiratory function mediated by the paraventricular nucleus. Respir Physiol Neurobiol. 2010; 174(1-2): 55-64.

Kc P, Balan KV, Tjoe SS, Martin RJ, Lamanna JC, Haxhiu MA, Dick TE. Increased vasopressin transmission from the paraventricular nucleus to the rostral medulla augments cardiorespiratory outflow in chronic intermittent hypoxia-conditioned rats. J Physiol. 2010; 588: 725-40.

Knight WD, Little JT, Carreno FR, Toney GM, Mifflin SW, Cunningham JT. Chronic intermittent hypoxia increases blood pressure and expression of FosB/DeltaFosB in central autonomic regions. American journal of physiology Regulatory, integrative and comparative physiology. 2011; 301: R131-39.

Krashes MJ, Koda S, Ye C, Rogan SC, Adams AC, Cusher DS, Maratos-Flier E, Roth BL, Lowell BB. Rapid, reversible activation of AgRP neurons drives feeding behavior in mice. The Journal of clinical investigation. 2011; 121:1424-28.

Kufoy E, Palma JA, Lopez J, Alegre M, Urrestarazu E, Artieda J, Iriarte J. Changes in the heart rate variability in patients with obstructive sleep apnea and its response to acute CPAP treatment. PloS One. 2012; 7:e33769.

Kunze DL. Reflex discharge patterns of cardiac vagal efferent fibres. J Physiol. 1972; 222: 1-15.

Lai CJ, Yang CC, Hsu YY, Lin YN, Kuo TB. Enhanced sympathetic outflow and decreased baroreflex sensitivity are associated with intermittent hypoxia-induced systemic hypertension in conscious rats. Journal of applied physiology. 2006; 100: 1974-82.

Landgraf R, Malkinson T, Horn T, Veale WL, Lederis K, Pittman QJ. Release of vasopressin and oxytocin by paraventricular stimulation in rats. Am J Physiol. 1990; 258: R155-9.

Large V, Hellstrom L, Reynisdottir S, Lonnqvist F, Eriksson P, Lannfelt L, and Arner P. Human beta-2 adrenoceptor gene polymorphisms are highly frequent in obesity and associate with altered adipocyte beta-2 adrenoceptor function. The Journal of clinical investigation. 1997; 100: 3005-13.

Leung RS. Sleep-disordered breathing: autonomic mechanisms and arrhythmias. Progress in cardiovascular diseases. 2009; 51:324-338.

Levy MN, Zieske H. Comparison of the cardiac effects of vagus nerve stimulation and of acetylcholine infusions. The American journal of physiology. 1969; 216: 890-7.

Llewellyn-Smith IJ, Kellett DO, Jordan D, Browning KN, Travagli RA. Oxytocinimmunoreactive innervation of identified neurons in the rat dorsal vagal complex. Neurogastroenterology and motility. The Official Journal of the European Gastrointestinal Motility Society. 2012; 24: e136-46.

Loewy AD, and Spyer KM editors. Central Regulation of Autonomic Functions. New York: Oxford University Press. 1990.

Loke YK, Brown JW, Kwok CS, Niruban A, Myint PK. Association of obstructive sleep apnea with risk of serious cardiovascular events: a systematic review and meta-analysis. Circulation Cardiovascular quality and outcomes. 2012; 5:720-28.

Luiten PG, Ter Horst GJ, Karst H, Steffens AB. The course of paraventricular hypothalamic efferents to autonomic structures in medulla and spinal cord. Brain Res. 1985; 329:374–78.

Machado BH, and Brody MJ. Role of the nucleus ambiguus in the regulation of heart rate and arterial pressure. Hypertension. 1988; 11: 602-07.

Mack SO, Kc P, Wu M, Coleman BR, Tolentino-Silva FP, Haxhiu MA. Paraventricular oxytocin neurons are involved in neural modulation of breathing. J. Appl. Physiol. 2002; 92:826–34.

Mack SO, Wu M, Kc P, Haxhiu MA. Stimulation of the hypothalamic paraventricular nucleus modulates cardiorespiratory responses via oxytocinergic innervation of neurons in pre-Botzinger complex. J. Appl. Physiol. 2007; 102:189–99.

Mastitskaya S, Marina N, Gourine A, Gilbey MP, Spyer KM, Teschemacher AG, Kasparov S, Trapp S, Ackland GL, Gourine AV. Cardioprotection evoked by remote ischemic preconditioning is critically dependent on the activity of vagal pre-ganglionic neurones. Cardiovasc Res. 2012; 95: 487-94.

McAllen RM, and Spyer KM. Two types of vagal preganglionic motoneurones projecting to the heart and lungs. The Journal of physiology. 1978; 282: 353-64.

McCall C, Singer T. The animal and human neuroendocrinology of social cognition, motivation and behavior. Nature neuroscience. 2012; 15:681-88.

McCann SM, Antunes-Rodrigues J, Jankowski M, Gutkowska J. Oxytocin, vasopressin and atrial natriuretic peptide control body fluid homeostasis by action on their receptors in brain, cardiovascular system and kidney. Prog Brain Res. 2002; 139: 309–26.

McGuire M, Bradford A. Chronic intermittent hypercapnic hypoxia increases pulmonary arterial pressure and haematocrit in rats. The European respiratory journal: official journal of the European Society for Clinical Respiratory Physiology. 2001; 18: 279-85.

Mendelowitz D, and Kunze DL. Identification and dissociation of cardiovascular neurons from the medulla for patch clamp analysis. Neuroscience letters. 1991; 132: 217-21.

Mendelowitz D. Firing properties of identified parasympathetic cardiac neurons in nucleus ambiguus. The American journal of physiology. 1996; 271: H2609-14.

Mendelowitz D. Nicotine excites cardiac vagal neurons via three sites of action. Clinical and experimental pharmacology & physiology. 1998; 25: 453-56.

Mendelowitz D. Advances in parasympathetic control of heart rate and cardiac function. News Physiol Sci. 1999; 14: 155-61.

Michelini LC. Oxytocin in the NTS. A new modulator of cardiovascular control during exercise. Ann NY Acad Sci. 2001; 940: 206–19.

Michelini LC, Marcelo MC, Amico J, Morris M. Oxytocinergic regulation of cardiovascular function: studies in oxytocin-deficient mice. American journal of physiology Heart and circulatory physiology. 2003; 284: H2269-76.

Mills E. Time course for development of vagal inhibition of the heart in neonatal rats. Life Sci. 1978; 23: 2717-20.

Mo ZL, Katafuchi T, Muratani H, Hori T. Effects of vasopressin and angiotensin II on neurones in the rat dorsal motor nucleus of the vagus, in vitro. J Physiol. 1992; 458: 561-77.

Mohring J, Schoun J, Kintz J, Robinson IC, McNeill JR. Vasopressin and oxytocin content are decreased in the brain stems of spontaneously hypertensive rats. Neuroendocrinology. 1983; 36: 457–61.

Morris M, Ross J, Sundberg DK. Catecholamine biosynthesis and vasopressin and oxytocin secretion in the spontaneously hypertensive rat: An in vitro study of localized brain regions. Peptides. 1985; 6: 949–55.

Motte S, Mathieu M, Brimioulle S, Pensis A, Ray L, Ketelslegers JM, Montano N, Naeije R, van de Borne P, Entee KM. Respiratory-related heart rate variability in progressive experimental heart failure. American journal of physiology. Heart and circulatory physiology. 2005; 289: H1729-35.

Nagel G, Szellas T, Huhn W, Kateriya S, Adeishvili N, Berthold P, Ollig D, Hegemann P, Bamberg E. Channelrhodopsin-2, a directly light-gated cation-selective membrane channel. Proc Natl Acad Sci U S A. 2003; 100: 13940-5.

Narkiewicz K, Somers VK. Sympathetic nerve activity in obstructive sleep apnoea. Acta physiologica Scandinavica. 2003; 177: 385-90.

Nawaratne V, Leach K, Suratman N, Loiacono RE, Felder CC, Armbruster BN, Roth BL, Sexton PM, Christopoulos A. New insights into the function of M4 muscarinic acetylcholine receptors gained using a novel allosteric modulator and a DREADD (designer receptor exclusively activated by a designer drug) Mol Pharmacol. 2008; 74: 1119–31.

Neff RA, Hansen MK, and Mendelowitz D. Acetylcholine activates a nicotinic receptor and an inward current in dorsal motor nucleus of the vagus neurons in vitro. Neuroscience letters. 1995; 195: 163-66.

Neff RA, Humphrey J, Mihalevich M, and Mendelowitz D. Nicotine enhances presynaptic and postsynaptic glutamatergic neurotransmission to activate cardiac parasympathetic neurons. Circulation research. 1998a; 83: 1241-47.

Neff RA, Mihalevich M, and Mendelowitz D. Stimulation of NTS activates NMDA and non-NMDA receptors in rat cardiac vagal neurons in the nucleus ambiguus. Brain research. 1998b; 792: 277-82.

Nishime EO, Cole CR, Blackstone EH, Pashkow FJ, Lauer MS. Heart rate recovery and treadmill exercise score as predictors of mortality in patients referred for exercise ECG. JAMA: the journal of the American Medical Association. 2000; 284: 1392-98.

Norman GJ, Cacioppo JT, Morris JS, Malarkey WB, Berntson GG, Devries AC. Oxytocin increases autonomic cardiac control: moderation by loneliness. Biological psychology. 2011; 86: 174-80.

de Oliveira DC, Chagas MH, Garcia LV, Crippa JA, Zuardi AW. Oxytocin interference in the effects induced by inhalation of 7.5% CO(2) in healthy volunteers. Human psychopharmacology. 2012; 27: 378-85.

Pachikara N, Mehra R. Treating obstructive sleep apnea with positive pressure therapy. Current treatment options in neurology. 2011; 13:458-72.

Pajolla GP, Accorsi-Mendonça D, Lunardi CN, Bendhack LM, Machado BH, Llewellyn-Smith IJ. Immunoreactivity for neuronal NOS and fluorescent indication of NO formation in the NTS of juvenile rats submitted to chronic intermittent hypoxia. Auton Neurosci. 2009; 148(1-2):55-62.

Pardini BJ, Patel KP, Schmid PG, and Lund DD. Location, distribution and projections of intracardiac ganglion cells in the rat. Journal of the autonomic nervous system. 1987; 20: 91-101.

Parish JM, Somers VK. Obstructive sleep apnea and cardiovascular disease. Mayo Clinic proceedings Mayo Clinic. 2004; 79: 1036-46.

Patton HD, and Howell WH. Textbook of physiology. Philadelphia: Saunders, 1989.

Pei Y, Rogan SC, Yan F, Roth BL. Engineered GPCRs as tools to modulate signal transduction. Physiology. 2008; 23: 313–21.

Peters JH, McDougall SJ, Kellett DO, Jordan D, Llewellyn-Smith IJ, Andresen MC. Oxytocin enhances cranial visceral afferent synaptic transmission to the solitary tract nucleus. J Neurosci. 2008; 28: 11731-40.

Petersson M, Alster P, Lundeburg T, Uvna¨s-Moberg K. Oxytocin causes a long time decrease of blood pressure in female and male rats. Physiol Behav. 1996; 60: 1311–15.

Petersson M, Lundeberg T, Uvnäs-Moberg K. Oxytocin decreases blood pressure in male but not in female spontaneously hypertensive rats. J. Auton. Nerv. Syst. 1997; 66: 15–18.

Petersson M. Cardiovascular effects of oxytocin. Prog Brain Res. 2002; 139: 281-88.

Petersson M, Uvna¨s-Moberg K. Effects of an acute stressor on blood pressure and heart rate in rats pretreated with intracerebroventricular oxytocin injections. Psychoneuroendocrinology. 2007; 32: 959–65.

Petreanu L, Huber D, Sobczyk A, Svoboda K. Channelrhodopsin-2-assisted circuit mapping of long-range callosal projections. Nat Neurosci. 2007; 10: 663-68.

Pickering TG, Gribbin B, Petersen ES, Cunningham DJ, Sleight P. Effects of autonomic blockade on the baroreflex in man at rest and during exercise. Circ Res. 1972; 30: 177- 85.

Pinol RA, Bateman R, Mendelowitz D. Optogenetic approaches to characterize the long-range synaptic pathways from the hypothalamus to brain stem autonomic nuclei. Journal of Neuroscience Methods. 2012; 210(2): 238-46.

Pinol RA, Jameson H, Popratiloff A, Lee NH, Mendelowitz D. Visualization of oxytocin release that mediates paired pulse facilitation in hypothalamic pathways to brainstem autonomic neurons. PLos One. 2014; 7; 9(11):e112138.

Raggenbass M, Dubois-Dauphin M, Charpak S, Dreifuss JJ. Neurons in the dorsal motor nucleus of the vagus nerve are excited by oxytocin in the rat but not in the guinea pig. Proc Natl Acad Sci U S A. 1987; 84: 3926-30.

Raggenbass M, Dreifuss JJ. Mechanism of action of oxytocin in rat vagal neurones: induction of a sustained sodium-dependent current. J Physiol. 1992; 457: 131-42.

Rardon DP, and Bailey JC. Parasympathetic effects on electrophysiologic properties of cardiac ventricular tissue. Journal of the American College of Cardiology. 1983; 2: 1200-09.

Ramezani A, Hawley RG. Generation of HIV-1-based lentiviral vector particles. Current protocols in molecular biology / edited by Frederick M. Ausubel ... [et al.], 2002; Chapter 16: Unit 16 22.

Ren J, Qin C, Hu F, Tan J, Qiu L, Zhao S, Feng G, Luo M. Habenula "cholinergic" neurons co-release glutamate and acetylcholine and activate postsynaptic neurons via distinct transmission modes. Neuron. 2011; 69: 445-52.

Richard S, Zingg HH. Identification of cis-acting regulatory elements in the human oxytocin gene promoter. Mol Cell Neurosci. 1991; 2: 501-10.

Rinaman L. Oxytocinergic inputs to the nucleus of the solitary tract and dorsal motor nucleus of the vagus in neonatal rats. J Comp Neurol. 1998; 399: 101-9.

Rinaman L. Visceral sensory inputs to the endocrine hypothalamus. Front Neuroendocrinol. 2007; 28: 50-60.

Ring RH, Malberg JE, Potestio L, Ping J, Boikess S, Luo B, Schechter LE, Rizzo S, Rahman Z, Rosenzweig-Lipson S. Anxiolytic-like activity of oxytocin in male mice: behavioral and autonomic evidence, therapeutic implications. Psychopharmacology. 2006; 185: 218-25.

Rogan SC, Roth BL. Remote control of neuronal signaling. Pharmacological reviews. 2011; 63: 291-315.

Rogers RC, Hermann GE. Hypothalamic paraventricular nucleus stimulation-induced gastric acid secretion and bradycardia suppressed by oxytocin antagonist. Peptides. 1986; 7: 695-700.

Rogers RC, Hermann GE. Oxytocin, oxytocin antagonist, TRH, and hypothalamic paraventricular nucleus stimulation effects on gastric motility. Peptides. 1987; 8: 505-13.

Rowan III WH, Campen MJ, Wichers LB, Watkinson WP. Heart rate variability in rodents: uses and caveats in toxicology studies. Cardiovasc Toxicol. 2007; 7: 28 51.

Russ RD, Walker BR. Oxytocin augments baroreflex bradycardia in conscious rats. Peptides. 1994; 15: 907–12.

Sanders MH, Kern NB, Costantino JP, Stiller RA, Strollo PJ, Jr., Studnicki KA, Coates JA, Richards TJ. Accuracy of end-tidal and transcutaneous PCO2 monitoring during sleep. Chest. 1994; 106: 472-83.

Saper CB, Loewy AD, Swanson LW, Cowan WM. Direct hypothalamo-autonomic connections. Brain Res. 1976; 117: 305-12.

Sasaki K, Suzuki M, Mieda M, Tsujino N, Roth B, Sakurai T. Pharmacogenetic modulation of orexin neurons alters sleep/wakefulness states in mice. PloS one. 2011; 6:e20360.

Sawchenko PE, Swanson LW. Immunohistochemical identification of neurons in the paraventricular nucleus of the hypothalamus that project to the medulla or to the spinal cord in the rat. J Comp Neurol. 1982; 205: 260-72.

Scher AM, Young AC. Reflex control of heart rate in the unanesthetized dog. Am J Physiol. 1970; 218: 780-89.

Sharpe AL, Calderon AS, Andrade M, Cunningham JT, Mifflin SW, Toney GM. Chronic intermittent hypoxia increases sympathetic control of blood pressure: role of neuronal activity in the hypothalamic paraventricular nucleus. American Journal of Physiology - Heart and Circulatory Physiology. 2013; 305(12): H1772-80.

da Silva AQ, Fontes MA, Kanagy NL Chronic infusion of angiotensin receptor antagonists in the hypothalamic paraventricular nucleus prevents hypertension in a rat model of sleep apnea. Brain research. 2011; 1368: 231-38.

Sofroniew MV, Schrell U. Evidence for direct projections from oxytocin and vasopressin neurons in the hypothalamic paraventricular nucleus in the medulla oblongata:Immunohistochemical visualization of both the horseradish peroxidase transported and peptide produced by the same neurons. Neurosci Lett. 1981; 22: 211–17.

Sofroniew MV. Vasopressin and oxytocin in the mammalian brain and spinal cord. Trends Neurosci. 1983; 6: 467-72.

Spyer KM. Neural organisation and control of the baroreceptor reflex. Rev Physiol Biochem Pharmacol. 1981; 88: 24-124.

Stauss HM. Heart rate variability. American Journal of Physiology - Regulatory, Integrative and Comparative Physiology. 2003; 285(5), R927-31.

Sternson SM, Roth BL. Chemogenetic tools to interrogate brain functions. Annu Rev Neurosci. 2014; 37: 387-407.

Stornetta RL, Guyenet PG, McCarty RC. Autonomic nervous system control of heart rate during baroreceptor activation in conscious and anesthetized rats. J Auton Nerv Syst. 1987; 20: 121-27.

Stuesse SL. Origins of cardiac vagal preganglionic fibers: a retrograde transport study. Brain research. 1982; 236: 15-25.

Sullebarger JT, Liang CS, Woolf PD, Willick AE, Richeson JF. Comparison of phenylephrine bolus and infusion methods in baroreflex measurements. J Appl Physiol. 1990; 69: 962-67.

Swanson LW, Sawchenko PE, Berod A, Hartman BK, Helle KB, Vanorden DE. An immunohistochemical study of the organization of catecholaminergic cells and terminal fields in the paraventricular and supraoptic nuclei of the hypothalamus. J Comp Neurol. 1981; 196: 271–85.

Swanson LW, Sawchenko PE. Hypothalamic integration: organization of the paraventricular and supraoptic nuclei. Annu Rev Neurosci. 1983; 6: 269-324.

Szulc J, Wiznerowicz M, Sauvain MO, Trono D, Aebischer P. A versatile tool for conditional gene expression and knockdown. Nat Methods. 2006; 3: 109-16.

Ter Horst GJ, Luiten PG, Kuipers F. Descending pathways from hypothalamus to dorsal motor vagus and ambiguus nuclei in the rat. J Auton Nerv Syst. 1984; 11: 59-75.

Thomas JS, Koh SH, Cooper GM. Haemodynamic effects of oxytocin given as i.v. bolus or infusion on women undergoing Caesarean section. British Journal of Anaesthesia. 2007; 98: 116–19.

Townend JN, Littler WA. Cardiac vagal activity: a target for intervention in heart disease. Lancet. 1995; 345: 937-38.

Troncoso Brindeiro CM, da Silva AQ, Allahdadi KJ, Youngblood V, Kanagy NL. Reactive oxygen species contribute to sleep apnea-induced hypertension in rats. American journal of physiology Heart and circulatory physiology. 2007; 293: H2971-76.

Valenstein T, Case B, Valenstein ES. Stereotaxic atlas of the infant rat hypothalamus. Developmental psychobiology. 1969; 2: 75-80.

Vanoli E, De Ferrari GM, Stramba-Badiale M, Hull SS, Jr., Foreman RD, Schwartz PJ. Vagal stimulation and prevention of sudden death in conscious dogs with a healed myocardial infarction. Circ Res. 1991; 68: 1471-81.

Varga V, Losonczy A, Zemelman BV, Borhegyi Z, Nyiri G, Domonkos A, Hangya B, Holderith N, Magee JC, Freund TF. Fast synaptic subcortical control of hippocampal circuits. Science. 2009; 326: 449-53.

Versteeg CAM, Bohus B, de Jong W. Inhibition of centrally evoked pressor responses by neurohypophysial peptides and their fragments. Neuropharmacology. 1982; 21: 1359- 64.

Voorn P, Buijs RM. An immuno-electronmicroscopical study comparing vasopressin, oxytocin, substance P and enkephalin containing nerve terminals in the nucleus of the solitary tract of the rat. Brain Res. 1983; 270: 169-73.

Vrontou S, Wong AM, Rau KK, Koerber HR, Anderson DJ. Genetic identification of C fibres that detect massage-like stroking of hairy skin in vivo. Nature. 2013; 493: 669–73.

Wang J, Irnaten M, and Mendelowitz D. Characteristics of spontaneous and evoked GABAergic synaptic currents in cardiac vagal neurons in rats. Brain research. 2001a; 889: 78-83.

Wang J, Irnaten M, Neff RA, Venkatesan P, Evans C, Loewy AD, Mettenleiter TC, and Mendelowitz D. Synaptic and neurotransmitter activation of cardiac vagal neurons in the nucleus ambiguus. Annals of the New York Academy of Sciences. 2001b; 940: 237-46.

Wang J, Irnaten M, Venkatesan P, Evans C, Mendelowitz D. Arginine vasopressin enhances GABAergic inhibition of cardiac parasympathetic neurons in the nucleus ambiguus. Neuroscience. 2002; 111(3): 699-705.

Wang J, Wang X, Irnaten M, Venkatesan P, Evans C, Baxi S, and Mendelowitz D. Endogenous acetylcholine and nicotine activation enhances GABAergic and glycinergic inputs to cardiac vagal neurons. Journal of neurophysiology. 2003; 89: 2473-81.

Warner MR, deTarnowsky JM, Whitson CC, and Loeb JM. Beat-by-beat modulation of AV conduction. II. Autonomic neural mechanisms. The American journal of physiology. 1986; 251: H1134-42.

White JD, Krause JE, McKelvy JF. In vivo biosynthesis and transport of oxytocin, vasopressin, and neurophysins to posterior pituitary and nucleus of the solitary tract. J Neurosci. 1984; 4: 1262-70.

Wsol A, Cudnoch-Jedrzejewska A, Szczepanska-Sadowska E, Kowalewski S, Puchalska L. Oxytocin in the cardiovascular responses to stress. J. Physiol. Pharmacol. 2008; 59 (Suppl 8):123–27.

Wsol A, Cudnoch-Jedrzejewska A, Szczepanska-Sadowska E, Kowalewski S, Dobruch J. Central oxytocin modulation of acute stress-induced cardiovascular responses after myocardial infarction in the rat. Stress. 2009; 12: 517-25.

Yamashita H, Kannan H, Kasai M, Osaka T. Decrease in blood pressure by stimulation of the rat hypothalamic paraventricular nucleus with L-glutamate or weak current. J. Auton. Nerv. Syst. 1987; 19: 229-34.

Yan B, Li L, Harden SW, Gozal D, Lin Y, Wead WB, Wurster RD, Cheng ZJ. Chronic intermittent hypoxia impairs heart rate responses to AMPA and NMDA and induces loss of glutamate receptor neurons in nucleus ambiguous of F344 rats. American journal of physiology Regulatory, integrative and comparative physiology. 2009; 296: R299-308.

Yang Z, Bertram D, Coote JH. The role of glutamate and vasopressin in the excitation of RVL neurones by paraventricular neurones. Brain Res. 2001; 908: 99-103.

Yeh ER, Erokwu B, LaManna JC, Haxhiu MA. The paraventricular nucleus of the hypothalamus influences respiratory timing and activity in the rat. Neurosci. Lett. 1997; 232: 63–66.

Zhao Y, Araki S, Wu J, Teramoto T, Chang YF, et al. (2011) An expanded palette of genetically encoded Ca(2)(+) indicators. Science. 2001; 333: 1888–91.

Zheng JQ, Seki M, Hayakawa T, Ito H, Zyo K. Descending projections from the paraventricular hypothalamic nucleus to the spinal cord: anterograde tracing study in the rat. Okajimas Folia Anat. Jpn. 1995; 72: 119–35.

Zhu H, Roth BL. DREADD: A Chemogenetic GPCR Signaling Platform. International Journal of Neuropsychopharmacology. 2014; 1–6.